Towards Low Dose Retrospective Dosimetry on Shelled Species

by

Amna Hassan

A thesis submitted to the
School of Graduate and Postdoctoral Studies in partial
fulfillment of the requirements for the degree of

Master of Applied Science

in

Nuclear Engineering

Faculty of Energy Systems and Nuclear Science

University of Ontario Institute of Technology
(Ontario Tech University)

Oshawa, Ontario, Canada

August 2020

Thesis Examination Information

Submitted by: **Amna Hassan**

Master of Applied Science in **Nuclear Engineering**

Towards Low Dose Retrospective Dosimetry on Shelled Species

An oral defense of this thesis took place on August 5, 2020 in front of the following examining committee:

Examining Committee

Chair of Examining Committee	Dr. Hossam Gaber
Research Supervisor	Dr. Edward Waller
Examining Committee Member	Dr. Kirk Atkinson
Thesis Examiner	Dr. Sean Forrester, Faculty of Science

The above committee determined that the thesis is acceptable in form and content and that a satisfactory knowledge of the field covered by the thesis was demonstrated by the candidate during an oral examination. A signed copy of the Certificate of Approval is available from the School of Graduate and Postdoctoral Studies.

Abstract

This work investigates calcified tissues of shelled species for retrospective dosimetry using electron paramagnetic resonance (EPR) spectroscopy. To determine applicable samples for low dose studies, shells of crustacean and mollusc species were irradiated to 10 Gy using a ^{137}Cs source. Reference dosimetry was performed with alanine powder using a specifically developed calibration curve. Characteristic Mn^{2+} signals were present in the EPR spectra of all studied species. Radiation-induced peaks were not detected in shells of any species except terrestrial snails. A dose-response curve for terrestrial snails was developed by irradiating shells to 2, 10, and 20 Gy. However, Mn^{2+} signals caused limitations in resolving radiation-induced peaks below 2 Gy. Environmental factors were assessed, and it was found that shell structure and habitat characteristics contribute to Mn^{2+} signals in EPR spectra. Since high-intensity Mn^{2+} signals obscured radiation-induced peaks, shells of the studied aquatic species were deemed unsuitable for low dose retrospective dosimetry.

Keywords: EPR dosimetry; retrospective dosimetry; alanine powder; calcified tissues; Mn^{2+}

Declaration of Authorship

- I hereby declare that this thesis consists of original work of which I have authored. This is a true copy of the thesis, including any required final revisions, as accepted by my examiners.
- I authorize the University of Ontario Institute of Technology to lend this thesis to other institutions or individuals for the purpose of scholarly research. I further authorize University of Ontario Institute of Technology to reproduce this thesis by photocopying or by other means, in total or in part, at the request of other institutions or individuals for the purpose of scholarly research. I understand that my thesis will be made electronically available to the public.

Signed: 

Date: August 12 2020

Statement of Contributions

Contributing individuals to the work in this thesis:

Dr. Margarita Tzivaki, Ontario Tech University, for providing the background information and procedures of operating the EPR spectrometer.

Lukas Felner, BSc, University of Applied Sciences Technikum Wien, for optimizing the alanine-EPR measurements used for secondary dosimetry.

Dr. Marilyne Stuart, Canadian Nuclear Laboratories (CNL), for performing irradiations of the alanine powder at the CNL GammaCell 220 facility.

Acknowledgements

First and foremost, I would like to express my deepest appreciation and gratitude to my supervisor Dr. Ed Waller for his continuous support, guidance, and encouragement of my research endeavors.

My sincere appreciation goes to Margarita Tzivaki for her endless advice, support, explanations, and the ever so helpful reality checks I have needed. Thank you also to Marta Kocemba for performing the bulk of my sample collection, and also for introducing me to the world of plants, which provided me with hours of necessary distraction.

Finally, thank you to my family for their loving support and their constant encouragement of my career aspirations.

The research work presented in this thesis has been funded by the National Sciences and Engineering Council of Canada (NSERC) and the University Network of Excellence in Nuclear Engineering (UNENE).

Contents

Abstract iii

Declaration of Authorship iv

Statement of Contributions v

Acknowledgements vi

1 Introduction 1

1.1 Motivation for the Study . . . 1

1.1.1 Radiation Protection of the Environment . . . 1

1.1.2 Retrospective Dosimetry . . . 2

1.2 Radiation Exposure in the Environment . . . 3

1.2.1 Global Fallout . . . 3

1.2.2 Nuclear Accidents . . . 4

1.2.3 Summary . . . 6

1.3 Retrospective Dosimetry using Shelled Species . . . 7

1.4 Objectives and Statement of Work . . . 8

2 Theoretical Background and Literature Review 11

2.1 Principles of Electron Paramagnetic Resonance . . . 12

2.2 Retrospective Dosimetry Techniques . . . 15

2.2.1 Physical Dosimetry . . . 15

2.2.2 Biological Dosimetry . . . 19

2.2.3 Summary . . . 20

2.3 Applications of EPR Dosimetry . . . 21

2.3.1 EPR Dosimetry with Alanine . . . 22
2.3.2 EPR Dosimetry on Shelled Species . . . 22
Crustacea . . . 23
Molluscs . . . 26
2.3.3 Environmental EPR Dosimetry . . . 28
2.3.4 Summary . . . 30

3 Experimental Work 32
3.1 Samples . . . 33
3.1.1 Studied Species . . . 33
3.1.2 Sample Preparation . . . 34
Crustacea . . . 34
Molluscs . . . 35
3.2 Irradiations and Dosimetry . . . 39
3.2.1 Cesium-137 Irradiations . . . 39
3.2.2 Dosimetry . . . 40
3.3 EPR Measurements . . . 41
3.3.1 Measurement Procedure . . . 42
3.3.2 Measurement Parameters . . . 43
3.3.3 Experimental Studies . . . 47
3.4 Alanine-EPR Dosimetry . . . 53
3.4.1 Samples and Irradiations . . . 53
3.4.2 EPR Measurements . . . 53
3.4.3 Dose Response . . . 56

4 Results and Discussion 62
4.1 Selection of Suitable Species . . . 62
4.1.1 American Lobster . . . 63
4.1.2 Freshwater Pond Snails . . . 64
4.1.3 Terrestrial Snails . . . 65
4.2 Effect of Chemical Etching on Snail Shells . . . 68
4.3 Terrestrial Snail Dose Response . . . 69
4.4 Effect of Manganese on the EPR Signal . . . 77

4.4.1 Crustacea 79
4.4.2 Molluscs 82
4.4.3 Summary 88
4.5 Applicability for Retrospective Dosimetry 90

5 Conclusions **93**
5.1 Overall Summary 93
5.2 Improvements of Experimental Methods and Recommendations . . 96
5.3 Future Work 98

Bibliography **100**

List of Figures

2.1 Zeeman splitting effect when materials with unpaired electrons are placed in a magnetic field and their energy levels split proportionally to the magnetic field. An absorption spectrum is acquired when the magnetic field matches the applied microwave frequency [23]. 13
2.2 An EPR spectrum displayed in the first derivative line shape with respect to the magnetic field. 13
2.3 Dose reconstruction based on the additive irradiation method. Additional dose is added to the sample and the EPR signal peak-to-peak height is measured after each iteration [21]. 15

3.1 Breakdown of a lobster for sample preparation. Pliers and dissection tools were used to obtain small pieces of shells. 35
3.2 Fragments of clean crustacean shells. 35
3.3 Cleaning of bivalvia shells. Remaining muscles attached to the shells were removed using dissection tools. 36
3.4 Samples of clean bivalvia shells. 36
3.5 Samples of clean gastropod shells. 37
3.6 Shells were crushed to grain sizes of 0.1 - 0.5 mm using a mortar and pestle and then filled into 0.6 mL micro-centrifuge tubes. 38
3.7 A 7 cm x 7 cm 3-D printed holder. Shells samples were clipped vertically and alanine dosimeters were clipped on the sides. 39
3.8 Irradiation setup for experiments. Sample holder was placed a distance of 34 cm from the center of the source. 40
3.9 Bruker EMX-Micro X-Band spectrometer. 41
3.10 Wilmad LabGlass quartz EPR tubes. 41

3.11 Power saturation curve plot for a terrestrial snail sample irradiated to 10 Gy. The sample was measured using microwave powers ranging from 0.3 mW to 10 mW. Increasing the microwave power increases the signal intensity until a point where the signal is no longer linear. 44
3.12 The effect of increasing the modulation amplitude on the peak-peak height of the radiation-induced peak for a terrestrial snail shell sample irradiated to 10 Gy. Measurements were recorded at a microwave power of 0.94 mW. 45
3.13 EPR spectra of terrestrial snail sample measured using a modulation amplitude of 0.3 G (top) and 3 G (bottom). At a higher modulation amplitude, the spectral resolution is improved; however, the signal beings to broaden. 46
3.14 A power saturation curve plot for an alanine dosimeter irradiated to 0.5 Gy. 54
3.15 EPR spectra of alanine powder dosimeters irradiated to doses ranging from 0.5 - 20 Gy. All three major resonance peaks (marked with 1, 2, and 3) show a dose-response relationship. Spectra are recorded using a microwave power of 9.36 mW. 56
3.16 Alanine powder calibration curve. The measurement point are averages of peak-to-peak heights of five samples in one dose group. . . 58

4.1 EPR spectra of American lobster shells before and after an irradiation dose of 10 Gy. The Mn^{2+} peaks are present and marked with an asterisk. No radiation-induced peak is detected for lobster shells at this dose. 64
4.2 EPR spectra of pond snail shells before and after an irradiation dose of 10 Gy. Characteristic Mn^{2+} peaks are present and marked with an asterisk. No radiation-induced peak is visible at this dose. 65
4.3 EPR spectra of terrestrial snail shells before and after an irradiation dose of 10 Gy. Characteristic Mn^{2+} peaks are present and marked with an asterisk. An additional peak is visible at this dose. 66

4.4 EPR spectra of terrestrial snail shells measured using a sweep width of 50 G. The unirradiated shells display only the native central peak. The irradiated shells display an additional peak characterized as the radiation-induced peak and is marked with an orange asterisk. This peak is visible at a magnetic field value of 3500 G. 67
4.5 EPR spectrum of an unirradiated terrestrial snail shell measured using a sweep width of 50 G. 70
4.6 EPR spectra of three terrestrial snail shells irradiated to doses of 2, 10, and 20 Gy. The black asterisk indicates native peaks. Peaks marked with a green asterisk are radiation-induced. 71
4.7 Terrestrial snail shell spectrum measured with the standard amplitude marked at a g-value of 1.98. The different peaks in terrestrial snail shell spectra are observed at g-values of 2.003, 2.0012, and 2.0016. 72
4.8 Dose-response curve for three terrestrial snail shell samples irradiated to doses of 2, 10, and 20 Gy. 75
4.9 EPR spectra of shrimp shells before and after an irradiation dose of 10 Gy. Marked with a black asterisk is a Mn^{2+} signal. A central peak is also displayed, marked with an orange asterisk. The signal marked with a blue asterisk is from the internal standard. 80
4.10 EPR spectra of American lobster shells before and after an irradiation dose of 10 Gy. Characteristic Mn^{2+} peaks are present and marked with an asterisk. 82
4.11 EPR spectra of oyster shells before and after an irradiation dose of 10 Gy. Characteristic Mn^{2+} peaks are present and marked with an asterisk. 83
4.12 EPR spectra of blue mussel shells irradiated to a dose of 10 Gy. The Mn^{2+} peaks are marked with black asterisks. A central peak is also displayed and marked with an orange asterisk. 84
4.13 EPR spectra of eliptio mussel shells before and after an irradiation dose of 10 Gy. The Mn^{2+} peaks are marked with an asterisk. 85

4.14 EPR spectra of pond snail shells before and after an irradiation dose of 10 Gy. Characteristic Mn^{2+} peaks are present and marked with an asterisk. 86
4.15 EPR spectra of terrestrial snail shells before and after an irradiation dose of 10 Gy. Characteristic Mn^{2+} peaks are present and marked with an asterisk. 87

List of Tables

2.1 A comparison of common physical and biological retrospective dosimetry techniques. Detection limits and time limitations for the common techniques are presented. Reproduced from [7] [42]. 21
2.2 Detection limits of freshwater and marine molluscs and one terrestrial gastropod. Reproduced from [32]. 31

3.1 A list of the shelled species used for this study. 33
3.2 EPR parameters for mollusc and crustacean samples. 47
3.3 Dosimetry measurements for the dose-response experiment of terrestrial snail shells. 50
3.4 EPR parameters used for alanine powder measurements. 55
3.5 Mean measurements of alanine dosimeters. Columns two and three represent the mean and standard deviations of fifteen measurements for one dose group. Columns four and five represent the means and standard deviations of average peak-to-peak measurements of each samples in a dose group. 59

4.1 g-values identified in terrestrial snail shells in this study and their corresponding radical species determined from literature. 71
4.2 Measurements of the density normalized peak-to-peak heights for three terrestrial snail shell samples. The peak-to-peak heights are the means of three measurements taken for one sample. 75
4.3 A summary of the various factors influencing EPR spectra in seven shelled species. 89

Chapter 1

Introduction

1.1 Motivation for the Study

The research work presented in this thesis has been motivated by the continuous interest in the protection of the environment from ionizing radiation. There has also been an emphasis on using terrestrial and aquatic species impacted by a radiological accident for retrospective dosimetry. The combination of these topics forms the basis of this research and will be presented in the following sections.

1.1.1 Radiation Protection of the Environment

Over the last few decades, protection of the environment from radiation exposure has attracted much interest. In the past, the International Commission on Radiological Protection (ICRP) has stated that the environment is protected if there have been suitable measures taken to protect humans from radiological risks [1]. It was acknowledged that this statement does not take different exposure scenarios into account where there can be a radiological risk primarily to the environment rather than to humans. This includes cases of unintentional releases, or in previous practices of disposing radioactive waste into the deep sea, where the aquatic environment would be exposed to high dose rates, which do not reflect the same for human exposures [2]. Therefore, with the growing awareness to protect the environment, in 2000 the ICRP created a Task Group to specifically target the

protection of the environment. This resulted in ICRP Publication 108, which derives content from the development of previous publications, stating that protection from ionizing radiation is necessary for non-human species and ecosystems [3].

Following the approach of radiation protection of humans by using the Reference Man, ICRP 108 set the concept of using a similar approach by introducing Reference Animals and Plants. The Reference Animals and Plants are described as generalized to the taxonomic level of family, which allows for numerous species to be considered within the 'set' [3]. As a result, the overall goals of an environmental protection system are needing to protect, conserve biological diversity, and maintain the health of natural habitats and ecosystems [3].

1.1.2 Retrospective Dosimetry

In the event of a radiological accident, dose assessments are required for affected organisms. For unplanned exposures, synthetic dosimeters are not available or in place at the time of the accident [4]. As a result, it becomes difficult to assess and quantify the absorbed dose to individuals and the surrounding environment. Therefore, retrospective dosimetry can be used to derive absorbed doses to exposed populations as more information regarding the incident becomes available. Fallout from nuclear weapons testing, reactor accidents, unintentional radiation releases, and regulatory monitoring are causes of potential exposure to radiation, and by extension, a reason to perform retrospective dosimetry [4].

In the acute phase of an accident, the primary concern is to assess the extent of the incident and estimate the immediate impact on exposed populations. This is achieved by performing conventional environmental monitoring sampling techniques used to provide initial protective measures to the public. These techniques are used to assess radiation in the environment by measuring radionuclide concentrations and activities in the contaminated areas by collecting air, soil, water, and vegetation samples [5]. The conventional sampling techniques are also implemented in the late (or recovery) stages of an accident to determine long-term environmental impacts.

Retrospective dosimetry techniques are further used in the late stages of an accident. Various materials available in the affected area can be used to determine precise local doses to the environment if they have been exposed during the time of the accident. To use these materials as natural dosimeters, it is important to ensure they are capable of retaining the accidental exposure history between the exposure and measurement period time [6]. Materials such as quartz, bricks, porcelain, cotton, and phone screens have all been extensively studied and used as natural or fortuitous dosimeters for retrospective dosimetry [7] [8]. Currently, there are many physical and biological retrospective dosimetry techniques available for various applications that provide dose assessments specific to the situation in question, and these will be discussed further in Chapter 2.

1.2 Radiation Exposure in the Environment

In the following sections, sources of radioactive releases in the environment will be presented. In particular, a brief overview of releases from global fallout and major nuclear accidents will be discussed, as these releases have resulted in the majority of radionuclides deposited in aquatic and terrestrial environments.

1.2.1 Global Fallout

Fallout from nuclear weapons testing between 1945 - 1980 resulted in the majority of anthropogenic radionuclides released into terrestrial and aquatic environments [9]. The fallout from these tests had a substantial regional deposition due to radionuclides dispersing from the stratosphere as fine particulates over many years [10]. Considering 70% of the Earth's surface is covered in water, the majority of radionuclides from nuclear weapons testing fallout now reside in aquatic environments. The total deposition of ^{137}Cs and ^{90}Sr from global fallout in the Earth's oceans is estimated to be 603 PBq and 376 PBq respectively [10] [11]. Though the fallout from testing was expected to be high, the global distribution was not predicted. Such was the case with rain-out, which caused higher radionuclide deposition in locations that were geographically far from the original testing sites [10].

1.2.2 Nuclear Accidents

Chernobyl

The Chernobyl accident in 1986 was the result of steam explosions in the core of the Unit 4 nuclear reactor at the Chernobyl Nuclear Power Plant, which released significant amounts of radioactive material into the atmosphere. The accident resulted in an increase in radionuclide concentrations in aquatic and terrestrial environments. The total activity of the release was estimated to be 1110 PBq and was widely distributed in various European countries and throughout the Northern Hemisphere [9] [12]. The most heavily affected body of water was the Baltic Sea, receiving 4.5 PBq of ^{137}Cs, and is becoming a leading source of ^{137}Cs entering the Atlantic Ocean [10].

Although significant quantities of more than 20 radionuclides were released by the accident, many were short-lived, and decayed within months after the accident [9]. Longer lived radionuclides, such as ^{137}Cs and ^{90}Sr, are still of concern in aquatic ecosystems today, since compounds incorporating these radionuclides tend to be soluble, allowing them to freely move around within bodies of water [9]. Though many radionuclides were diluted in larger seas, smaller rivers and lakes had considerably high concentrations of radionuclides present. For instance, in the Pripyat river, the ^{137}Cs concentration was estimated to be 20 000 Bq/kg in suspended sediments, and ^{90}Sr activity was found to be 4200 Bq/kg in sludge deposits and around 66 Bq/kg in bank and river deposits [13]. The water concentrations of ^{137}Cs and ^{90}Sr in the Pripyat river were estimated to be 22 kBq/m^3 and 1.9 kBq/m^3, respectively [13]. The concentrations of ^{137}Cs and ^{90}Sr in the river steadily decreased, and by 1995 were reported to be 0.1 kBq/m^3 and 0.3 kBq/m^3 [13]. Additionally, the ^{137}Cs concentrations in aquatic species were reported to be 15 kBq/kg in Prussian carp and 90 kBq/kg in pike [14].

Fukushima

The Fukushima nuclear accident in 2011 was the result of a 9.0 magnitude earthquake followed by a tsunami that disabled the emergency power supply and cooling systems of the reactors at the Fukushima-Daiichi nuclear station in Japan. The

venting of gases, coupled with hydrogen explosions and a fire in the spent fuel pond of Unit 4, resulted in radioactive contaminant releases into the atmosphere [15]. The accident had an estimated release of 7 - 20 PBq of ^{137}Cs into the atmosphere, which was approximately 11% of what was released from Chernobyl [10][16]. Contaminated water from the reactor buildings resulted in an additional 27 PBq of radionuclides being directly released into the sea [10] [15]. Radiologically significant radionuclides released into the environment were ^{137}Cs, ^{134}Cs, ^{131}I, and smaller quantities of strontium and plutonium isotopes [16].

The exposure pathway into the sea had little radiological impact on neighboring countries, as most discharged radionuclides were quickly diluted in the Pacific Ocean. However, radioactive materials attached to suspended sediments were deposited into riverbed sediments and plants, which caused higher activity concentrations near shore, in soil, and in sediment [16]. The concentrations of ^{137}Cs in bottom-dwelling and demersal biota were high and exceeded the regulatory limit of 100 Bq/kg [16]. Furthermore, the ^{137}Cs concentration in sediments was found to be the leading source of contamination in benthic invertebrates [16]. Though the concentrations of radiocesium gradually decreased in marine environments, shallow waters near the power plant were reported to have elevated amounts [16]. The shorter half-life ^{131}I was present in the environment until a few months after the accident. There is more concern about the longer half-life cesium, strontium, and plutonium isotopes that are persistent in terrestrial and aquatic ecosystems for a longer period of time.

Mayak Production Complex

There have been significant impacts on the Techa River ecosystem in Russia due to radioactive contamination releases from 1949 - 1957 from the Mayak Nuclear Materials Production Complex. Between 1949 - 1952, 100 PBq of radioactive materials were discharged into the river, with ^{90}Sr and ^{137}Cs amounting to approximately 10 PBq each [17]. In 1951, significant levels of ^{90}Sr and ^{137}Cs were reported in river water. It was estimated that 78 km from the site, concentrations of ^{90}Sr and ^{137}Cs in the water were 27 kBq/L and 7.5 kBq/L, respectively [18].

The Mayak Complex also stored large quantities of high-level radioactive waste in metal tanks that were kept in concrete vaults. In 1957, failure of a temperature controlled tank resulted in a thermal explosion that led to 740 PBq of radionuclides released into the environment [19]. The radioactive plume from the accident dispersed over the atmosphere and eventually settled on terrain and in water bodies, which led to high levels of contamination in an area of 20 000 km^2 [19].

1.2.3 Summary

Environmental exposure to radiation from weapons testing and nuclear accidents have resulted in elevated concentrations of anthropogenic radioactive material in both terrestrial and aquatic ecosystems. In managing nuclear accidents, the primary concern is having an effective emergency preparedness response and ensuring appropriate measures have been taken to protect the public. These protective measures include evacuation and sheltering procedures while also limiting the consumption of food and water in the immediate vicinity of an accident. In the months to years following an unplanned exposure, environmental studies can be conducted to determine the long-term effects of the exposure and the resulting impact on non-human biota.

Radioactive materials initially released into the atmosphere result in a radioactive plume that disperses in the direction of the wind, and eventually deposits on the ground and water. Exposure pathways can lead to radioactive materials being distributed throughout the environment, resulting in radionuclide deposition in multiple ecosystems. As such, retrospective dosimetry techniques can be implemented years after an accident to provide dose assessments, even where the exposure has subsided, to evaluate the impact on the environment.

1.3 Retrospective Dosimetry using Shelled Species

This work investigates the feasibility of using shelled species for retrospective dosimetry. Namely, the shelled species being considered are from the crustacean and mollusc families, as they are abundantly available in both the terrestrial and aquatic environments.

Previous studies of using solid crystalline materials as natural dosimeters suggest that materials composed of a similar structure could be used for this purpose. The shells of various terrestrial and aquatic species are primarily composed of calcium carbonate, and are similar to those materials. These similarities are specifically defined by crystallinity. Materials such as quartz, porcelain, and bricks are formed as defined crystalline structures. Similarly, crustacean and mollusc shells are formed through calcification, which includes the uptake of calcium and carbonate ions, and results in species forming their shells in an arranged structural order [20].

The interaction of ionizing radiation in calcified tissues, such as shells, results in the production of free electrons. Free electrons can be captured in the crystal structure of the calcium carbonate matrix and form radical centers that are stable for a long period of time [21]. Using an appropriate measurement technique, radiation-induced radical centers can be quantified in these materials, which allows for an attempt at dose reconstruction. For the basis of this work, the primary retrospective dosimetry technique being considered is Electron Paramagnetic Resonance (EPR) spectroscopy. The principles and applications of EPR for dosimetry will be discussed further in Chapter 2.

Shelled species are commonly used for assessment of metal pollution in the environment, as they are ubiquitous in their habitats and accumulate high concentrations of metals [22]. Various bivalve and gastropod species have previously been studied and used as indicators of metal pollution in their respective ecosystems [22]. Similarly, in the case of radiological accidents, crustacean and mollusc species will naturally be found in the resulting contaminated areas. Species living in the vicinity of these accidents could be exposed to high levels of radioactive contamination. They could then be collected and studied to extrapolate the absorbed dose in

their contaminated environments. Using these species allows for further measurements of absorbed doses to the animal itself. Typically through environmental sampling measurements and estimating bioaccumulation factors, absorbed doses to the animals are approximated. Using calcified tissues of shelled species found in the vicinity of nuclear accidents allows an opportunity to measure the dose to the animal directly. However, it is important to note that the dose measured in the animal flesh will be different than what is measured in calcified shells. For instance, ^{90}Sr will be accumulated more in calcified tissues, which will result in a higher estimation of the absorbed dose. Measuring the absorbed doses in calcified tissues of species in various ecosystems will be beneficial in providing a necessary response for long-term environmental protection and remediation.

1.4 Objectives and Statement of Work

The objective of this work is to investigate whether the calcified tissues of certain aquatic and terrestrial shelled species are applicable to use for retrospective dosimetry. For this work, EPR spectroscopy is used as the retrospective dosimetry technique for dose assessments. Therefore, the practical applications of EPR as a dosimetry technique are also assessed.

The experimental work for this thesis can be summarized into the following objectives:

- Identifying shelled species suitable to use for retrospective dosimetry.
- Developing sample preparation procedures and assessing measurement parameters for EPR analysis.
- Characterizing radiation-induced peaks in irradiated samples to establish a dose-response relationship for the studied species.
- Identifying limiting factors for low dose EPR dosimetry.

The shelled species collected for this work are from the crustacean and mollusc families. Specifically, the species being considered are the American lobsters (*Homarus americanus*), giant tiger prawns (*Penaeus monodon*), Eastern oysters (*Crassostrea*

virginica), blue mussels (*Mytilus edulis*), Eastern elliptio mussels (*Elliptio complanata*), freshwater pond snails (*Lymnaea stagnalis*), and terrestrial grove snails (*Cepaea nemoralis*).

The primary goal of this work is to identify shells of species that can be used for environmental dose assessments after a radiological accident. Through exposure pathways, anthropogenic radioactive materials released from accidents can lead to possible contamination in aquatic and terrestrial ecosystems. Therefore, it is critical to identify and sample the shelled species which will be significantly impacted by radiological accidents. Once samples have been collected, sample preparation methods for each species need to be developed. Sample preparation involves cleaning and grinding shells in a way that does not influence the EPR signals when performing spectral analysis. Next, irradiation experiments are conducted on prepared samples. An additional peak becomes present in an EPR spectrum as a result of shells being exposed to ionizing radiation. This peak is known as the radiation-induced peak. The irradiated samples are analyzed qualitatively to determine if radiation-induced peaks in an EPR spectrum can be detected at the investigated doses. If radiation-induced peaks are detected in the EPR spectrum, samples can be further used to determine detection limits of the species and consequently, their relevance to environmental dosimetry.

As these calcified shells are meant to be used for environmental dose assessments, a low dose range for shells needs to be resolved. As a result, preliminary experiments in establishing a dose-response of a species is conducted, where samples are irradiated to doses of 2, 10, and 20 Gy. A quantitative analysis can be performed by measuring the peak-to-peak height of the radiation-induced peak using a processing software. The height of the radiation-induced peak increases with increasing irradiation dose, and this relationship can be used to develop a dose-response curve for the studied species. The development of a dose-response curve is a method that is widely used in EPR spectroscopy [21] [23] and is therefore used as the primary method for dose assessments in this work. The EPR measurement parameters are also evaluated to ensure that optimal spectral resolution for quantitative analysis is achieved.

Finally, limiting factors for low dose retrospective dosimetry using EPR spectroscopy are considered. This includes assessing environmental factors of different shelled species that contribute to the EPR signals in a spectrum and would potentially limit the use of EPR for low dose studies. Experimental methods in quantifying various environmental factors are presented, and the applicability of low dose EPR dosimetry on shelled species is discussed.

Chapter 2

Theoretical Background and Literature Review

The following chapter is separated into three topics:

1. A theoretical background describing the principles of Electron Paramagnetic Resonance (EPR) spectroscopy. This information provides the fundamentals of EPR spectroscopy and the basis for why it is applicable to this work.
2. A review of standard physical and biological retrospective dosimetry techniques. A comparison of detection limits and applicability for long-term detection for these techniques is also discussed.
3. A literature review of the various EPR dosimetry applications. The applications discussed provide the means to understand sample selection, detection limits, environmental factors, and spectra analysis using EPR spectroscopy. The gaps from this review provide insight on unexplored research areas, one of which is presented in this work.

2.1 Principles of Electron Paramagnetic Resonance

Electron Paramagnetic Resonance spectroscopy is used to identify and analyze materials containing unpaired electrons. It is based on measuring the resonance absorption of microwave energy in paramagnetic materials, which occurs when there is a transition of the spin of an unpaired electron between energy levels in the presence of a strong magnetic field [21].

Unpaired electrons in paramagnetic materials occupy one of two spin states ($m_s = +\frac{1}{2}, -\frac{1}{2}$) in the absence of a magnetic field [21]. When they are placed in a strong magnetic field, their energy levels split proportionally to the magnetic field (known as the Zeeman effect, shown in Figure 2.1) with a greater number of electrons found in the lower energy state [21] [23]. Hyperfine splitting also occurs in the case of interaction with the nuclear field of the atom. An electron in the lower energy level can transition to the higher energy level when it absorbs a quantum of electromagnetic radiation energy ($h\nu$). For EPR spectroscopy, this energy is in the form of microwave energy. The direction of the electron's spin will change under the following resonance condition:

$$h\nu = g\beta B \tag{2.1}$$

where h is Planck's constant, ν is the resonance microwave energy, g is a spectroscopic splitting factor, β is the Bohr magneton, and B is the magnetic field induction [23].

The absorption spectrum in EPR spectroscopy is acquired by varying the magnetic field and keeping a fixed frequency of microwave radiation, which causes the two energy levels to split proportionally to the magnetic field. A resonance condition occurs when the microwave radiation is equal to the difference between the two energy levels. EPR spectra are displayed as the first derivative of the absorption with respect to the magnetic field. The spectra can be evaluated based on their shape, spectrum line-width, intensity, and splitting factor (g-value) [21]. The g-value is an important parameter since unpaired electrons in different crystal structures have

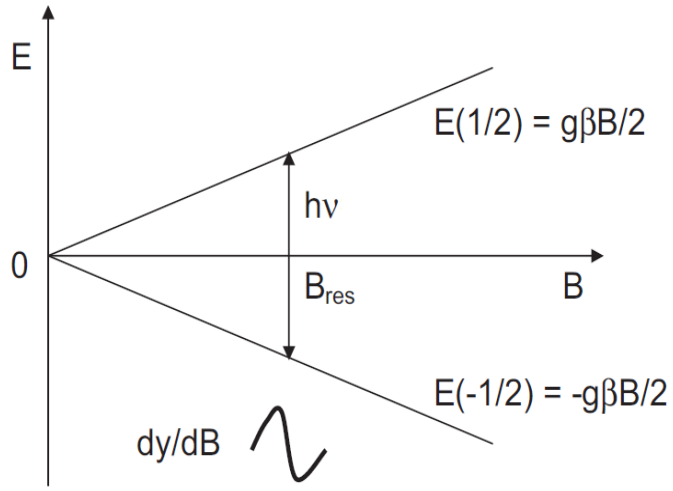

FIGURE 2.1: Zeeman splitting effect when materials with unpaired electrons are placed in a magnetic field and their energy levels split proportionally to the magnetic field. An absorption spectrum is acquired when the magnetic field matches the applied microwave frequency [23].

different g-values [24]. Simply put, the g-value is a characteristic value of the material in question and can be used to classify different radicals in the spectrum. An example of an EPR spectrum is presented in Figure 2.2.

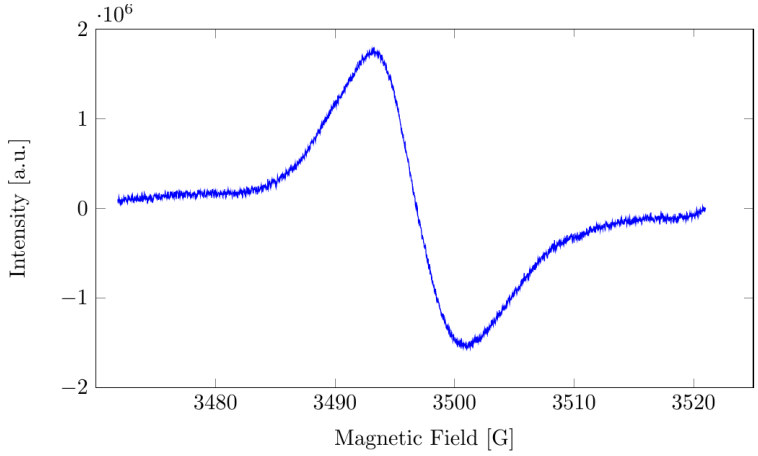

FIGURE 2.2: An EPR spectrum displayed in the first derivative line shape with respect to the magnetic field.

In calcified tissues, EPR can be used on measurements of the radiation-induced radicals in hydroxyapatite [$Ca_{10}(PO_4)_6(OH)_2$] present in teeth and bones, and calcium carbonate [$CaCO_3$] present in shelled species. Carbonate ions are incorporated into the crystalline lattice of these materials. When ionizing radiation interacts with these ions, free electrons are formed. The free electrons can be captured in the crystal matrix and form radical centers (CO_2^- and CO_3^-), which can be used to measure the accumulated radiation exposure [21]. As a result, materials that contain unpaired electrons due to absorption of ionizing radiation can be measured, since the intensity of the electron transitions is proportional to the number of radical centers formed in the target material [21]. The proportionality of the intensity to the number of radical centers formed is subsequently proportional to the absorbed dose received by that material [21]. This proportionality allows for calcified tissues to be used as natural or fortuitous dosimeters.

Dose assessments for various samples are achieved through measurements of the peak-to-peak height of the radiation-induced peak obtained from the EPR spectrum. Dose reconstruction can be achieved through two standard methods: an additive irradiation method and a dose-response calibration curve [21] [23]. The additive method is based on re-irradiating the sample in addition to its original exposure [21]. The dose reconstructed is specific to the sample being tested, since this method measures the dose for one individual sample at a time. Figure 2.3 shows this method based on adding known dose in a controlled environment and measuring the subsequent EPR signal intensity after each iteration. By back-extrapolating the dose-response curve, the initial or "accidental" dose can be determined.

The calibration curve method creates a more general dose-response curve by using a large number of samples that averages the sample-to-sample variances [21]. A constructed calibration curve allows for samples of unknown dose to be measured. This method works by measuring the peak-to-peak heights of radiation-induced peaks and converting them to the dose using the developed calibration curve. The calibration curve method is less time consuming than the additive method, and ultimately non-destructive since additional dose is not added to the sample.

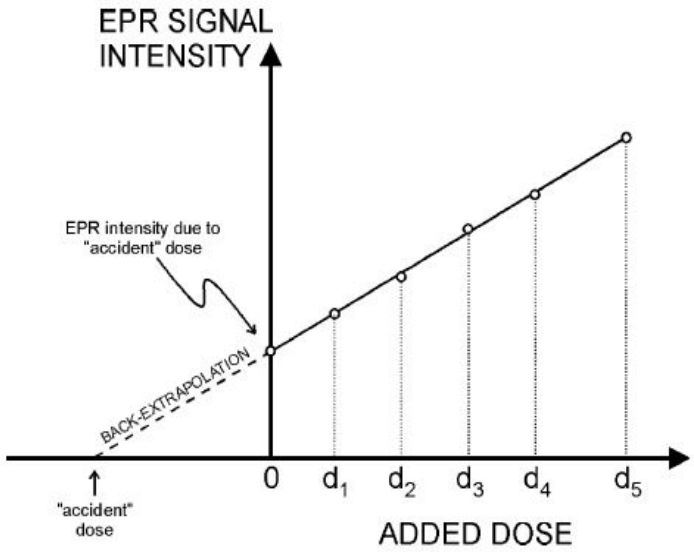

FIGURE 2.3: Dose reconstruction based on the additive irradiation method. Additional dose is added to the sample and the EPR signal peak-to-peak height is measured after each iteration [21].

2.2 Retrospective Dosimetry Techniques

The purpose of retrospective dosimetry is the determination of absorbed dose to human and non-human biota in the event of unplanned exposures. Retrospective dosimetry techniques are categorized according to measurements of absorbed doses to individuals or providing general radiation doses in the environment [10]. The purpose of this section is to provide a brief overview of the commonly used physical and biological dosimetry techniques. A comparison of their detection limits and applicability for long-term detection is also discussed.

2.2.1 Physical Dosimetry

Electron Paramagnetic Resonance Dosimetry

Electron paramagnetic resonance is a physical, non-destructive retrospective dosimetry technique used in a wide range of applications. As discussed in Section 2.1,

when ionizing radiation interacts with tissues containing carbonates, radical centers are formed. In carbonates, these radical centers are long-lived and stable, which is beneficial for EPR dosimetry as it can be used for dose assessments for long periods of time. Materials can function as dosimeters for absorbed radiation, if the EPR signal intensities of radiation-induced radical centers in those materials have a linear relationship with dose [25].

Crystalline materials such as carbohydrates, amino acids, and tooth enamel can be used for retrospective dosimetry, as they produce strong and stable radiation-induced radicals after exposure to ionizing radiation [10]. Retrospective dosimetry using tooth enamel is the most common application of EPR dosimetry, as it uses the stable free radical of the hydroxyapatite compound [21] [26]. The hydroxyapatite compound comprises up to 95-97% in tooth enamel, 70-75% in dentin, and 60-70% in bones [21]. The signal intensity of the formed radical centers in spectra are shown to not decay at room or body temperatures [26]. EPR dosimetry using tooth enamel has previously been conducted for studies of atomic-bomb survivors, Chernobyl workers, and Techa river populations [27] [28] [26]. Extensive research and future studies have been conducted and proposed on using EPR dosimetry on calcified tissues for large-scale radiation incidents [29].

Plastic materials such as credit cards, phone screens, and buttons have also been used for dose reconstruction after a radiological accident. For most plastic samples, the radiation-induced peaks at room temperature decay up to 50% within 20-30 hours after irradiation and are indistinguishable from the background signals after one week [30]. EPR dosimetry has also been widely used for the detection of irradiated food and dating of fossils. These applications use higher doses and will be further discussed in Section 2.3. Sample preparation protocols for various materials are well established and straightforward to implement. Measurement readouts largely depend on the material being studied, and range between a few minutes to hours [7]. Repeated measurements of the same sample are also possible, as the readout is non-destructive when the sample exits the resonance condition. When samples are removed from the external magnetic field, the original number of electrons with magnetic moments in the two energy levels are restored, allowing this

technique to be used repeatedly for dose assessments over many years. Detection limits for this technique largely depend on the material being studied. Doses as low as 0.1 Gy have been measured for tooth enamel [31] [7] and 0.2 Gy for marine molluscs [32].

Though this technique is widely used, there are certain limitations that must be considered. First, when using this technique on tooth enamel, the method is highly invasive as it requires multiple sample extractions from individuals. It also determines cumulative lifetime dose, which includes dose components from natural, background, medical, accidental, and occupational sources [21] [33]. As a result, secondary methods for lifetime dose-estimations are required from these exposures to measure only the accidental dose. Interfering signals such as UV or from other paramagnetic species in the sample can be present in spectra, which will potentially mask radiation-induced peaks at low doses. Lastly, the EPR spectra can be influenced by various sample preparation methods such as chemical treatment, annealing of samples, and grinding [34]. To ensure optimal signal resolution is obtained in all spectra, sample preparation protocols should be followed thoroughly. Improvements for lowering the limit of detection for this technique are based on well-established sample preparation protocols as well as on improving spectral resolution and reproducibility of results [35].

Luminescence Dosimetry

Luminescence dosimetry is another physical technique used for retrospective dosimetry and geological dating. Optically stimulated luminescence (OSL) and thermoluminescence dosimetry (TLD) work based on using light and heat, respectively, to stimulate a luminescence signal from materials that have been exposed to ionizing radiation [36]. When crystalline materials are exposed to ionizing radiation, electron-hole pairs are formed, and some electrons become trapped in the lattice sites of those materials. When light or heat is applied to the material, electrons transition from their trapped excited state back to the ground state and recombine with holes. This results in an energy emission that is quantified in proportion to

dose. Crystalline materials are capable of retaining these electrons in the traps for many years, allowing this technique to be used for retrospective dosimetry.

Materials used for these measurements include quartz extracted from bricks, tiles, and porcelain collected from contaminated areas [37]. The sample preparation procedures are well-established and can take between 1 hour to 1 day to process depending on the material being tested [7]. Luminescence dosimetry has been applied to materials collected from contaminated environmental areas of the atomic bomb detonation, nuclear fallout testing sites, and settlements of the Chernobyl and Techa River regions [38].

The detection limits of luminescence dosimetry greatly depend on the tested materials. The Lowest Limit of Detection (LLD) of bricks that are a few decades old have been reported in the order of 20-25 mGy [7]. Materials such as quartz, mortar, and concrete show detection limits higher than 100 mGy [7]. Personal materials such as phones, electronic cards carried by individuals, and various other materials found in urban environments can also be used as fortuitous dosimeters. The electronic components of mobile phones are promising to use for luminescence dosimetry, as studies have shown inductors removed from mobile phones have luminescence properties, and a linear dose-response over a dose range of $0.1 - 5$ Gy [39]. Studies performed on table salt reported that salt could also be used effectively as a natural dosimeter, as it provides high thermoluminescence (TL) peaks with a LLD of 30 mGy [40]. Additionally, the detection limits for tooth enamel range from 1-5 Gy [7]. Similarly to EPR dosimetry, the response of ionizing radiation in different materials and time stability is dependent on the materials being tested.

Limitations of these technique arise mainly from signal fading of most materials with increasing storage time. Personal materials are reported to show partial signal fading [7], allowing these materials to only be useful in the months after an accident for accurate dose estimates. Similarly to EPR dosimetry, materials used in luminescence dosimetry determine cumulative dose, which includes doses from natural radiation sources. Therefore, the age of the material is of importance to determine an accident dose. Repeated measurements of samples are also of concern for TLD, since the dosimetric signal for TL is read out destructively. Applying heat to the

material results in electrons transitioning back from their trapped excited states to the ground state. As a result, repeated measurements of the sample cannot be achieved as the electrons are released from their traps and recombine with holes.

2.2.2 Biological Dosimetry

Biodosimetry techniques are used for determining absorbed doses to individuals after exposure to ionizing radiation. As ionizing radiation induces various cytogenetic damage, biodosimetry techniques can be implemented to estimate the dose received.

Dicentric Chromosome Assay

Dicentric chromosome assay (DCA) is a biodosimetry technique used for dose assessments after exposure to ionizing radiation. Exposure to radiation induces various types of chromosome aberrations in an individual's peripheral blood lymphocytes (PBLs) [41]. A dicentric aberration is one example that is formed as a result of breaks in each of the two separate pre-replication chromosomes. This results in the formation of two centromeres in one chromosome (dicentric) and an accentric fragment. As this aberration is commonly induced as a result of exposure to ionizing radiation, this biodosimetry technique can be used to determine absorbed doses to individuals. Due to the low background level of dicentric chromosomes in general, the sensitivity of the assay is high and can detect whole-body doses up to 0.1 Gy [41] [7]. The technique can be used for dose assessments a few days after exposure, or in the case of a triage, a smaller number of cells can be analyzed for a rapid assessment [7].

A limitation of this technique arises from the formed dicentrics being unstable and as a result, the aberrations are eliminated with time (which depends on the dose received). Therefore, this method is only useful within a few days to months of irradiation.

Fluorescence *in situ* Hybridization

Fluorescence *in situ* Hybridization (FISH) is another common biodosimetry technique used to assess chromosome damage to individuals. This technique is based on fluorescent dyes that are attached to a specific region of the genome, which can help identify chromosomal damage. This biodosimetry technique is based on scoring stable chromosome damage, such as translocations and insertions, that can be detected with FISH chromosomes. Translocation frequencies are persistent over many years in circulating lymphocytes, allowing this technique to be used for decades after exposure [7]. This technique has been performed for whole-body exposures for atomic-bomb survivors, Chernobyl workers, and the Goiania and Techa river populations [42]. As chromosome damage can be induced through various situations, such as exposure to ionizing radiation and UV, this retrospective dosimetry technique is useful in determining doses received to individuals. Furthermore, this technique has been shown to be beneficial in providing an understanding of risks associated with long-term exposure to ionizing radiation in individuals [42].

The limitations of this technique arise from pre-existing aberrations caused by exposures other than ionizing radiation, such as smoking or exposure to UV. The detection limit for this technique is approximately 0.5 Gy cumulative lifetime dose for an individual basis, and can be down to 0.2 Gy for non-smoking individuals [7].

2.2.3 Summary

Retrospective dosimetry techniques can be implemented for a wide range of applications. These techniques determine absorbed doses to human and non-human biota in the cases of unplanned exposures. As conventional dosimeters are not available at the time of an accident, retrospective dosimetry techniques can be used to derive absorbed doses to exposed populations and determine doses to the environment. Table 2.1 compares the above techniques in terms of important factors to consider for retrospective dosimetry for exposure to ionizing radiation. These factors include detection limits and the time frame in which dose signals are stable. These two considerations decide which technique is best suited for the situation in need of assessment. Physical techniques such as EPR and luminescence dosimetry would

be better suited for long term retrospective dosimetry, where the primary concern is not a reflection of a biological response. Physical retrospective dosimetry techniques would additionally be better suited in determining doses to the environment using natural materials. In contrast, biodosimetry techniques are more suited for changes in biological parameters, which can be used for both long and short term applications.

TABLE 2.1: A comparison of common physical and biological retrospective dosimetry techniques. Detection limits and time limitations for the common techniques are presented. Reproduced from [7] [42].

Technique	Detection limits (Gy)	Time limitations
EPR	0.1 for tooth enamel	years
	0.2 for marine mollusc	years
	> 2 for personal items	days
Luminescence	0.1 for quartz	years
	1-5 for tooth enamel	
	> 0.01 for personal items	months
DCA	0.1 for whole body	months
FISH	0.1-4	years

2.3 Applications of EPR Dosimetry

In Section 2.2, an overview of different retrospective dosimetry techniques is provided. However, as stated earlier, there are various dosimetry applications associated with EPR spectroscopy, and the following section will provide a review of other applications.

Most measurements for EPR dosimetry are performed using an X-band spectrometer with a microwave frequency of 9.5 GHz and a magnetic field of 0.33 T [43]. High frequency bands, such as Q-bands, produce spectra with higher resolution that allow for more detailed information to be extracted from signals [44]. However, an X-band spectrometer is applicable to use for a majority of applications.

2.3.1 EPR Dosimetry with Alanine

Alanine-EPR dosimetry is an increasingly useful application due to its wide range of detection limits. Alanine-EPR measurements are most commonly used for reference dosimetry, quality assurance dosimetry, and calibration purposes by radiation laboratories [45]. The most common forms of alanine-EPR dosimeters include rods, powder, and pellets, which are based on the organic microcrystalline L-α amino acid [CH_3-CHNH_2-COOH] [46] [47]. The process of irradiating alanine forms a stable radical of $CH_3-CH-COOH$ [46] that can be read out non-destructively and repeatedly, similarly to other materials using EPR. As a result, EPR measurements can be performed over many years, since the formed radical has a long-term stability.

The EPR spectra of irradiated alanine display three distinct peaks that all increase with irradiation dose. The peak-to-peak heights of the center resonance peak are commonly used for dose assessments. However, peak-to-peak heights of all three major peaks can also be summed to evaluate the dosimetric signal [45]. Irradiated alanine has been shown to have a linear dose-response from 0.01 Gy to 10 kGy [45], and has an energy-independent response for photons above 100 keV [47]. Therefore, alanine is a suitable reference dosimeter due to its dynamic range, long-term stability, and linear dose-response.

2.3.2 EPR Dosimetry on Shelled Species

Detection of irradiated foodstuffs and dating natural carbonates for archeological purposes are common applications of EPR. Though the doses delivered for both applications are high (ranges from 0.1 to 10 kGy [48]), the literature regarding these methods is still of importance. This review provides insight into EPR dosimetry applications of non-human biota and provides information on EPR spectra of unirradiated and irradiated shelled species.

Radical centers induced by ionizing radiation in foodstuffs are generally short-lived, making them difficult to detect. In shelled species that contain $CaCO_3$, EPR measurements of radiation-induced radicals of CO_2^-, CO_3^{3-}, and SO_3^- are longer

lived and can therefore be used for detection purposes [48] [49] [50]. Irradiated crustacean and mollusc shells are most commonly used for detection using EPR and will be discussed further. Although both families contain $CaCO_3$ as the main constituent of their shells, either in the crystalline structure of aragonite, calcite, or a combination of both, various other components of the shell matrix also contribute to their EPR signals, thus making EPR detection species dependent [49].

Sample preparation methods used to perform EPR measurement for both crustacean and mollusc species consist of similar protocols. The flesh or muscle is removed, and shells are thoroughly washed [51] [52] [53]. Clean shell samples can either be air or freeze-dried before irradiation. Samples can be irradiated either by using a sliver of the shell or a powdered form. Powdered samples allow for a more homogeneous sample and allow for a greater number of samples to be irradiated at once [50]. Methods used to obtain samples such as excessive grinding, cutting, or heating results in mechanically-induced signals in addition to native signals already present [30] [34]. Chemical etching of samples using a low concentration of acetic acid has been shown to remove surface defects produced from grinding during sample preparation procedures [54] [55].

Crustacea

The physical structure of a crustacean shell is made of a cuticle containing four layers: epicuticle, exocuticle, endocuticle, and a membranous layer [56]. The epicuticle is a thin layer surrounding the animal, while the exocuticle and endocuticle layers consist of mineralized chitin-proteins and calcium carbonate [57] [56]. Species that contain a harder exoskeleton, such as crabs and lobsters, contain higher amounts of $CaCO_3$. Species with more flexible exoskeletons, such as shrimp, contain more chitin-proteins.

The unirradiated shells of most crustacea display a variety of peaks in the EPR spectra. These peaks are a result of organic components in the shell structures and impurities, such as characteristic Mn^{2+} paramagnetic ions [49]. The majority of the spectra are dominated by six resonance peaks from Mn^{2+} ions. The intensity of Mn^{2+} signals is largely based on the crystalline structure of shells and does not

increase with irradiation [48]. The spectra for most irradiated shells contain an additional peak at the center of the Mn^{2+} signals [58] [59]. This peak is known as the radiation-induced peak and is shown to be dose-dependent. As a result, measurements of the radiation-induced peak can provide an estimate of the absorbed dose to the species in question.

Most members of the crustacean family undergo a molting process as they grow. This requires their whole exoskeleton to be replaced by a new cuticle, which grows underneath the existing one. The change in the shell structure results in differences in the amounts of calcium deposition in the shell [60], which can then have an impact on the resulting EPR signals. Therefore, when sampling crustacean species, it would be beneficial to have some knowledge of the animal's age and stage of molt [60]. The geographical region from which crustacean species are sampled also affects the shape of the EPR signal [61]. The main differences between the EPR signals are due to the Mn^{2+} signals, where some species collected from one region display weaker Mn^{2+} signals compared to others [61]. As radiation detection in crustacea is mainly species dependent, the EPR detection of three crustacean species commonly used in the detection of irradiated foodstuffs will be discussed further.

Norway Lobster

The Norway lobster (*Nephrops norvegicus)* undergoes a calcification process by depositing calcium carbonate as calcite, vaterite, and hydroxyapatite into the organic matrix of the cuticle [61]. Similarly to unirradiated shells, the irradiated shells of the Norway lobster display six characteristic Mn^{2+} signals. At the center of the six resonances is a radiation-induced peak with a g-value of 2.0009 [61] [62] [63]. The additional peak at this g-value allows for qualitative assessments of irradiated lobsters, which is important since many countries have strict laws on the irradiation of foodstuffs. The peak-to-peak height of the radiation-induced peak can further be used to perform a quantitative analysis on the dose estimations for this species. There is a significant increase in the peak-to-peak height of the radiation-induced peak in irradiated Norway lobster shells with increasing dose. The additive dose method, described in Section 2.1, is a reliable method for determining the initial dose applied to the Norway lobster [61]. Concerning the stability of the formed

radical centers, samples stored at chilled temperatures are found to have stronger signal intensities than those kept at warmer temperatures due to the decay of radicals being minimal in a frozen state [61].

Shrimp

The exoskeleton of shrimp is different from those of other hard-shelled crustacea. Its shell is more flexible and less rigid, suggesting the species contains more chitin in the exoskeleton. In the identification of pink shrimps (*Parapenaeus longirostris*), the EPR spectra of unirradiated shells display strong sextet Mn^{2+} signals, which are reported to have no effect on shape or intensity when compared to irradiated shells [64]. The EPR spectra of shells irradiated to doses between 1-10 kGy show CO_2^- radical center peaks at g-values of 2.0013 and 1.9959 [64]. These peaks increase with dose and are easily distinguishable from the spectra of unirradiated shells. Dose assessments of pink shrimp have also been conducted by Aydaş et al. in which the estimation of the initial dose in shrimp shells was quantified by applying the additive dose method [64].

Other species of shrimp, such as the *Pandalus montagui*, have shown very little presence of Mn^{2+} in their spectra. The spectra of irradiated shells for this species display strong radiation-induced peaks at g-values of 2.0010 and 1.9970 [63]. The difference between the presence of Mn^{2+} in shrimp shells is attributed to the different crystal structure of the species, as well as the geographical location from which the species was sampled. Furthermore, there has been a linear response to radiation dose measured in both Mediterranean crevette and pink shrimp shells from dose ranges between 1 - 5 kGy [61]. However, the signal intensity between these species of shrimp presents contrasting results. It is reported that shrimp shells that contain a more rigid structure have shown a more intense signal compared to shrimps that contain a flexible and thin exoskeleton [61] [65]. As a result, the detection of irradiated shrimp vastly differs depending on the species. Some pink shrimp species display radiation-induced peaks derived from the chitin component of their exoskeleton [53] [61], while others display peaks from the CO_2^- radical [64]. The difference in the origin of radiation-induced peaks is possibly due to the shell matrix of the species, which is dependent on the habitat. These results suggest

that the detection of radiation-induced peaks in shrimp shells is possible only if the species and its geographical location are known.

Crab

A study conducted on crab shells by Maghraby [66] showed that unirradiated crab shells displayed characteristic Mn^{2+} signals, which have been present in previously discussed crustacean species as well. The spectra of irradiated crab shells show a complicated signal with various radicals present. However, the most prominent signal can be attributed to the CO_2^- radical, with an average g-value of 2.0005 [66]. The irradiated crab shells have shown a linear response associated with radiation dose, ranging from 1 - 5 kGy, to signal intensity. However, the different components of the exoskeleton display varying EPR signal intensities. The crab's walking legs (dactyl) have the strongest EPR-intensity-dose correlation, whereas the swimming legs display the weakest [66]. The differences between intensities with regards to the different exoskeleton components can be attributed to the degree of crystallinity in each component. As is the case for crabs, the walking legs are harder and more rigid than the back swimming legs. The difference in signal intensities suggest that when performing EPR dosimetry with larger crustacean species, caution must be given to which part of the cuticle is used.

Molluscs

Mollusc shells are primarily composed of $CaCO_3$, either in the form of aragonite, calcite, or a combination of both [20], in addition to an organic component known as conchiolin [50] [67]. The separate layers of the mollusc shell are the perisostracum (a thin uncalcified layer), the prismatic (a thick calcareous layer), and the hypostracum (the innermost layer that contains stacks of aragonite and calcite) [20]. The shape of EPR spectra from the different layers have not been shown to differ amongst one another [48] [20]; however, there is a difference depending on the crystal form of $CaCO_3$. Shells that contain calcite as their main crystal also contain large amounts of Mn^{2+}, which can obscure radiation-induced peaks at low doses [32].

As previously mentioned, the shells of mollusc species can be composed of one or a combination of the two common polymorphs of calcium carbonate: calcite and aragonite. Aragonite is known to be the major crystal form of most freshwater and terrestrial molluscs [68], with smaller amounts of calcite present in some species. The shells of marine molluscs are mainly composed of calcite or aragonite and smaller amounts of $Ca_3(PO_4)_2$, $Mg(CO_3)$, $Ca(SO_4)$, and SiO_2 [69]. The aragonite structure has a higher density and hardness than calcite [69] [68]. As a result, it is important to note that structural differences in mollusc shells can be a major limitation in EPR dosimetry since the crystallinity in the shell mineral influences the EPR signal intensity and shape [25] [70].

EPR detection for various mollusc species has been studied, and similarly to crustacea, is also species dependent. The EPR spectra of mussel [53] [69] [71] and oyster shells [51] [71] [72] have displayed high intensity Mn^{2+} signals, while the shells of some clam and scallop species have displayed no detectable Mn^{2+} signals [71] [69]. The intensities of Mn^{2+} signals in the EPR spectra can be attributed to the crystal form of $CaCO_3$, the age of the sample, as well as the sampling location. Live clams have displayed no detectable Mn^{2+} signals [71] while fossilized clams have [73]. The presence of strong Mn^{2+} signals in EPR spectra cause a limitation in detection for some species. For instance, radiation-induced peaks for oyster shells are difficult to resolve for samples irradiated with doses lower than 10 Gy due to the high intensity Mn^{2+} signals [74]. Additionally, the color of mollusc shells contribute to EPR spectra, where darker shells contain more paramagnetic ions (Mn^{2+}) compared to uncolored shells, and as a result produce strong Mn^{2+} signal intensities [25] [75].

Since the shell of a mollusc is unique to its species, it is important to note the chemical composition of the shell and assign the appropriate chemical structure to the EPR signals [50]. Radical centers induced by ionizing radiation in the calcium carbonate matrix of mollusc shells can be attributed to CO_2^-, CO_3^-, CO_3^{3-}, SO_2^-, and SO_3^- with g-values in the range of 2.0010-2.0062 [67]. In most cases, carbonates, phosphate impurities, and organic matter contribute to the EPR signals [50]. Detection limits for mollusc samples also vary depending on the species and the sampling location. Freshwater molluscs have dose detection levels reported

at 2 Gy for zebra mussels and as low as 0.2 Gy for marine clams [32].

In addition to the detection of irradiated foodstuffs, EPR dosimetry using fossilized mollusc shells has also been used for archaeological purposes. Common samples for this application include the shells of the gastropod species. This species is viable for EPR dosimetry due to its shell, because although the live animal has a relatively short life-span, its shell remains intact in the surrounding environment. As a result, the gastropod species can be used for dating or dose reconstruction purposes. Similarly to other mollusc shells, the shells of gastropods contain $CaCO_3$ as their main constituent, which can be in the form of aragonite, calcite, or a combination of the two [55]. The spectra of unirradiated gastropod shells display strong Mn^{2+} signals similar to those observed in other carbonate samples. The intensity of these signals has been shown to not increase with absorbed dose [67]. Additional peaks are present between the third and fourth peaks of Mn^{2+} signals of the irradiated shells and can be attributed to radicals of CO_2^-, SO_2^-, and CO_3^{3-} with g-values of 2.0016, 2.0057, and 2.0012 respectively [68] [76]. The signals of the CO_2^- and CO_3^{3-} radicals are more commonly used for detection due to the long stability of the trapped electron and linear response to increasing dose [55] [68] [76].

2.3.3 Environmental EPR Dosimetry

Although the most common applications of EPR dosimetry on shelled species are the detection of irradiated foodstuffs and dating, species that contain calcified tissue in either their bones or shells can also be used for environmental dosimetry. EPR for environmental dosimetry has been conducted, with most studies performed in heavily contaminated environmental areas from unintentional releases or major accidents.

The majority of EPR environmental dosimetry has been conducted in the Techa River ecosystem. Dose reconstruction protocols have been developed for aquatic species living in contaminated habitats from the liquid radioactive waste released from the Mayak PA. In particular, a study conducted by Ivanov et al. [77] utilized otoliths of three different fish species for dose reconstruction using EPR. Samples

of perch, roach, and pike fish were caught from storage reservoirs of liquid radioactive waste, and their otoliths were removed and prepared for measurements. The otolith contains the largest amount of calcified tissue in a fish and is composed of $CaCO_3$. EPR measurements can then be performed similarly to methods described for crustacean and mollusc shells. For dose reconstruction, an additive irradiation method was applied to each species in which the radiation-induced peak increased linearly with radiation dose. An important outcome to note from this study was the EPR dose-response of each species. The pikes' otoliths were observed to have a higher radiation sensitivity than both the roach and perch, which agrees with earlier findings of EPR dosimetry being largely species dependent.

The use of mollusc shells has been a reliable method in the detection of foodstuff irradiation; however, as discussed in Section 2.3.2, these doses are generally high and easier to measure. Detection limits for eight freshwater and seventeen marine molluscs have been reported in a study conducted by Stachowicz et al. to establish their suitability for environmental radiation detection. Table 2.2 (reproduced from [32]) presents the detection limit findings from the study. In this study, samples native to freshwater and marine habitats were collected, prepared, and irradiated to doses of 10 Gy initially. If a radiation-induced peak was visible, samples were irradiated to lower doses to determine detection limits. Out of the eight freshwater mollusc samples (and one terrestrial gastropod), four displayed a radiation-induced peak, with the lowest detection limit reported at 2 Gy for *Dreissena polymorpha* (zebra mussels) and *Capaea homoralis* (terrestrial snail) [32]. Marine molluscs were observed to have a greater sensitivity to radiation, and the lowest detection limit for a marine mollusc was at 0.2 Gy [32]. The difference in radiation sensitivity can be based on the crystallinity of each shell, as well as its sampling location. This preliminary investigation into the detection limits of molluscs suggests a methodical protocol for choosing samples for environmental dosimetry is needed.

2.3.4 Summary

Retrospective dosimetry has been shown to be useful in assessing radiation dose to individuals and the environment in the case of emergencies, accidents, and regulatory monitoring. EPR dosimetry, in particular, is a promising physical method as it is a non-destructive technique with straightforward sample preparation methods and relatively fast measurement readouts. The majority of EPR spectroscopy applications in dosimetry are centered around accidental dosimetry using tooth enamel or identification and detection methods for food irradiations. EPR for environmental dosimetry has been shown to be effective for areas of high concentrations of contamination using the calcified tissues of various species. The applications of using EPR for accidental dosimetry and detection of irradiated foodstuffs are useful resources to enhance the knowledge for low dose retrospective dosimetry on shelled species. There are limiting factors of this technique, but further investigations into low dose retrospective dosimetry using EPR is a viable method for radiation detection. Since Mn^{2+} signals introduce a potential limiting factor for low dose studies, the environmental factors which influence the presence of these signals in an EPR spectrum must also be assessed. Low limits of detection are of paramount importance for environmental retrospective dosimetry, along with extensive research in determining suitable species for dosimetric studies.

TABLE 2.2: Detection limits of freshwater and marine molluscs and one terrestrial gastropod. Reproduced from [32].

Species	Dose detection limit [Gy]
Fresh Water Molluscs	
Planobarium corneus	10
Viviparus contectus	3.0
Dreissena polymorpha	2.0
Anodonta complanata Rossm	No EPR Signal
Anodonta anatina	No EPR Signal
Anodonta callensis	No EPR Signal
Unio pictorum	No EPR Signal
Unio tumidus Retz	No EPR Signal
Capaea homoralis	2.0
Marine Molluscs	
Arcidae sp	0.2
Tonna galea	0.3
Venus sp	0.3
Corithium sp	0.3
Cardium sp	0.5
Meleagrina vulgaris	0.5
Lambis lambis	0.5
Tridacna squamosa	1.0
Lambis chiragra	2.0
Strombus sinuatus	2.0
Coralliophila sp	2.0
Pecten sp	3.0
Fusinus colus	3.0
Turitella terebra	5.0
White coral	0.3
Red starfish	2.0
Balanus	4.0

Chapter 3

Experimental Work

This chapter will discuss the experimental methods completed for this work. Some methods used are primarily based on the literature discussed in Chapter 2, and others have been developed specifically for this work.

The experimental work for this thesis can be divided into three main objectives:

1. Identifying shelled species suitable for low dose retrospective dosimetry. This includes developing sample preparation procedures and irradiating samples for qualitative EPR analysis.
2. Establishing a dose-response relationship for the studied species. This consists of irradiating samples to various doses and performing EPR analysis to refine measurement parameters for quantitative assessments.
3. Assessing limiting factors for low dose EPR dosimetry. This includes examining various shelled species and determining how environmental factors might influence an EPR signal.

3.1 Samples

3.1.1 Studied Species

Seven species from the crustacea and mollusca family were obtained to determine which aquatic and terrestrial calcified tissues would be suitable for retrospective dosimetry. Table 3.1 lists the specific species obtained for this work. Sample preparation procedures were developed for each species, along with preliminary experiments to determine the species studied specifically for dose assessments.

TABLE 3.1: A list of the shelled species used for this study.

Lobster	*Homarus americanus*	Crustacean
Shrimp	*Penaeus monodon*	Crustacean
Blue mussels	*Mytilus edulis*	Bivalve
Oysters	*Crassostrea virginica*	Bivalve
Eliptio mussels	*Elliptio complanata*	Bivalve
Freshwater pond snails	*Lymnaea stagnalis*	Gastropod
Terrestrial snails	*Cepaea nemoralis*	Gastropod

The species obtained for this work were selected based on their habitats. As EPR dosimetry using calcified tissues is largely species dependent, it was necessary to sample species from different aquatic and terrestrial biomes. *Homarus americanus* and *Penaeus monodon* are representative of marine benthic crustacea. *Crassostrea virginica* and *Mytilus edulis* are marine bivalves that are native to the Atlantic Ocean and found in various estuaries. *Elliptio complanata* and *Lymnaea stagnalis* are freshwater bivalves and gastropods and found commonly in lakes, streams, rivers, and ponds throughout Ontario. Finally, *Cepaea nemoralis* are representative of terrestrial gastropods, and found in habitats containing soil and grass. As the freshwater and terrestrial molluscs studied for this work are ubiquitous in Oshawa, sample collection from the wild was also possible.

An additional factor in selecting these specific species is that they inhabit various substrates. The accumulation of trace metals in species' shells, based on their occupancy on different substrates, provides information on environmental factors contributing to EPR signals in spectra. Furthermore, crustacean and mollusc shells

are composed of calcium carbonate, either in the form of aragonite, calcite, or a combination of both. By sampling species whose shells are composed of different calcium carbonate minerals, further insight into the influence of shells' structural differences in EPR spectra is possible.

The initial species selected for dose assessments were the American lobsters, pond snails, and terrestrial snails, as this included species from both aquatic and terrestrial ecosystems. Preliminary experiments were conducted on these species to determine if radiation-induced peaks at environmentally relevant doses could be detected. The remaining species listed in Table 3.1 were used for investigating limiting factors when choosing a particular species for low dose studies. All experimental work regarding choosing a suitable species is explained in detail in Section 3.3.3.

3.1.2 Sample Preparation

For this work, sample preparation procedures have been developed based on methods that are conventionally used for EPR detection of shelled species [50] [51] [53].

Crustacea

Sample preparation for all crustacean species was performed in the same manner. Samples of lobster and shrimp were purchased from a local supermarket. Lobster samples were prepared by breaking down the whole organism using pliers and dissection tools, as shown in Figure 3.1. The various components of the lobster exoskeleton were divided and placed in separate beakers. Shrimp shells were simply peeled off the entire organism. The inside of the shells was scraped off using a scalpel to remove muscles or flesh attached to the shell. Shells were then placed in a 500 mL solution of 1.2% sodium hypochlorite for 24 hours. The solution consisted of 100 mL household bleach diluted with 400 mL reverse osmosis (RO) water. This solution helped to remove any odors from the shells and assisted in removing a thin membrane attached to the inside of the lobster shells. Next, the shells were repeatedly rinsed with RO water to remove any remaining material attached to the shell. Shell fragments were inspected individually to ensure all flesh was removed.

The shells were placed in Petri dishes to dry in a desiccator for up to two weeks, as shown in Figure 3.2. For the lobster shells, the Petri dishes containing the different exoskeleton components were labeled.

FIGURE 3.1: Breakdown of a lobster for sample preparation. Pliers and dissection tools were used to obtain small pieces of shells.

(A) Lobster shells (B) Shrimp shells

FIGURE 3.2: Fragments of clean crustacean shells.

Molluscs

Bivalves

The two species of bivalvia used were blue mussels and oysters. Samples of each species were purchased from a local supermarket and the muscle was removed. Any pieces of muscle attached to the shells was scraped off using dissection tools, as shown in Figure 3.3. The bivalve shells were placed in a 500 mL solution of 1.2%

sodium hypochlorite for 24 hours. The sodium hypochlorite solution assisted in disinfecting the shells and removing odors due to any remaining muscle attached to the shell. Each shell was individually rinsed and scrubbed with water. Oyster shells, in particular, were thoroughly scrubbed and inspected to ensure no small rock debris was attached or stuck in the grooves of their shells. The shells were placed in Petri dishes and left to dry in a desiccator for up to two weeks, as shown in Figure 3.4.

FIGURE 3.3: Cleaning of bivalvia shells. Remaining muscles attached to the shells were removed using dissection tools.

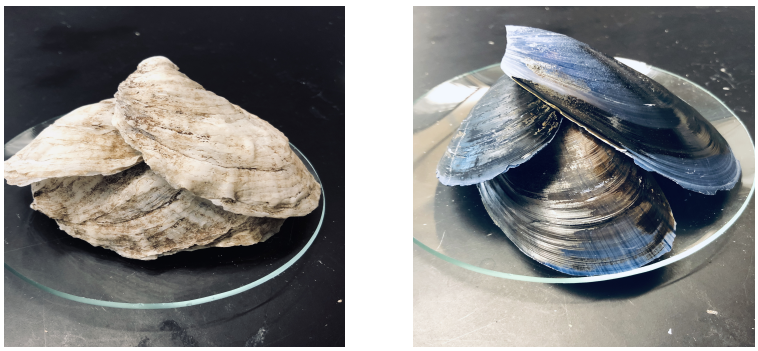

(A) Oyster shells (B) Blue mussel shells

FIGURE 3.4: Samples of clean bivalvia shells.

Gastropods

The two gastropod species were obtained from the wild. Shells of terrestrial grove

snails and freshwater pond snails were retrieved from around the Ontario Tech University campus and storm-pond. As only empty shells were collected for both species, there was no requirement to remove the organism or perform dissection procedures. Empty shells were thoroughly washed and scrubbed with water to remove dirt from both the outside and inside of the shells. Any rocks or small debris embedded inside the shells were cleaned out using nylon brushes. Shells were left in a beaker of water for 24 hours to ensure all dirt was washed out and then individually inspected. The shells were placed in Petri dishes and left to dry in a desiccator for two weeks, as shown in Figure 3.5.

(A) Freshwater pond snail shells

(B) Terrestrial grove snail shells

FIGURE 3.5: Samples of clean gastropod shells.

Sample Grinding

As discussed in Chapter 2, samples for EPR dosimetry can be irradiated by either using shell fragments or powdered shells. As powdered shells allow for a greater number of samples to be placed in front of a radiation source, all shell samples were first ground and then irradiated.

Shells of lobsters, oysters, and blue mussels were first crushed between two wooden planks to obtain smaller pieces. Only the claws were crushed for the lobster samples, as this component of the organism's exoskeleton has the hardest and most rigid structure. For the smaller species, samples of one shell were ground individually using a mortar and pestle to grain sizes of 0.1 - 0.5 mm. The grain sizes were separated using Advantech stainless steel mesh sieves with nominal wire opening

sizes of 0.5 mm (#35) and 0.1 mm (#140). The configuration of the sieves included a stainless steel pan at the bottom with the #140 size and #35 size sieves stacked on top, respectively. Crushed shell samples were placed inside the #35 size sieve and gently sifted to allow the smaller grain sizes to fall through the wire openings. Any larger grain sizes that did not fall through the opening were transferred back into the mortar and crushed again. This process was repeated until the entire shell was ground.

Once the shell was ground, the sieve stack was taken apart, and the powdered shells in the #140 size sieve were taken out and transferred into 0.6 mL micro-centrifuge tubes. The weight of each sample was measured using an analytical balance. Depending on the species, the weight of the shells ranged between 350 ± 1 mg to 500 ± 1 mg. Each sample was individually weighed before irradiation and EPR measurements as well.

All samples were stored in the desiccator until irradiation experiments. The desiccator was used to ensure the laboratory environment would not affect the samples. Humidity in a laboratory environment can cause the samples to absorb moisture and affect the resulting EPR signal intensity. Figure 3.6 displays a powdered sample for snail shells, along with the samples stored in micro-centrifuge tubes.

(A) Sample of a crushed snail shell.

(B) Crushed samples stored in micro-centrifuge tubes.

FIGURE 3.6: Shells were crushed to grain sizes of 0.1 - 0.5 mm using a mortar and pestle and then filled into 0.6 mL micro-centrifuge tubes.

3.2 Irradiations and Dosimetry

3.2.1 Cesium-137 Irradiations

All irradiations were performed at Ontario Tech using a Hopewell Design G-10 ^{137}Cs gamma source. A total of five irradiation experiments were performed throughout this work. The activity of the source as of the first irradiation experiment on November 12$^{\text{th}}$, 2018 was 6.7 Ci.

Shell samples were clipped vertically along a 7 cm x 7 cm 3-D printed holder. Powdered alanine dosimeters were clipped to the sides, as shown in Figure 3.7. Due to the small beam profile of the ^{137}Cs source, a maximum of nine samples could be irradiated at once (excluding the alanine dosimeters). For each irradiation experiment, the samples were placed at a distance of 34 cm from the center of the source, as shown in Figure 3.8.

FIGURE 3.7: A 7 cm x 7 cm 3-D printed holder. Shells samples were clipped vertically and alanine dosimeters were clipped on the sides.

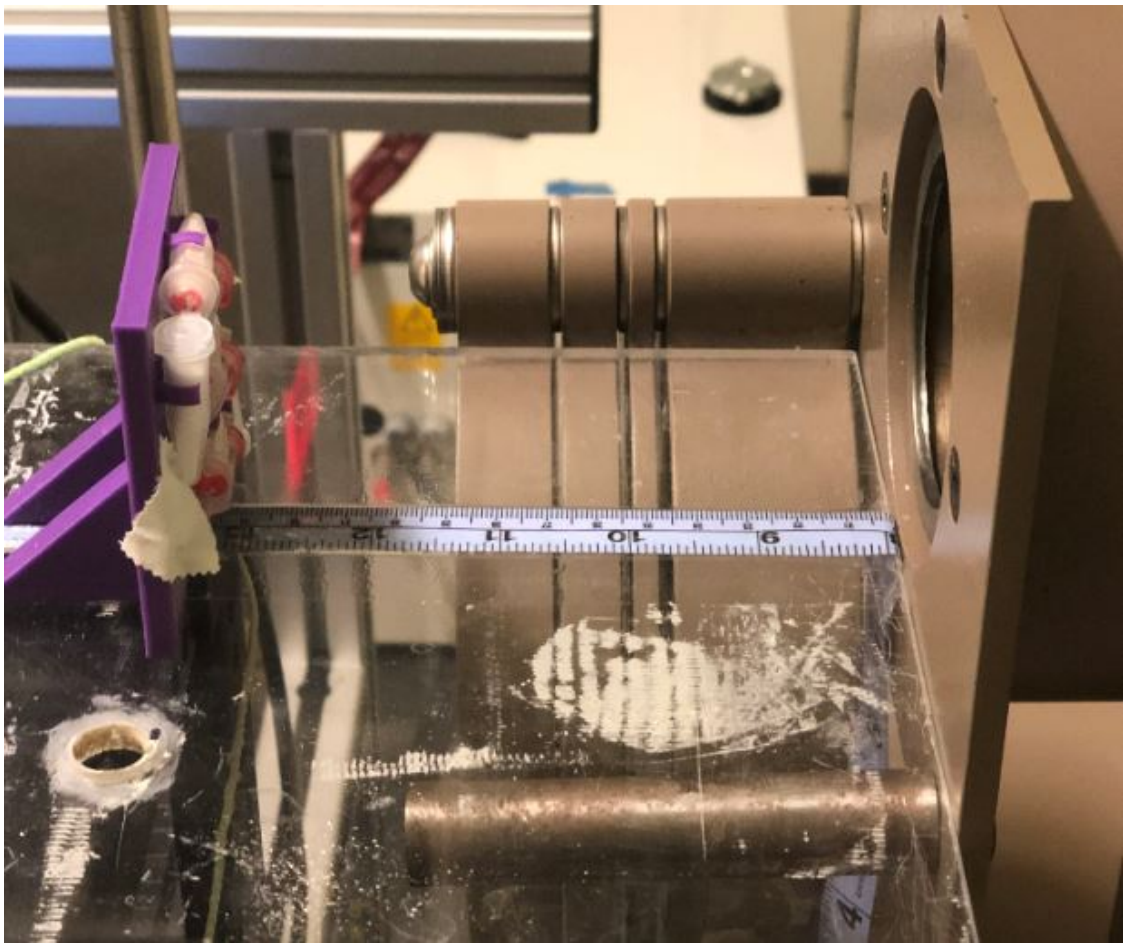

FIGURE 3.8: Irradiation setup for experiments. Sample holder was placed a distance of 34 cm from the center of the source.

3.2.2 Dosimetry

Reference dosimetry was performed with alanine powder dosimeters. A minimum of two alanine dosimeters were used for each experiment. Alanine powder was weighed to 350 $\pm$ 1 mg and filled in each micro-centrifuge tube. The samples were filled at the time of the irradiation experiment. An alanine calibration curve was developed to provide dose estimates for all irradiation experiments. The details of the calibration curve are explained further in Section 3.4.

3.3 EPR Measurements

All EPR measurements were performed using a Bruker EMX-Micro X-Band spectrometer, as shown in Figure 3.9. Samples were measured using the Wilmad LabGlass quartz EPR tubes (710-SQ-100 M), shown in Figure 3.10.

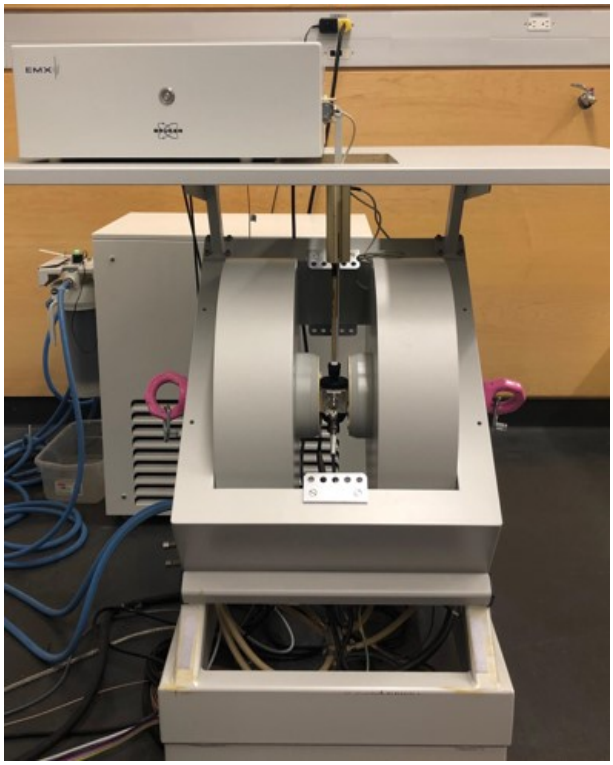

FIGURE 3.9: Bruker EMX-Micro X-Band spectrometer.

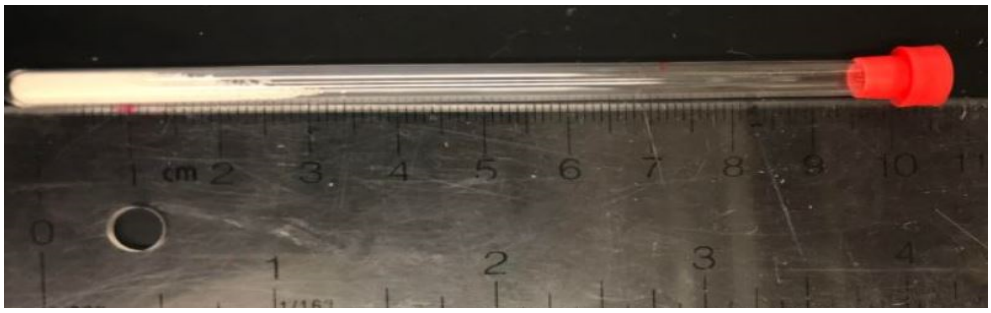

FIGURE 3.10: Wilmad LabGlass quartz EPR tubes.

3.3.1 Measurement Procedure

To generate reproducible EPR spectra for analysis of samples, a measurement procedure was established and followed for all sample measurements.

Before any irradiation experiment, measurements of unirradiated shell samples were taken as a control background. For EPR measurements, shell samples were transferred from mirco-centrifuge tubes into EPR tubes and weighed. The EPR tubes were packed with enough sample to ensure the active volume of the resonator (3.4 cm) would be filled. To establish that enough sample would be present in the active volume of the resonator, the fill height of the sample in the EPR tubes was measured. The fill height was measured from the bottom of the tube to the height of the sample in the tube using a ruler. In future measurements, a digital caliper was used.

To make sure tubes would be placed in the EPR cavity in the same position for every measurement, the tubes were marked with a line at 8.3 cm. This line was measured from the bottom of the tube using digital calipers. Wearing gloves, the tubes were additionally wiped using KIMTECH Kimwipes and ethanol. The Kimwipes were used to remove any dust or small particulates on the outside of the EPR tubes. Care was taken to ensure the line marked at 8.3 cm was not wiped off in this process. Next, the tubes were gently tapped on a hard surface to achieve a compacted sample in the tube. The tubes were then inserted in the resonator, and care was taken to ensure the sample stand was outside the cavity. After EPR measurements of each sample, the tubes were carefully pulled out, and the fill height was measured and recorded again. The purpose of measuring the mass and fill height of the samples was to determine the packing density of the sample in the tubes.

EPR spectra for all mollusc samples were recorded using the parameters listed in Table 3.2. Parameters were slightly altered for the crustacean species and are also listed in Table 3.2. The derivation of parameters for EPR measurements will be discussed in further detail in Section 3.3.2. An internal standard marker was also installed in the EPR spectrometer resonator. This standard has a known g-value

at $g = 1.98$ and was used for measuring repeatability and for determining g-factors of various peaks.

It should be noted that in one experiment, the active volume of the resonator was not fully filled. The fill heights for the first experiments with terrestrial and freshwater snail shells were measured at 2.7 cm. Sample preparation procedures for snails shells later included grinding enough sample to ensure the active volume of the resonator would be filled for subsequent experiments.

3.3.2 Measurement Parameters

In order to perform quantitative analysis of materials, the EPR measurement parameters must be examined. Various measurement parameters influence EPR signals in spectra, which can lead to signal distortion and cause misinterpretation of results. The following section will discuss the experiments conducted on a terrestrial snail shell sample irradiated to 10 Gy in order to determine the optimal measurement parameters for this species.

Microwave Power

The EPR signal intensity increases with the square root of the microwave power. At higher powers, the EPR signal begins to broaden, and the response of the signal intensity with respect to the microwave power is no longer linear. Therefore, using high microwave powers will not result in a stronger EPR signal, due to relaxation. Ideally, samples are measured using a microwave power below the value that begins to deviate from linearity in a power saturation curve [78]. In order to determine the optimal microwave power, a progressive saturation study can be conducted. A progressive saturation study includes measuring a sample at various microwave powers to observe its EPR signal intensity.

The sample used to perform the progressive saturation study was a terrestrial snail shell sample (TGS-10), which had previously been irradiated to 10 Gy. Measurements were performed with microwave powers ranging from 0.3 mW to 10 mW. The peak-to-peak height of the radiation-induced peak was measured and plotted against the square root of the microwave power, and is shown in Figure 3.11.

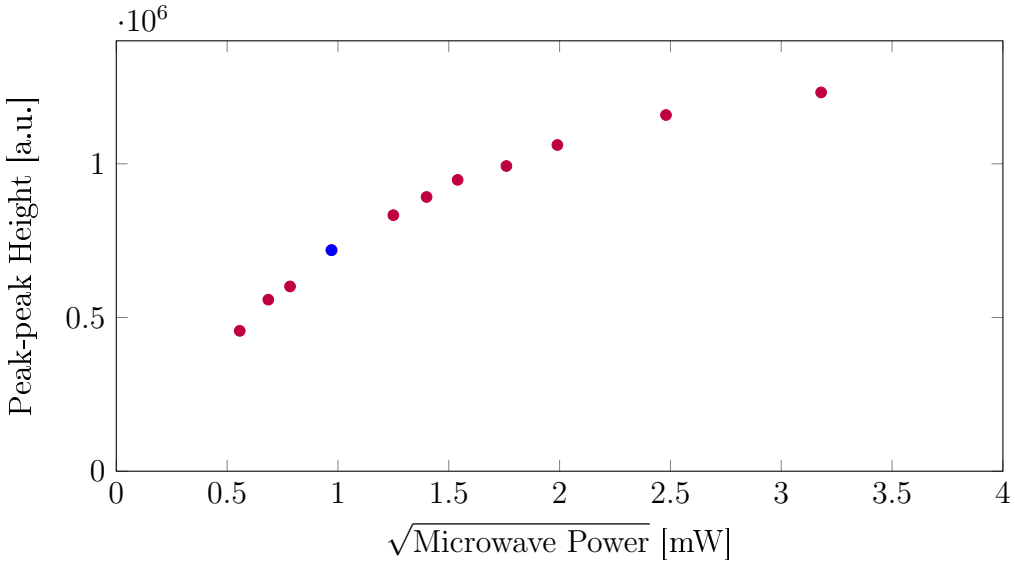

FIGURE 3.11: Power saturation curve plot for a terrestrial snail sample irradiated to 10 Gy. The sample was measured using microwave powers ranging from 0.3 mW to 10 mW. Increasing the microwave power increases the signal intensity until a point where the signal is no longer linear.

From Figure 3.11, the peak-to-peak height of the radiation-induced peak increases with increasing microwave power; however, at higher powers, the signal begins to saturate. Additionally, at the higher microwave powers, the signal lines begin to broaden. A microwave power of 0.94 mW was decided as an appropriate power level to use for the terrestrial snail species, since at this power level the peak-to-peak height of the radiation-induced peak is measured within the unsaturated region.

A saturation test was performed for each species to determine if Mn^{2+} signals were also measured in the linear range when using the selected microwave power. One method to check if a signal is measured in the linear range is by decreasing the attenuation by 6 dB, which is a factor of four increase in the microwave power. By decreasing the attenuation by 6 dB, the signal amplitude should increase by a factor of two [78]. The signal amplitude was observed to increase by this factor, and the selected microwave power of 0.94 mW was kept.

Modulation Amplitude

The modulation amplitude is another parameter that influences the shape and intensity of the EPR signal. Increasing the modulation amplitude increases the EPR signal intensity since the signal is averaged over more points. However, increasing the modulation amplitude can lead to signal broadening. The modulation amplitude value should be small enough that signal lines are not distorted [78]. The TGS-10 sample was measured at modulation amplitudes ranging from 0.1 G to 5 G, and at a microwave power of 0.94 mW. The behavior of the radiation-induced peak with the varying modulation amplitudes is shown in Figure 3.12.

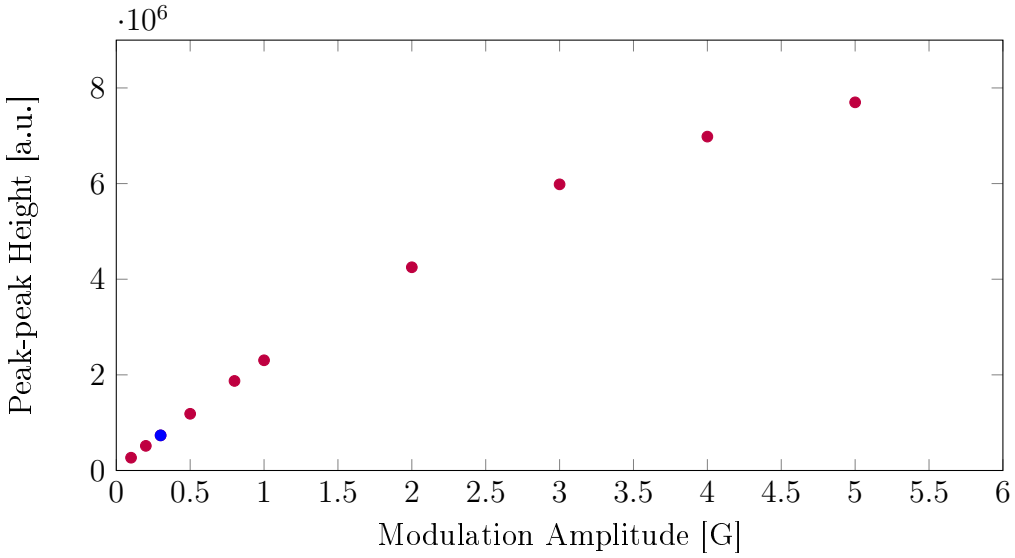

FIGURE 3.12: The effect of increasing the modulation amplitude on the peak-peak height of the radiation-induced peak for a terrestrial snail shell sample irradiated to 10 Gy. Measurements were recorded at a microwave power of 0.94 mW.

It can be seen that at higher modulation amplitudes, the peak-to-peak height of the radiation-induced peak increases until a small plateau is achieved. This is due to adjacent signal lines broadening and forming a singular peak, as shown in Figure 3.13. Figure 3.13 displays the EPR spectra of a terrestrial snail shell sample measured at a modulation amplitude of 0.3 G and 3 G. At a higher modulation amplitude, the EPR signal is over-modulated, with a distinct broadening of the

signal. The modulation amplitude chosen for the terrestrial snail species measurements was 0.3 G, as it provided an appropriate signal resolution with little signal broadening.

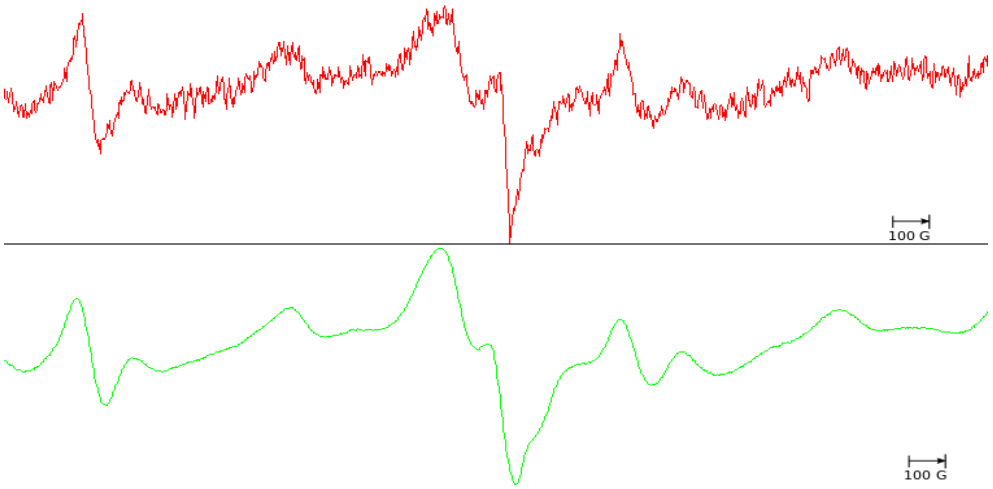

FIGURE 3.13: EPR spectra of terrestrial snail sample measured using a modulation amplitude of 0.3 G (top) and 3 G (bottom). At a higher modulation amplitude, the spectral resolution is improved; however, the signal beings to broaden.

Time Constant

The time constant is used to improve the signal-to-noise (S/N) ratio by slowing the response time of the spectrometer. A higher time constant will improve the signal resolution by decreasing the noise. However, the EPR signal can be distorted or filtered out if a long time constant is chosen. A general guideline to follow is to ensure the time constant takes less than 1/10 of the time to scan the narrowest line in the spectrum [78]. This is determined using Equation 3.1:

$$\frac{\text{spectrum width [G]}}{\text{line width [G]}} \times \frac{\text{time constant [s]}}{\text{sweep time [s]}} < 0.1 \tag{3.1}$$

Using the TGS-10 sample, an EPR measurement was performed to determine which time constant would be most suitable. From the measurements and the calculation (shown below), a time constant of 20.48 ms was chosen.

$$\frac{100\ \text{G}}{1.77\ \text{G}} \times \frac{0.02048\ \text{s}}{120\ \text{s}} = 0.0096$$

Table 3.2 presents the EPR parameters used for measurements of terrestrial snail samples in Section 3.3.3. Quick saturation tests were performed for each species, and it was deemed that the parameters used for the terrestrial snail shells were also applicable for the other mollusc samples. Parameters for the crustacean species are also listed.

TABLE 3.2: EPR parameters for mollusc and crustacean samples.

	Mollusc Parameters	Crustacean Parameters
Receiver Gain	$1.00 \cdot 10^4$	$1.00 \cdot 10^4$
Modulation Frequency	100 kHz	100 kHz
Modulation Amplitude	0.3 G	0.3 G
Center Field	3510 G	3510 G
Sweep Width	800.00 G	800.00 G
Time Constant	20.48 ms	20.48 ms
Sweep Time	120 s	120 s
Microwave Power	0.94 mW	2.25 mW

3.3.3 Experimental Studies

The following section describes the experimental studies conducted for this work. The objective of these studies was to identify a shelled species suitable for low dose retrospective dosimetry. Studies included investigating sample preparation methods as well as establishing dose-response relationships. Additionally, experiments assessing limiting factors for EPR dosimetry are presented.

Experiment 1 - Selecting a Species

The first experiment conducted was to determine which species would be suitable for low dose retrospective dosimetry. The American lobster was chosen as the initial species. One lobster was obtained from the local supermarket and prepared

according to the sample preparation methods described in Section 3.1.2. To determine if American lobster shells were suitable for low dose studies, a dose of 10 Gy was chosen for this experiment.

Before irradiation experiments, three samples of ground lobster claw shells were transferred from micro-centrifuge tubes into EPR tubes and weighed. Measurements of unirradiated samples were taken using the measurement parameters listed in Table 3.2. All spectra of unirradiated shelled displayed characteristic Mn^{2+} signals. The spectra for unirradiated samples provided control spectra that could be compared to the irradiated samples. After measurements, the samples were transferred back into micro-centrifuge tubes and clipped onto the 3-D printed sample-holder, along with two alanine dosimeters. The samples were placed 34 cm from the center of the source and irradiated to a dose of 10 Gy. After irradiation, all samples were transferred back into EPR tubes and weighed once more (to account for any sample loss between transfers). EPR measurements of irradiated samples were performed using the same parameter settings and procedures as the unirradiated samples.

A qualitative analysis of the measurements was performed to determine if the shells of the American lobster species displayed a radiation-induced peak at 10 Gy. All samples showed characteristic Mn^{2+} signals post-irradiation; however, no radiation-induced peak was detected.

Since the American lobster shells did not display a detectable radiation-induced peak at a dose of 10 Gy, this experiment was repeated using the freshwater pond snail and terrestrial snail shells.

Samples of snail shells were obtained from the wild and prepared according to the sample preparation methods outlined in Section 3.1.2. Three individual shell samples were used for each species. Before irradiation, samples were transferred into EPR tubes and weighed. Background measurements for each sample were taken using the parameters listed in Table 3.2. After background measurements, samples were clipped on to the sample-holder, along with two alanine dosimeters, and placed 34 cm from the center of the source. Similarly to the lobster experiment,

samples of snail shells were irradiated to a dose of 10 Gy. After irradiations, the shells were transferred into EPR tubes, weighed, and measured.

A qualitative analysis of the measurements was performed for both species, where a distinguishable difference between the unirradiated and irradiated shells was seen only for the terrestrial snail shells. It was then decided that based on the abundance of the terrestrial snail in the wild, and the shells of this species displaying a radiation-induced peak, that it should be chosen as the studied organism for dose assessments.

Experiment 2 - Chemical Etching

The purpose of this experiment was to determine if a chemical etching process would improve the EPR signal by removing surface defects from terrestrial snail shell samples. Chemical etching has been shown to remove surface defect signals caused by excessive grinding during sample preparation methods [54] [55]. Two samples of terrestrial snail shells were used for this experiment: TGS-U and TGS-I. The TGS-U sample was an unirradiated sample, and the TGS-I sample was a sample that had previously been irradiated to 10 Gy.

Before the etching process, EPR measurements for both samples were performed to acquire control background spectra. Samples were transferred from micro-centrifuge tubes into EPR tubes and weighed. The measurements were performed using the parameters listed in Table 3.2. After EPR measurements, the samples were transferred back into their micro-centrifuge tubes.

For the etching procedure, a 500 mL solution of 0.05 M acetic acid was made. From the prepared solution, 3 mL was transferred into two 50 mL beakers. Each sample was taken out of the micro-centrifuge tube and placed into the 50 mL beaker for 3 minutes. After the allotted time, the samples were filtered using a filter paper into a separate 100 mL beaker. The samples in the filter paper were then repeatedly washed with distilled water. The process of washing the samples was continued for approximately 5 minutes. The samples were left to dry in a fume-hood for two weeks and then transferred to the desiccator.

Once dried, the samples were transferred into EPR tubes, weighed, and measured using the parameter settings listed in Table 3.2. The peak-to-peak heights of the background native peak and the radiation-induced peak were assessed to determine if the etching procedure had any effect on the signal intensities.

Experiment 3 - Terrestrial Snail Dose Response

All previous experiments were performed with a dose of 10 Gy. Although a radiation-induced peak was present for the terrestrial snail shells, it was important to determine if a relationship between signal height and irradiation dose could be established. For this experiment, three terrestrial snail shell samples were used. The shells were prepared according to the sample preparation procedure discussed in Section 3.1.2. One sample for each dose group was used; TGS-A, TGS-B, and TGS-C, which were irradiated to doses of 2, 10, and 20 Gy respectively.

Before irradiation, EPR measurements of samples were performed. Samples were transferred from micro-centrifuge tubes into EPR tubes, weighed, and measured using the parameter settings listed in Table 3.2. After measurements, the samples were clipped onto the sample-holder and placed 34 cm from the center of the source. Samples were then irradiated to the target doses. After irradiation, samples were transferred back into EPR tubes, weighed, and measured using the same parameters as the unirradiated samples. Each irradiated sample was measured three times. Similarly, two alanine dosimeters were used and were measured three times. Table 3.3 displays the irradiation and dosimetry data for this experiment.

TABLE 3.3: Dosimetry measurements for the dose-response experiment of terrestrial snail shells.

Irradiation Time [Hours]	Calculated Dose [Gy]	Measured Alanine Dose [Gy]
11.00	2	2.05 ± 0.27
55.00	10	10.15 ± 0.02
109.89	20	19.41 ± 0.01

Experiment 4 - The Effect of Manganese

Previous experimental work displayed high intensity Mn^{2+} signals in the lobster and snail shell spectra. Due to the high intensity Mn^{2+} signals present in the EPR spectra, shells of lobster and freshwater pond snails were deemed unsuitable for low dose studies. As a result, an investigation into the manganese concentrations in shelled species and their influence on the resulting EPR spectra was instigated. This experiment was conducted in two components: irradiating half of the samples of various shelled species to 10 Gy, and measuring the concentration of manganese in the other half of the shells. Manganese concentrations in shells were measured using samples that had not been irradiated.

The species used for this experiment are listed in Table 3.1. Before irradiations, samples were prepared according to the sample preparation methods outlined in Section 3.1.2. One sample for each species was used. Before irradiations, EPR measurements of unirradiated samples were performed. After background measurements, the samples were transferred into micro-centrifuge tubes and clipped onto the sample-holder. The samples were placed 34 cm from the center of the source, and irradiated to a dose of 10 Gy. After irradiations, the samples were transferred back into EPR tubes, weighed and subsequently measured using the same parameter settings as the unirradiated sample measurements. For each sample, the peak-to-peak heights of the highest Mn^{2+} signal were recorded along with the peak-to-peak heights of the radiation-induced peak (if one was present).

The second portion of this experiment was determining the manganese concentration in the shells. To measure the concentration, samples were first dissolved and prepared for a readout using inductively coupled plasma - optical emission spectroscopy (ICP-OES). Samples were prepared by grinding the shells of each species individually in a mortar and pestle until a fine powder was obtained. The powdered samples used for ICP-OES were smaller than grain sizes of 0.1 mm. Each powdered sample was weighed to 200 mg and transferred into a 50 mL beaker. The beakers were placed on a hotplate, which was placed inside a fumehood. Wearing the appropriate protective equipment (lab coat, goggles, and gloves), 1 mL of 67% concentrated nitric acid was added to each beaker. The beakers containing

the powdered samples and nitric acid were heated to begin the open-vessel digestion process. The samples were heated at a constant temperature of 60 °C for 30 minutes, or until all of the sample had dissolved. The solution with the dissolved samples was then filtered using a Whatman # 42 filter paper into a 50 mL volumetric flask. The volumetric flask was filled up to mark with deionized water.

Additionally, a manganese standard stock solution of 100 mg L^{-1} was used to prepare calibration standard solutions. Five calibration standards were prepared: 0.5 mg L^{-1}, 3 mg L^{-1}, 9 mg L^{-1}, 15 mg L^{-1}, and 20 mg L^{-1}. The calibration standards were prepared by diluting the appropriate volume of the stock solution. For example, to make the 20 mg L^{-1} calibration standard, 10 mL of the manganese stock solution was transferred into a 50 mL volumetric flask and diluted with 39 mL of deionized water. To match the acid concentration used in the sample digestion procedure, 1 mL of nitric acid was added to the flask. Prepared samples were stored in the fume-hood until measurements using the ICP-OES were performed.

The experiments using the ICP-OES are currently on hold, and therefore, the results of this experiment will mainly focus on the EPR measurements of shells. Moreover, the results will focus on the Mn^{2+} signals in EPR spectra and the possible factors that affect the signal intensities.

3.4 Alanine-EPR Dosimetry

EPR dosimetry using alanine, mostly in the form of pellets, is a common application of EPR spectroscopy. Alanine-EPR dosimetry is primarily used for reference dosimetry, quality assurance, and calibration purposes. As discussed in Chapter 2, the EPR measurements for alanine are based on the production of the stable radical of $CH_3-CH-COOH$ [46]. The formed radical is stable for many years and has a linear dose response from 0.01 Gy to 10 kGy [45].

The following section discusses the experimental work performed for the development of an alanine calibration curve. The calibration curve was used to provide dose estimates for all irradiation experiments.

3.4.1 Samples and Irradiations

For the measurements associated with the calibration curve, DL-α-alanine powder was used for all samples. A total of forty samples were prepared with 350 mg of alanine weighed and filled in micro-centrifuge tubes.

The samples were labeled, packed, and transported to the Canadian Nuclear Laboratories (CNL) GammaCell 220 facility for irradiations. The samples were irradiated using a ^{60}Co gamma source. The dose rate of the source was 1.9 Gy/min the day of irradiations (May 2nd, 2019). Samples were irradiated to doses from 0.2 to 20 Gy, with five samples used for each dose point. After irradiations, the samples were sent back to Ontario Tech for EPR measurements.

3.4.2 EPR Measurements

The alanine samples were measured using the Bruker EMX-Micro EPR spectrometer. The measurement procedure outlined in Section 3.3.1 was used for all EPR measurements. The measurement parameters used will be discussed in more detail in the following.

Measurement Parameters

To determine the optimal parameters for measurement, advice from the literature was followed [79] [80]. However, power saturation tests were still performed on irradiated samples to verify the saturation behaviours of the samples. The parameters selected were based mainly on a good compromise between spectrum resolution, the height of the signal relative to the background signal, and acquisition time.

The modulation amplitude selected for alanine samples was 12 G. From literature, it is common practice to use a modulation amplitude for alanine that overmodulates the radiation-induced peaks [45]. The high modulation amplitude parameter provides better spectral resolution at the lower doses, which allows for easier measurements of the peak-to-peak heights.

A progressive power saturation study was performed on unirradiated and irradiated samples to test if the literature parameter for microwave power (10 mW) would be applicable to use for these samples as well. The sample AL-7 was used, which had been irradiated to a dose of 0.5 Gy. The sample was measured with varying microwave powers, and the peak-to-peak height of the central peak was recorded after each measurement. Figure 3.14 displays the plotted saturation curve.

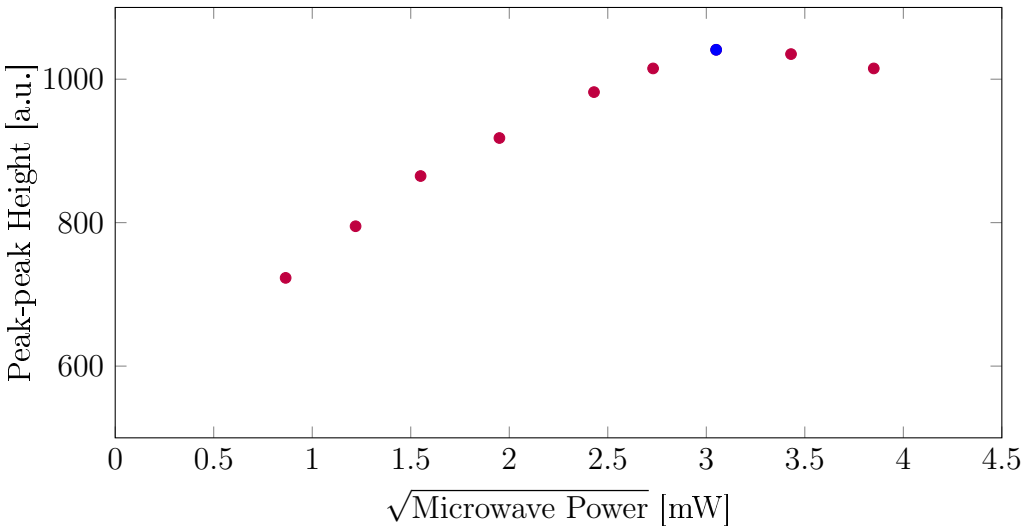

FIGURE 3.14: A power saturation curve plot for an alanine dosimeter irradiated to 0.5 Gy.

A microwave power of 9.3 mW was selected, since, from Figure 3.14, the peak-to-peak height of the radiation-induced peak was highest at this point. There is a slight deviation from linearity at this value; however, this was deemed acceptable. The proportionality of signal height increasing with the square root of the microwave power is only valid when the signal is not overmodulated. However, this relationship still holds for the area under the peak. Since the microwave power is in the saturation region, the signal height cannot be corrected for spectrometer power fluctuations. However, small power fluctuations will not affect the peak-to-peak height as much when the signal is saturated. The slight saturation in microwave power was accepted as the changes between the signal intensity of both unirradiated and irradiated samples were still observed using this microwave power. Therefore, the value of 9.3 mW was kept for a better signal resolution for samples at each dose point. At higher powers, it can be seen that the peak-to-peak height of the radiation-induced peak begins to decrease, which would make it unsuitable for dosimetric measurements.

The remaining parameters selected were tested based on acquisition time. By selecting a large time constant, the signal-to-noise ratio is improved as the spectrometer's response time is slowed. This time constant results in a longer measurement time for one sample and a higher signal resolution is attained. Overall, the parameters selected for alanine samples resulted in a total measuring time of 3 minutes for one sample. The parameters used to measure all alanine samples are listed in Table 3.4.

TABLE 3.4: EPR parameters used for alanine powder measurements.

Receiver Gain	$1.00 \cdot 10^4$
Modulation Frequency	100 kHz
Modulation Amplitude	12 G
Center Field	3510 G
Sweep Width	200 G
Time Constant	81.92 ms
Sweep Time	180 s
Microwave Power	9.36 mW

3.4.3 Dose Response

A quantitative analysis of the dose-response for the alanine dosimeters was performed to establish a relationship between the signal intensity and irradiation dose. The dose-response plot is displayed in Figure 3.15 and shows the EPR spectrum of one sample each from dose groups of 0.5 Gy, 2 Gy, 5 Gy, 9 Gy, 15 Gy, and 20 Gy. Here, a clear increase of the peak-to-peak height with the dose is observed. Alanine powder has three distinct peaks formed when exposed to ionizing radiation. All three peaks increase with irradiation dose and can be used for quantitative analysis. Furthermore, a smaller peak at a magnetic field value of 3450 G is observed at the higher doses. The peak displayed at a magnetic field value of 3550 G is the internal standard marker.

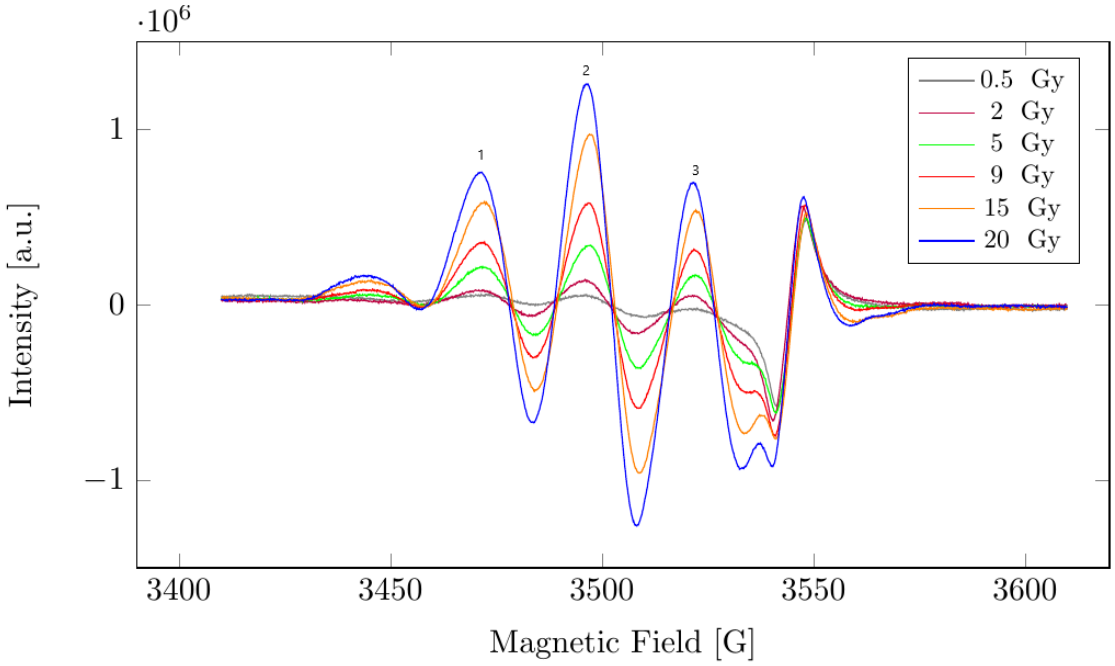

FIGURE 3.15: EPR spectra of alanine powder dosimeters irradiated to doses ranging from 0.5 - 20 Gy. All three major resonance peaks (marked with 1, 2, and 3) show a dose-response relationship. Spectra are recorded using a microwave power of 9.36 mW.

The peak-to-peak heights of the central resonance signal are commonly used to evaluate the dosimetric signal for alanine, mainly for practical reasons. There have

been instances where the peak-to-peak heights of all three major peaks have been summed for dosimetry measurements [45]. The third peak in the EPR spectrum (seen on the right) could not be used in the analysis for this study since the internal standard signal overlapped with this peak at the lower doses. As a result, only the first (left) and second (center) peaks were considered.

A comparative analysis of measuring the peak-to-peak heights of both the left and central peaks and only the central peak was performed. The analysis showed that the relative error was higher when summing the two peaks at the low doses compared to using only the central peak. At the 0.2 Gy dose group, summing the two peaks resulted in a relative error of 18%, which decreased to 9% when using only the central peak. Similarly, the 20 Gy dose point displayed a relative error of 2.4% when summing both peaks and 1.8% when only using the central peak. Since the left peak was not as prominent at the lower doses compared to the central peak, the measurements of the peak-to-peak heights were challenging to perform. Therefore, only the peak-to-peak heights of the central peak were used for evaluation.

The EPR measurements for samples were performed as follows: each sample from the eight dose groups was measured three times. After one measurement, the spectrometer was placed on "standby", the sample tube was entirely removed from the cavity, and then inserted back. This process was repeated for all samples as a method to reduce the measurement uncertainty from sample placement. Since one dose group had five samples, three measurements of each sample were performed, giving a total of fifteen measurements for one dose group. The peak-to-peak heights of the central peak were measured using the Bruker WinEPR processing software to develop the calibration curve. The spectra were uploaded into the processing software from the acquisition program after each measurement. The peak-to-peak heights for each sample were measured by adding the absolute values of the highest and lowest points of the central peak. The measured peak-to-peak heights for each sample were plotted against the dose. The derived calibration curve of the means is shown in Figure 3.16.

Figure 3.16 displays the dose-response of the alanine samples in the dose ranges

between 0.2 - 20 Gy. A linear relationship between the peak-to-peak heights and irradiation dose is observable from this calibration curve. The measurement points are calculated as the averages of the five samples in each dose group. As each sample was measured three times, the error bars represent the standard deviation of the fifteen sample measurements for one dose group.

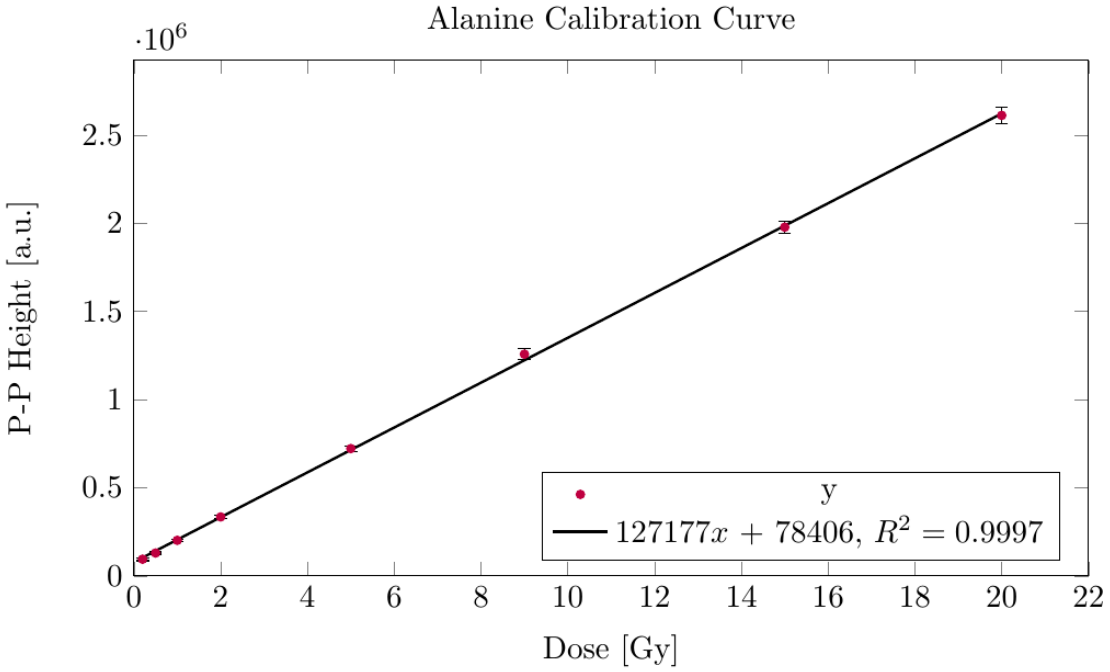

FIGURE 3.16: Alanine powder calibration curve. The measurement point are averages of peak-to-peak heights of five samples in one dose group.

Two methods of quantifying the means and standard deviations are presented in Table 3.5. Columns two and three represent the data used to develop the calibration curve in Figure 3.16. Here, the means for one dose group were calculated as the average of the fifteen measurements. These columns present the means and standard deviations of samples within a dose group. Columns four and five represent the means and standard deviations of one measurement instance for the five samples in one dose group. In this case, the average of the peak-to-peak heights of each sample measured three times was calculated. From the average of the peak-to-peak heights of each sample, the average for the dose group was calculated. These

columns, similarly, represent the means and standard deviations of samples within the same dose group. The two methods present the same means since the calculations were based on the same sample measurements. The standard deviations are also relatively close in value for both methods, with column five showing slightly lower values. This is due to the second method presenting the standard deviation of the averages of sample measurements, which provides the uncertainty of samples within a group.

TABLE 3.5: Mean measurements of alanine dosimeters. Columns two and three represent the mean and standard deviations of fifteen measurements for one dose group. Columns four and five represent the means and standard deviations of average peak-to-peak measurements of each samples in a dose group.

	5 samples, measured 3 times		1 measurement, 5 samples	
Dose [Gy]	Mean p-p height	st.dev.	Mean p-p height	st.dev.
0.2	$9.47 \cdot 10^4$	$0.908 \cdot 10^4$	$9.47 \cdot 10^4$	$0.847 \cdot 10^4$
0.5	$1.30 \cdot 10^5$	$0.625 \cdot 10^4$	$1.30 \cdot 10^5$	$0.609 \cdot 10^4$
1	$2.02 \cdot 10^5$	$0.740 \cdot 10^4$	$2.02 \cdot 10^5$	$0.654 \cdot 10^4$
2	$3.35 \cdot 10^5$	$1.00 \cdot 10^4$	$3.35 \cdot 10^5$	$0.900 \cdot 10^4$
5	$7.21 \cdot 10^5$	$1.47 \cdot 10^4$	$7.21 \cdot 10^5$	$1.33 \cdot 10^4$
9	$1.26 \cdot 10^6$	$3.18 \cdot 10^4$	$1.26 \cdot 10^6$	$3.10 \cdot 10^4$
15	$1.98 \cdot 10^6$	$3.32 \cdot 10^4$	$1.98 \cdot 10^6$	$3.24 \cdot 10^4$
20	$2.61 \cdot 10^6$	$4.77 \cdot 10^4$	$2.61 \cdot 10^6$	$4.37 \cdot 10^4$

A linear fit of the calibration curve is observed after quantifying the mean peak-to-peak heights of the samples. The calibration equation produced by fitting the line through the data points is presented in Figure 3.16 and shown in Equation 3.2. The equation from this calibration curve was used to provide dose estimates for all irradiation experiments. The equation produced from the fit has a coefficient of determination of 99.97%.

$$y = 127177x + 78406 \tag{3.2}$$

Challenges in experimental work

The development of an effective calibration curve can allow for alanine powder to be standardized as an inexpensive dosimeter for a variety of applications. For this work, alanine powder was used as reference dosimeters for all irradiation experiments. Furthermore, the irradiation geometry of the alanine powder dosimeters matches all shell samples used for this work. Measurements of alanine dosimeters are performed with fast readouts, and as with all EPR measurements, the dosimetric signal is read out non-destructively and the measurements can be performed repeatedly. However, there are experimental challenges of using alanine powder which must be discussed.

The major experimental problem faced when using the powdered form of alanine is that the powder is very easily affected by laboratory conditions. Humidity in a laboratory environment can cause the alanine powder to absorb moisture. Excess amounts of moisture in alanine not only affect the signal intensity but also provide challenges in sample preparation. The Wilmad EPR tubes have an inner diameter of 4 mm, and samples are transferred into the tubes via a funnel. To transfer the alanine powder into the EPR tubes, continuous tapping of the tubes was required. The added moisture in alanine powder increases the time it takes to transfer the samples into EPR tubes.

Silica gel packs can be stored in the alanine container to manage this challenge. Silica gel packs contain a desiccant that absorbs water and keeps materials in a dry state. As silica gel packs were not acquired for this work, an alternative method was storing the prepared alanine dosimeters in the desiccator. In the beginning, the sample preparation of alanine powder resulted in exceedingly long times. However, storage of the samples in the desiccator shortened the overall sample preparation times to some extent.

Future Work

Future experimental work can be considered for optimizing the alanine calibration curve. First, sample measurements should be repeated to compare standard deviations of the samples in each dose group from one measurement instance to samples

measured from multiple dates. Additionally, signal fading should be examined by performing measurements a few months or years after irradiation. Signal fading has been studied in a previous experiment using alanine powder, where it was reported that the dosimetric signal showed no noticeable fading 1.5 months after irradiation, provided the dosimeters were stored in a dark environment [79]. Finally, a comparison of the radiation response of alanine dosimeters to conventional dosimeters, such as optically stimulated luminescent (OSL) and thermoluminescent (TLD) dosimeters, should be explored. These experiments will provide a comparative analysis between the detection limits and dose-responses of conventional dosimeters with alanine powder dosimeters.

Chapter 4

Results and Discussion

EPR spectroscopy is a promising retrospective dosimetry technique in assessing radiation doses to non-human biota. It is used as a qualitative and quantitative technique in identifying an irradiated sample, as well as estimating the absorbed dose in a sample. As previously discussed in Chapter 2, calcified tissues of shelled species using EPR spectroscopy have most commonly been used to detect irradiated foodstuffs and for geological dating. These applications use doses in the ranges of 1-10 kGy, which are multiple orders of magnitude higher than environmental doses. To test the feasibility of using calcified tissues for low dose studies, a significantly lower dose range needs to be detected. Preliminary studies of using mollusc species for detection of ionizing radiation in the environment have shown promising results, with the lowest doses reported at 2 Gy for freshwater molluscs and 0.2 Gy for marine molluscs [32] [75].

4.1 Selection of Suitable Species

Initial experiments were conducted to identify suitable species to use for low dose studies. The tested species were American lobsters (*Homarus americanus*), freshwater pond snails (*Lymnaea stagnalis*), and terrestrial snails (*Cepaea nemoralis*). Shell samples were obtained and prepared following the sample preparation methods described in Section 3.1.2. EPR spectra for unirradiated shells were measured to establish control spectra for all samples. Samples were irradiated with a dose of 10 Gy using a ^{137}Cs gamma irradiator. Reference dosimetry was performed with

alanine powder. If a radiation-induced peak could not be detected for a species at 10 Gy, it was eliminated from the study at this stage, as any environmentally relevant doses are well below this value. The following sections describe the qualitative spectra analysis performed in determining a suitable species to use for dose assessments.

4.1.1 American Lobster

The EPR spectra of unirradiated and irradiated American lobster shells are presented in Figure 4.1. Both spectra were measured over a magnetic field range of 3100 G to 3900 G (800 G sweep width). This was to ensure the entirety of the signal would be displayed, in order to observe all composite signals measured for this species. For comparative purposes, the spectra for unirradiated and irradiated shells are plotted together in Figure 4.1.

In the literature, both the unirradiated and irradiated shells of the majority of crustacea display the characteristic Mn^{2+} signals. The irradiated shells should show an additional radical peak at the center of the Mn^{2+} signals, between the third and fourth Mn^{2+} peaks [58] [59]. The presence of this peak indicates that the sample has been irradiated, and should be visible close to 3495 G [62].

In Figure 4.1, the spectra of unirradiated and irradiated American lobster shells display the six Mn^{2+} signals that are equally spaced, and as expected, are independent of dose. These signals are marked with an asterisk above each peak. The irradiated shell sample shows no deviation from the unirradiated sample. There is also no additional radiation-induced peak visible near 3495 G. This is expected when the intensity of Mn^{2+} signals is this pronounced, as it will obscure peaks induced by radiation at low doses. As the American lobster shells did not display a detectable peak at a dose of 10 Gy, they were eliminated from the dose assessment study. The lobster shells were further used for determining limiting factors of EPR spectroscopy, discussed in Section 4.4.

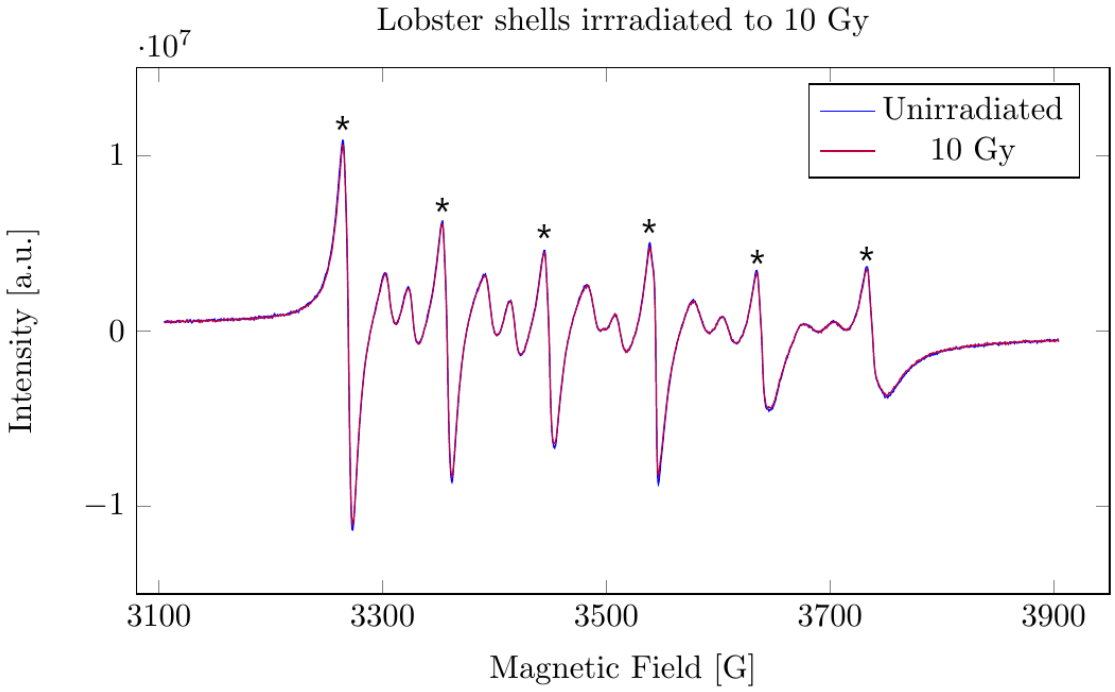

FIGURE 4.1: EPR spectra of American lobster shells before and after an irradiation dose of 10 Gy. The Mn^{2+} peaks are present and marked with an asterisk. No radiation-induced peak is detected for lobster shells at this dose.

4.1.2 Freshwater Pond Snails

Figure 4.2 displays the EPR spectra of unirradiated and irradiated freshwater pond snail shells. The shape of the EPR signal derived from the pond snail shells are different from those of the American lobster. The EPR signal for this species is more complex, yet still shows the characteristic Mn^{2+} signals. The intensity of these signals is comparable to those found in the American lobster shells.

In the literature, irradiated freshwater mollusc shells show additional radical peaks present between the third and fourth Mn^{2+} peaks, at g-values of 2.0014, 2.0016, and 2.0057 [32] [68]. The additional peaks are typically associated with carbonates and have been shown to be radiation dependent.

In Figure 4.2, an additional radical peak is not observed in irradiated shells. Similarly to the American lobster shells, the high intensity of the Mn^{2+} signals obscured

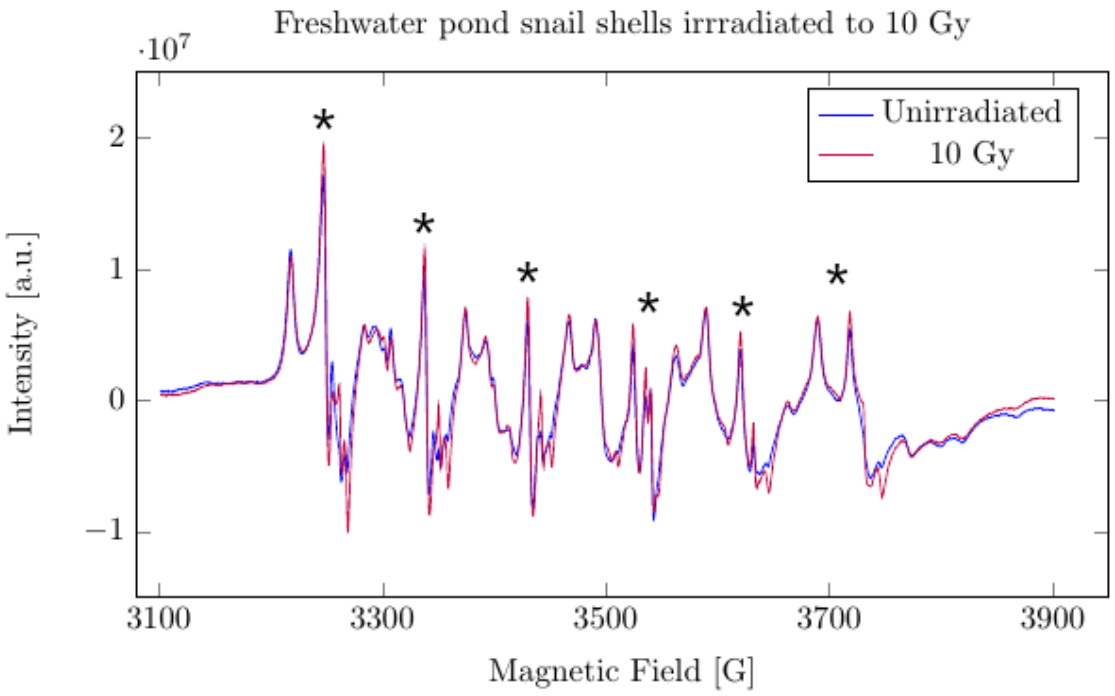

FIGURE 4.2: EPR spectra of pond snail shells before and after an irradiation dose of 10 Gy. Characteristic Mn^{2+} peaks are present and marked with an asterisk. No radiation-induced peak is visible at this dose.

any radiation-induced peaks for quantification purposes. As a radiation-induced peak could not be detected at a dose of 10 Gy in the pond snail shells, this species was discarded from further low dose studies as well.

4.1.3 Terrestrial Snails

The EPR spectra of terrestrial snail shells were initially measured using a sweep width of 800 G and are presented in Figure 4.3. The shape of the EPR signal produced by these shells differs from the American lobster and pond snail shells. The spectra of both the unirradiated and irradiated samples display the characteristic Mn^{2+} signals and are marked with an asterisk. Here, the intensity of the Mn^{2+} signals is an order of magnitude lower than what was displayed for the American lobster and pond snail shells. The intensity of signals from various other impurities

in the terrestrial snail shells are also lower than the pond snail shells. As a result, the Mn^{2+} signals are easily identifiable, and the native central peak is more pronounced. Similarly to other gastropod species, the irradiated shells should show an additional peak between the third and fourth Mn^{2+} peaks [32].

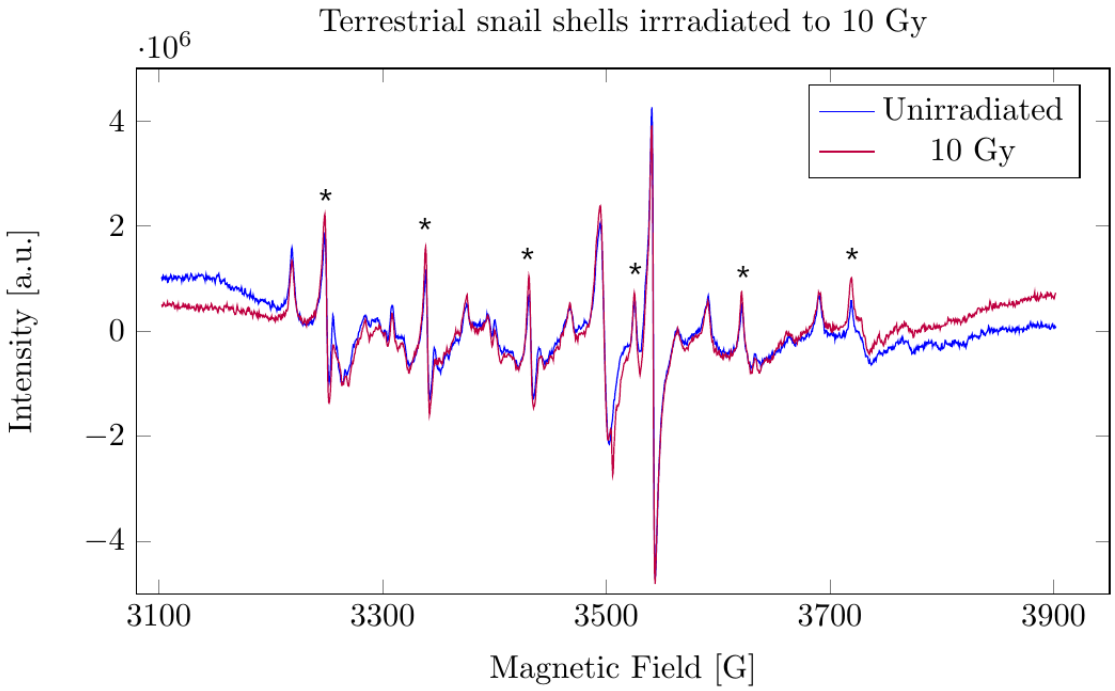

FIGURE 4.3: EPR spectra of terrestrial snail shells before and after an irradiation dose of 10 Gy. Characteristic Mn^{2+} peaks are present and marked with an asterisk. An additional peak is visible at this dose.

In Figure 4.3, the irradiated sample shows an additional peak in the center of the spectrum. To observe this peak more closely, the central part of the spectrum was scanned using a smaller sweep width of 50 G. Figure 4.4 shows the derived EPR signal, and it can be seen that an additional peak is easily distinguishable from the unirradiated sample. Based on a visible radiation-induced peak for the terrestrial snail shells, this species was selected as the most suitable calcified tissue to use for further dose assessment studies. Additional experiments were conducted to characterize the radiation-induced peak.

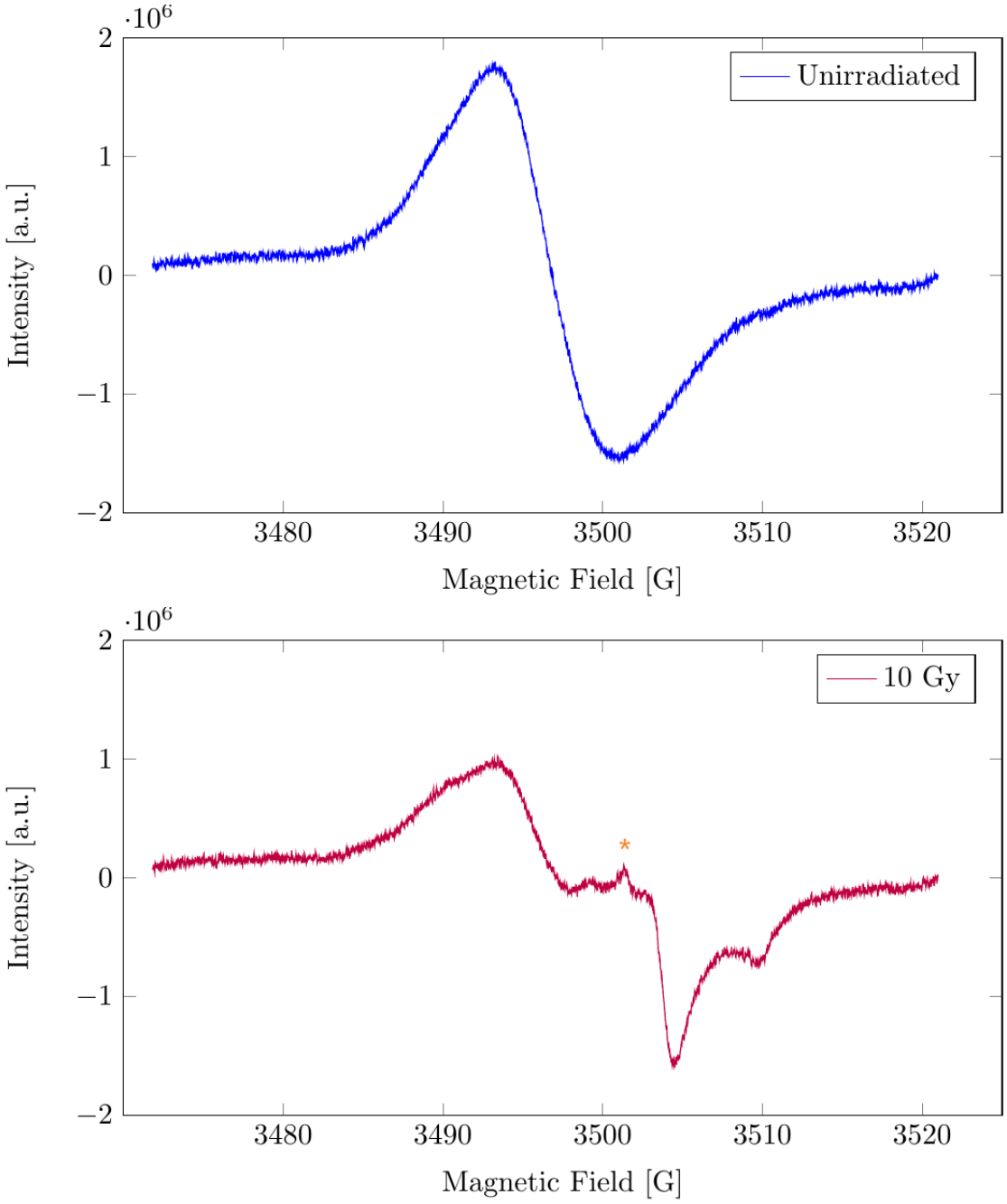

FIGURE 4.4: EPR spectra of terrestrial snail shells measured using a sweep width of 50 G. The unirradiated shells display only the native central peak. The irradiated shells display an additional peak characterized as the radiation-induced peak and is marked with an orange asterisk. This peak is visible at a magnetic field value of 3500 G.

4.2 Effect of Chemical Etching on Snail Shells

A method of removing surface defects and possible grinding-induced signals was tested as a sample preparation method on terrestrial snail shells. The objective of this study was to investigate if etching through a chemical process would improve the EPR signal. In studies of dating fossilized gastropod shells, chemical etching has been used to remove the surface defect peak introduced through grinding or milling processes during sample preparation procedures [54]. The additional peak that appears in the EPR spectrum is reported to be at a g-value of 2.0002 [54] [55].

For this experiment, two samples of terrestrial snail shells were used: TGS-U and TGS-I, with the former being an unirradiated sample and the latter a sample that had previously been irradiated to 10 Gy. Both samples were ground using a mortar and pestle. The etching and measurement procedures are described in Section 3.3.3.

EPR measurements of both samples were performed before the etching process to acquire spectra that could be compared to samples after etching. The absence of a signal at $g = 2.0002$ in both spectra before etching indicated that there was no mechanically-induced signal by grinding the shells. The etching procedure was still implemented to examine if this method would improve the overall EPR signal.

After etching the samples, a minimal decrease in intensity was detected for both samples. The TGS-U sample showed a decrease of 5% in signal intensity of the native central peak. The radiation-induced peak for the TGS-I sample had a decrease of 6% in signal intensity. In the literature, chemical etching has been shown not to influence the intensities of other peaks present in the EPR spectrum [54]. As a result, other factors could have caused a decrease in the signal intensity of these samples.

The decrease in intensity could be due to the storage conditions of the samples. Samples before the etching procedure were kept outside the desiccator, and the humidity of the laboratory likely contributed to the higher initial signals. After the etching procedure, samples were kept in the fume-hood and then transferred to the desiccator and kept in a controlled environment. Since a second experiment in

validating the decrease in signal intensities was not conducted due to the minimal amount of sample available, this remains uncertain.

The process of chemically etching samples also did not affect the intensity of Mn^{2+} signals. This was expected, as this method is primarily used to remove surface defects from grinding shells. Chemical etching should not affect the intensities of other signals present in the EPR spectrum [54]. Since there was a decrease in the intensity of the radiation-induced peak after etching, this method was not further pursued for samples that had previously been irradiated. There was no evidence of chemical etching significantly improving the overall EPR signal. As the literature reported peak at $g = 2.0002$ was not present in the spectra for either samples, this technique was not used in future sample preparation procedures. However, the effects of chemical etching on shell samples can still be studied and implemented if future samples display mechanically-induced peaks.

4.3 Terrestrial Snail Dose Response

Although a radiation-induced peak was present for the terrestrial snail shells, it was important to determine if a relationship between signal height and irradiation dose could be established for this species. The experimental procedures for this study are outlined in Section 3.3.3. Figure 4.5 shows the EPR spectrum of an unirraidated terrestrial snail shell, where no radiation-induced peak is observed. Figure 4.6 shows the spectra of three terrestrial snail shell samples irradiated to doses of 2, 10, and 20 Gy.

A relationship between the radiation-induced peak and dose is notable in Figure 4.6. The native central peak, observed in all terrestrial snail shells, is seen at the magnetic field value of 3490 G. This peak (marked with a black asterisk in Figure 4.6) does not increase with irradiation, and was therefore not used for dose assessments. At an irradiation dose of 2 Gy, an additional peak is observed, which is not present in unirradiated shells. The new peak, which is a result of the shells being exposed to ionizing radiation, is marked with a green asterisk in Figure 4.6. This peak is observed at the magnetic field value of 3500 G and seen to increase

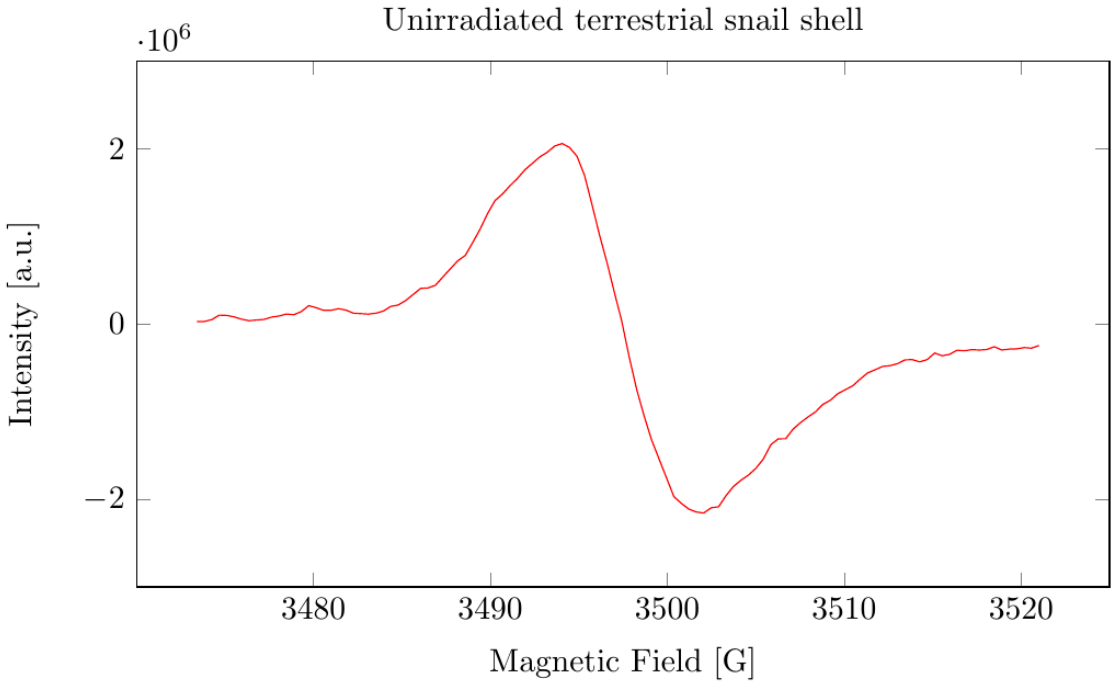

FIGURE 4.5: EPR spectrum of an unirradiated terrestrial snail shell measured using a sweep width of 50 G.

with dose. Although the increase in intensity is small, the relationship of this increase can be used to develop a dose-response curve for terrestrial snail shells. Furthermore, at an irradiation dose of 20 Gy, additional smaller peaks are resolved near the primary radiation-induced peak that are not easily distinguishable in the 2 Gy signal. This resulted in further characterization of the radiation-induced peaks.

As discussed in Chapter 3, an internal amplitude standard was available for EPR measurements. This standard has a known g-value at $g = 1.98$ and was used for the purposes of measuring repeatability, determining g-values of different peaks, and as an amplitude standard. In the literature, the peaks most commonly used for radiation detection in gastropod species are at g-values of 2.0012 [76] and 2.0016 [68], associated with the CO_3^{3-} and CO_2^{-} radicals respectively . Both peaks are commonly used in dating applications of EPR dosimetry. These peaks are shown to have a linear relationship with dose and the lifetime of the trapped electron is

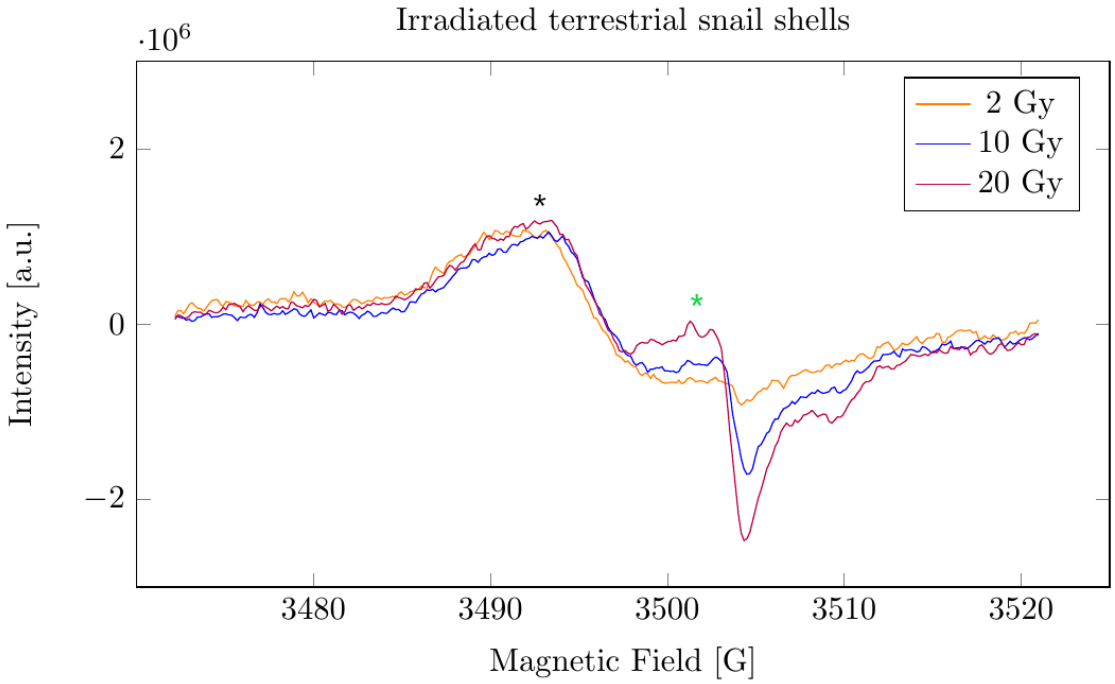

FIGURE 4.6: EPR spectra of three terrestrial snail shells irradiated to doses of 2, 10, and 20 Gy. The black asterisk indicates native peaks. Peaks marked with a green asterisk are radiation-induced.

stable for a long period of time [55] [68] [76]. Using the internal standard, the following g-values listed in Table 4.1 were determined for the terrestrial snail shells from the spectrum in Figure 4.7:

TABLE 4.1: g-values identified in terrestrial snail shells in this study and their corresponding radical species determined from literature.

g-value	Radical Species	Reference
2.003	O^-	[81]
2.0012	CO_3^{3-}	[76]
2.0016	CO_2^-	[69] [55] [68]

The peak at a g-value of 2.0016 was used for radiation detection and all dose assessments in this study. This peak was observed to increase with dose and was resolved at a dose of 2 Gy. The peak at a g-value of 2.0012 was not easily detected at 10 Gy and was not evident at the 2 Gy dose. Moreover, the peak at a g-value

of 2.003 did not increase with irradiation dose. This peak was attributed to the radical species O^- and is reported to be due to surface defects instead [81].

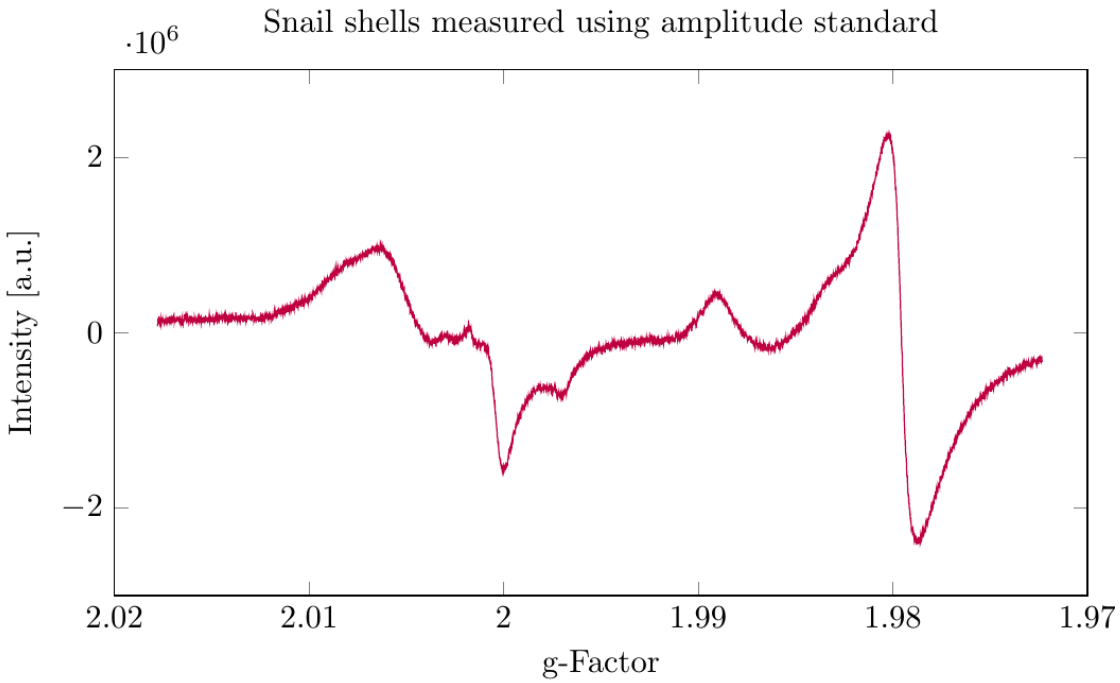

FIGURE 4.7: Terrestrial snail shell spectrum measured with the standard amplitude marked at a g-value of 1.98. The different peaks in terrestrial snail shell spectra are observed at g-values of 2.003, 2.0012, and 2.0016.

Using the peak at $g = 2.0016$, a dose-response curve for the terrestrial snail shells was developed. Figure 4.8 shows the peak-to-peak heights of one sample measured at each dose. All spectrum measurements were performed using the available Bruker WinEPR software. To calculate the signal height for a sample, spectra were uploaded into the processing software from the acquisition program. The peak-to-peak height of the $g = 2.0016$ signal for each sample was measured by determining the highest and lowest points of the peak and adding their absolute values. This process was repeated for all irradiated shells. As observed in Figure 4.5, the unirradiated shells did not display a radiation-induced peak, and therefore the peak-to-peak height of the 0 Gy measurement is zero.

The dose-response plot in Figure 4.8 is normalized based on the packing density for each sample. This was done to reduce errors associated with the amount of sample present in the EPR cavity. The packing density takes into account the amount of material packed into an EPR tube and can differ between samples. For this normalization, the peak-to-peak height of the sample was divided by the density for that sample. The density was calculated by dividing the mass of the sample by the volume of the sample in the tube, taken as a cylinder and a semi-sphere (Equation 4.3) [82]. The heights for the volume calculations are based on the fill height measurements of the sample in each tube, as discussed in Section 3.3.1. Calculations for the normalization of samples based on weight and fill height are shown below.

$$V_{cylinder} = \pi r^2 h \tag{4.1}$$

$$V_{semi-sphere} = \frac{1}{2} \cdot \frac{4}{3} \pi r^3 \tag{4.2}$$

$$V_{sample} = V_{cylinder} + V_{semi-sphere} \tag{4.3}$$

To calculate the density, the mass of the sample is divided by the volume, as shown in Equation 4.4:

$$\rho = \frac{m_{sample}}{V_{sample}} \tag{4.4}$$

Finally, the normalized intensity is calculated by dividing the intensity (measured peak-to-peak height from the WinEPR software) by the density (Equation 4.5):

$$I_{norm} = \frac{I_{measured}}{\rho} \tag{4.5}$$

The peak-to-peak height measurement points are averages of three measurements taken for one sample, which have been normalized based on the weight and fill height measurements. The EPR measurements of samples were performed on the same day without turning the EPR off, and the one sample was measured three times. Therefore, the measurement points represent the averages of the three measurements of one sample. The error bars represent the standard deviation of the three measurements taken for the one sample, which also account for the uncertainties in the packing density. The measurement uncertainties for the peak-to-peak height are presented below.

The fill height measurements for these sample were performed using a ruler and the uncertainty from those measurements are $\Delta h = 0.5\ mm$. The uncertainty of the mass measurements can be taken as the instrument uncertainty of the analytical balance as $\Delta m = 1\ mg$.

Next, the error of the volume calculations are based on Equation 4.6:

$$\Delta V_{sample} = \pi r^2 \Delta h_{measured} \tag{4.6}$$

Through error propagation, the errors for the density are calculated as:

$$\Delta\rho = \sqrt{\left(\frac{\Delta V_{sample}}{V_{sample}}\right)^2 + \left(\frac{\Delta m}{m}\right)^2} \cdot \rho \tag{4.7}$$

Finally, the normalized intensity error is calculated using Equation 4.8:

$$\Delta I_{norm} = \sqrt{\left(\frac{\Delta I_{measured}}{I_{measured}}\right)^2 + \left(\frac{\Delta\rho}{\rho}\right)^2} \cdot I_{norm} \tag{4.8}$$

The measurements and standard deviations for the dose-response plot are presented in Table 4.2. Since only one sample was irradiated to a single dose point, the standard deviations in Table 4.2 represent the uncertainties associated with the measurement method.

TABLE 4.2: Measurements of the density normalized peak-to-peak heights for three terrestrial snail shell samples. The peak-to-peak heights are the means of three measurements taken for one sample.

Measured Dose [Gy]	Mean p-p Height [a.u.]	st.dev. [a.u.]
2.05	$1.11 \cdot 10^6$	$3.51 \cdot 10^4$
10.15	$1.58 \cdot 10^6$	$3.58 \cdot 10^4$
19.41	$1.93 \cdot 10^6$	$3.79 \cdot 10^4$

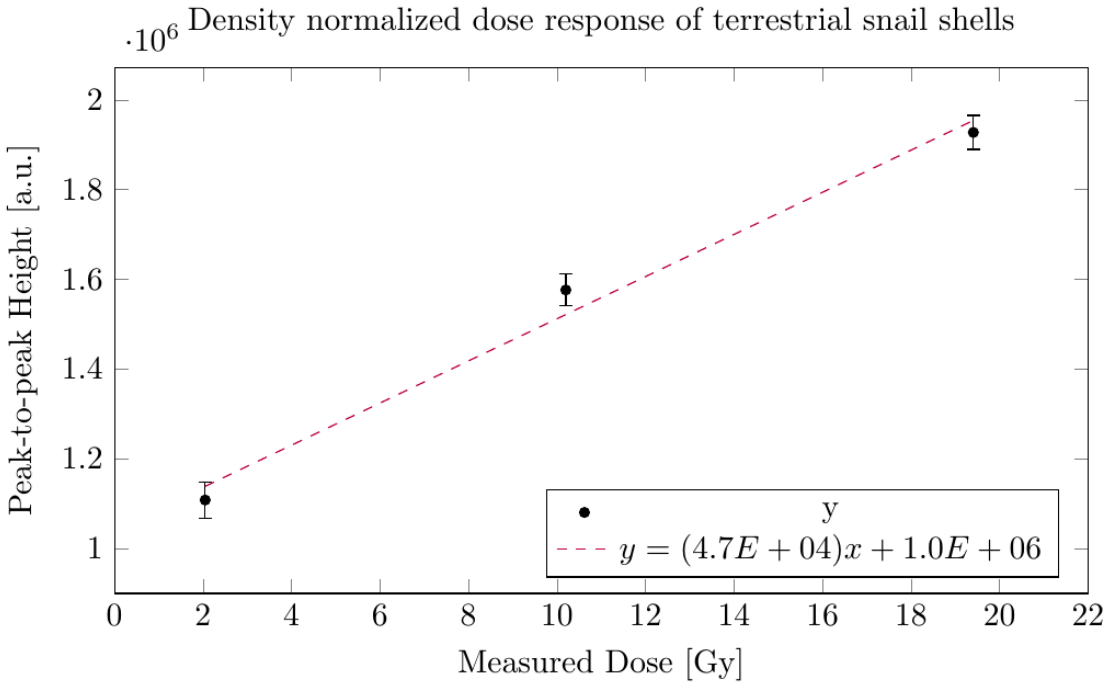

FIGURE 4.8: Dose-response curve for three terrestrial snail shell samples irradiated to doses of 2, 10, and 20 Gy.

The relative error of the 2 Gy measurements is 4% and 2% for the 10 Gy and 20 Gy measurements. The high measurement uncertainty is expected for the 2 Gy sample, since the signal was difficult to resolve due to the adjacent Mn^{2+} signals.

The dose-response of terrestrial snails was assessed through a linear fit. The equation produced by fitting the line through the data points is shown in Figure 4.8.

Considering the measurement error bars, a linear relationship between the peak-to-peak height of the $g = 2.0016$ signal and irradiation dose is observable through the three dose points. As discussed earlier, the native central peak of terrestrial snail shells did not increase with dose and was not used for dose assessments. Since the unirradiated shells did not display a radiation-induced peak, the peak-to-peak height of the 0 Gy dose point is considered zero.

Although the dose-response only accounts for three dose points, each with just one sample, this preliminary experiment shows promising results. A relationship at this trial stage is observed between peak height and dose, which can justify using the terrestrial snail species as potential dosimeters for retrospective dosimetry. Using these species in a dose range realistic for environmental dosimetry will require further experiments. To consider terrestrial snail shells for environmental dosimetry, samples will need to be irradiated to doses below 2 Gy to determine their detection limit.

In literature, the lowest limit of detection for a terrestrial snail species (*Cepaea homoralis*) is reported at 2 Gy [32] [75]. Based on the results of this experiment, a radiation-induced peak is detectable at 2 Gy, since there was no radiation-induced peak present for unirradiated samples. In order to detect a signal in a dose range suitable for environmental dosimetry, several experimental and measurement procedures need to be considered. First, an increase in sample size will be necessary, as this will allow for statistical evaluation of sample peak-to-peak heights in one dose group. Additionally, the resolution of a signal below 2 Gy will require further refinements in measurement parameters. This can include increasing the modulation amplitude, the time constant, and the number of scans used to derive the EPR signal. Finally, the high Mn^{2+} signal intensities provide a considerable amount of uncertainty in quantifying the radiation-induced peak at 2 Gy. Therefore, the presence of Mn^{2+} signals will need to be accounted for in subsequent experiments when resolving peaks at doses below 2 Gy for this species.

4.4 Effect of Manganese on the EPR Signal

As discussed in Chapter 2 and seen from previous experiments in this work, the Mn^{2+} impurities in EPR spectra introduced a significant limiting factor for low dose studies. It has been reported that high Mn^{2+} intensities in EPR spectra will obscure radiation-induced peaks at low doses [32] [75].

The intensity of Mn^{2+} signals for various shelled species are dependent on multiple factors, which must be considered when selecting a species for environmental EPR dosimetry. The intensities of Mn^{2+} signals are independent of radiation, and are instead attributed to the crystal form of $CaCO_3$, the age of a shell sample, and the geographical location from which species are sampled. The color of a shell also contributes to the EPR spectra. Darker colored shells contain more paramagnetic ions compared to uncolored shells, and thus result in high Mn^{2+} signal intensities [25] [75].

Manganese is a naturally abundant metal found in the environment and comprises approximately 0.1% of the Earth's crust [83]. The element is commonly found in soils and sediments in combination with other compounds and minerals. Manganese exists in several oxidation states and is extensively studied due to its toxicity effects in biological systems [84]. Crustacea and molluscs naturally accumulate manganese into their bodies during their lifetime, and consequently, trace amounts of the metal are found in the shells of most species.

The accumulation of manganese in a species' shell is largely dependent on the crystal form of the shell. Shelled species are primarily composed of one, or a combination of the two common polymorphs of calcium carbonate; aragonite and calcite [20] [85]. Manganese is chemically more stable in calcite than aragonite, as Mn^{2+} ions can enter the Ca^{2+} sites in calcite without causing significant crystallographic defects in the structure [86] [87]. This is mainly due to the similar structural properties of calcite and rhodochrosite ($MnCO_3$) [87]. As a result, shells that are mainly composed of calcite will contain more Mn^{2+} ions [32]. When classifying species based on their crystal mineral, it is reported that shells of decapod

crustacea are mainly composed of calcite [85]. The shells of freshwater and terrestrial molluscs are composed of aragonite [68], with smaller amounts of calcite present in some species. As a result, Mn^{2+} will be present in the shells of most species but will have varying concentrations depending on the crystal mineral.

The Mn^{2+} ions present in EPR spectra cause serious limitations in the quantification of radiation-induced peaks in some species at lower doses. As a result, an investigation into the manganese concentrations in shelled species and its influence on the resulting EPR spectra was instigated. The purpose of this experiment was to correlate the concentration of manganese in the shells of various species to their EPR Mn^{2+} signal intensities. The outcome of this experiment can be used to assess the feasibility of using certain shelled species for dosimetry studies. For instance, manganese detection can be used as a triage method in selecting species applicable to use for low dose EPR dosimetry. This can lead to further studies, where creating a methodical protocol when choosing samples for environmental EPR dosimetry might become necessary.

Seven species from the crustacean and mollusc families were chosen for this experiment, and are listed in Table 3.1. The selection was primarily based on the substrates these species inhabit. Species can be classified based on the occupancy of their substrates. For instance, some species burrow themselves in the sediment, while others live on the sediment surface. Some bivalve species live in intertidal zones and estuaries and live on substrates such as rocks, algae, or various submerged items in water. Terrestrial gastropods commonly inhabit soil or grass surfaces.

As discussed earlier, manganese is present in various concentrations in soils and in sediments. Manganese concentrations (in dry weight) have been reported in the range from 3550-8960 mg/kg in surface sediments of the Baltic Sea, 410-6700 mg/kg in river sediments from the South Platte River Basin in the United States, and 300-600 mg/kg in natural soil [83]. The concentration of manganese in sediments and soils will vary depending on the locations, but concentrations are higher in sediment. A species' occupancy on substrates has a significant influence on the accumulation of manganese in shells. Species that occupy different substrates will be exposed to varying concentrations of manganese and thus incorporate some of

the element into their shells during the calcification or molting process. As a result, species from different habitats will have a certain concentration of the element in their shells and, consequently, have varying Mn^{2+} signal intensities in their EPR spectra. Species that contain high intensity Mn^{2+} signals from high manganese concentrations in their shells will be unsuitable to use as environmental samples for low dose studies.

Initially, this experiment was conducted in two components: irradiating half of the shells of a species to 10 Gy, and measuring the concentration of manganese in the other half of the shells. The irradiated shells were measured using the EPR spectrometer in order to measure the peak-to-peak heights of the highest Mn^{2+} signal of that shell, and the radiation-induced peak (if one was present). In parallel, ICP-OES was meant to be used to quantify the manganese concentrations in the shells. As the latter portion of this experiment is currently on hold, only the results of the EPR measurements will be discussed. The sample preparation procedures for each species, along with the irradiation setup and EPR measurements, are outlined in Section 3.3.3. The EPR spectra for all species were measured using the parameters listed in Table 3.2 and are presented below. For comparative purposes, the spectra of unirradiated and irradiated shells are plotted together.

4.4.1 Crustacea

The shells of the two crustacean species used were the giant tiger prawn and the American lobster.

Shrimp

The EPR spectra for shrimp shells are presented in Figure 4.9. The central peak (marked with an orange asterisk) has a weak intensity, which does not increase with dose. The Mn^{2+} signal for this species also has a weak intensity and is marked with a black asterisk. The more prominent peak in the spectra (blue asterisk) is the internal standard. No radiation-induced peak is detected for this species, which was expected due to the less rigid structure of shrimp shells. As the exoskeleton of shrimp contains higher amounts of chitin-proteins, there is less calcium carbonate present in the shell structure. This is supported by the literature,

which states that shrimp shells that contain a flexible and thin exoskeleton have lower signal intensities than shells that are more rigid [61] [65]. Due to the presence of more chitin-proteins in the exoskeleton, the electron traps are unstable from less calcification, which makes detection of radical centers difficult.

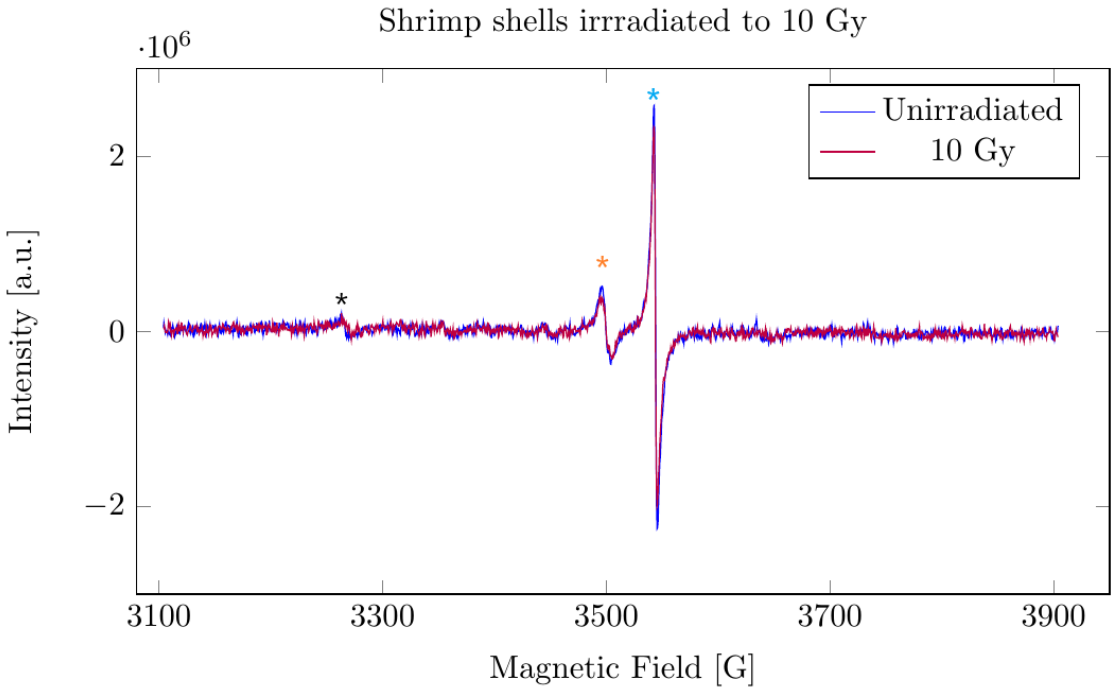

FIGURE 4.9: EPR spectra of shrimp shells before and after an irradiation dose of 10 Gy. Marked with a black asterisk is a Mn^{2+} signal. A central peak is also displayed, marked with an orange asterisk. The signal marked with a blue asterisk is from the internal standard.

The absence of Mn^{2+} signals in the EPR spectra is unexpected. As giant tiger prawns live in areas of deep water and bury themselves in muddy or rocky bottoms, it was presumed their shells would accumulate manganese [83]. Additionally, as tiger prawns are decapod crustacea, the shells are composed of calcite. Calcite is known to incorporate manganese more easily into its structure. A possible explanation is that the shrimp used in this experiment were bought from a local grocery store. It can be assumed these shrimp were not harvested from the wild and were

instead farmed. Farming crustacea, and especially *Penaeus monodon*, is a well-established industry. The species are grown in a controlled environment and kept in various tanks depending on their larval stage. Water quality parameters such as salinity, temperature, and pH are controlled and measured regularly [88]. The feeding of organisms is also controlled. Since high concentrations of manganese are detrimental to biological systems, it would be reasonable to assume farmed species are kept in clean and regulated environments. As a result, the chemical composition of the shell from farmed species is not comparable to the shells of species collected from the wild.

American Lobster

The EPR spectra for the American lobster shells are presented in Figure 4.10. As discussed in Section 4.1, the EPR spectra show high intensity Mn^{2+} signals and no radiation-induced peak. The absence of a radiation-induced peak is most likely due to the Mn^{2+} signals since it is established high intensity Mn^{2+} signals will obscure radiation-induced peaks at low doses [32] [75].

The high intensity Mn^{2+} signals were expected for this species. American lobsters are marine crustacea with shells composed of calcite. Mn^{2+} is chemically more stable in calcitic shells, which suggests a higher concentration of the element in this structure. Furthermore, manganese is known to be accumulated in the majority of benthic fauna [83]. As lobsters are benthic organisms, there is a possibility of higher concentrations of manganese present in the exoskeleton. It is important to note that lobsters undergo a molting process as they grow. Their whole exoskeleton is replaced by a new cuticle, which grows underneath the existing one. As lobsters molt, they re-absorb minerals from their existing cuticle and incorporate them into the new exoskeleton. As such, there will be differences in the amounts of calcium deposition in the shells [60], and presumably, manganese based on availability in the previous cuticle and environmental conditions. As the concentration of manganese was not measured in the current work, it is difficult to quantify the effect in the EPR spectra. However, evidence is found in the literature that lobsters, as benthic crustacea, accumulate increased amounts of manganese.

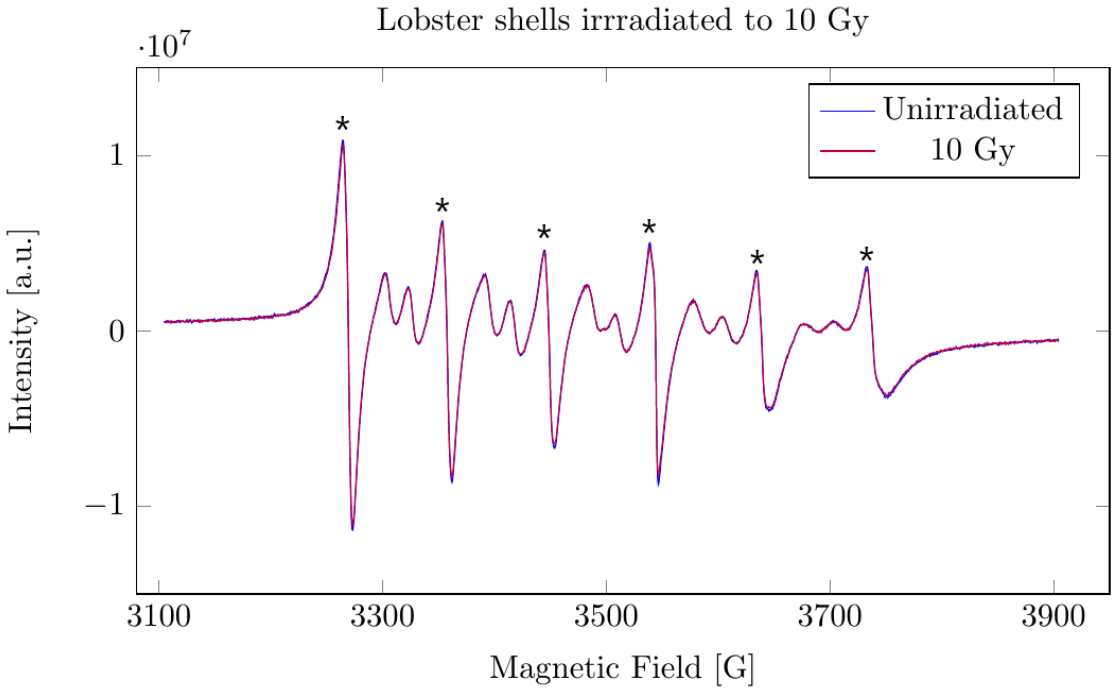

FIGURE 4.10: EPR spectra of American lobster shells before and after an irradiation dose of 10 Gy. Characteristic Mn^{2+} peaks are present and marked with an asterisk.

4.4.2 Molluscs

The three bivalve species used for this experiment were oysters, blue mussels, and Eastern eliptio mussels. The two gastropod species were the freshwater pond snails and terrestrial grove snails.

Eastern Oyster

The EPR spectra of Eastern oyster shells are presented in Figure 4.11. The characteristic Mn^{2+} signals are present and marked with an asterisk. A further qualitative assessment of the spectrum shows no detectable radiation-induced peak for the irradiated shells. In the literature, a radiation-induced peak for Pacific oyster shells is reported at a g-value of 2.0038 at an irradiation dose of 0.5 kGy [72]. The absence of a radiation-induced peak at 10 Gy in this work is likely due to the high intensity Mn^{2+} signals. As the high intensity Mn^{2+} signals effectively masked a radiation-induced peak at the investigated dose, oyster shells would not be suited

for environmental EPR dosimetry. This is consistent with the literature, where it has been reported that spectra for irradiated oyster shells, using the radical species of CO^{2-}, is difficult to resolve for samples irradiated with doses lower than 10 Gy [74].

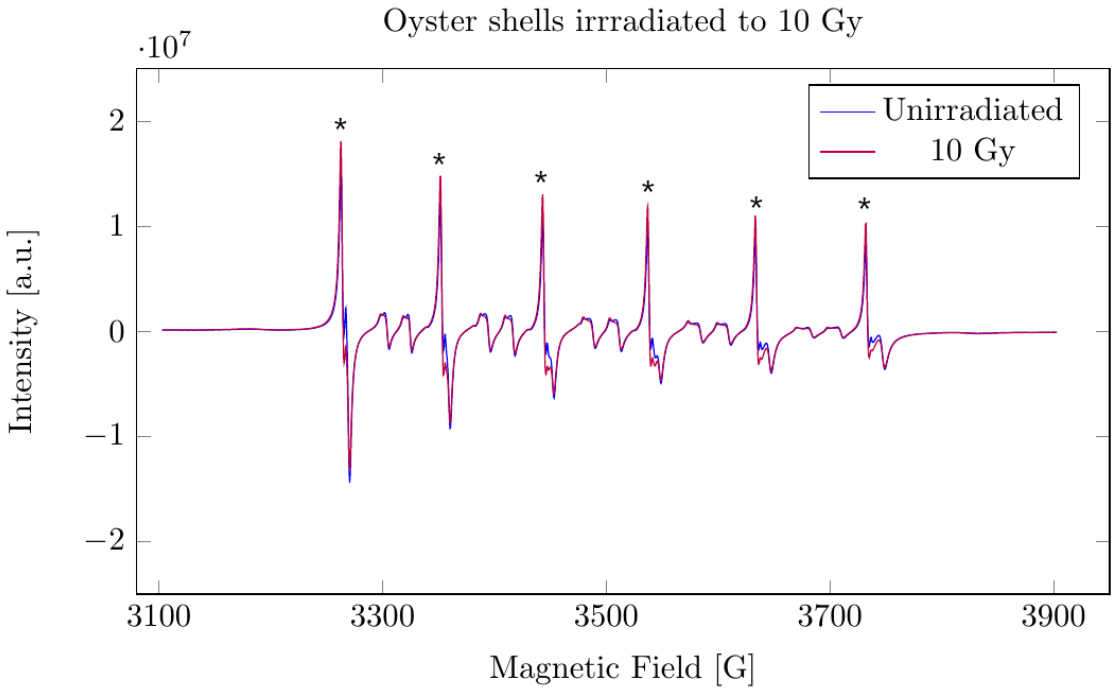

FIGURE 4.11: EPR spectra of oyster shells before and after an irradiation dose of 10 Gy. Characteristic Mn^{2+} peaks are present and marked with an asterisk.

In the case of oyster shells, the intensity of the Mn^{2+} signals is slightly higher than the American lobster shells. Similarly to lobsters, oysters are marine animals, and their shells are mainly composed of calcite. Oyster shells are primarily composed of $CaCO_3$ and smaller amounts of organic components [20] [72]. Furthermore, oysters colonize in groups on substrates, such as rocks and shells, where they grow for the remainder of their lives. The majority of oyster reefs are directly on the sediment surface, and it can be assumed that trace amounts of manganese are accumulated in the shells.

Blue Mussel

The EPR spectra for blue mussel shells is presented in Figure 4.12. The Mn^{2+} signals are visible (marked with black asterisks) along with a central peak (marked with an orange asterisk). Blue mussel shells do not display a radiation-induced peak at a dose of 10 Gy. The absence of a radiation-induced peak was expected for this species for multiple reasons. First, blue mussels are marine molluscs, suggesting that the $CaCO_3$ polymorph is in the form of calcite. Manganese is more stable in calcite and shells with this crystal form display high intensity Mn^{2+} signals [32]. Additionally, blue mussels have dark colored shells, which further suggests the incorporation of paramagnetic ions in the shells. Darker colored shells are known to contain more paramagnetic ions compared to uncolored shells, which have shown high Mn^{2+} signal intensities in the EPR spectra [75]. Blue mussels are also found in subtidal and intertidal zones, where they permanently inhabit hard substrates embedded in sediment.

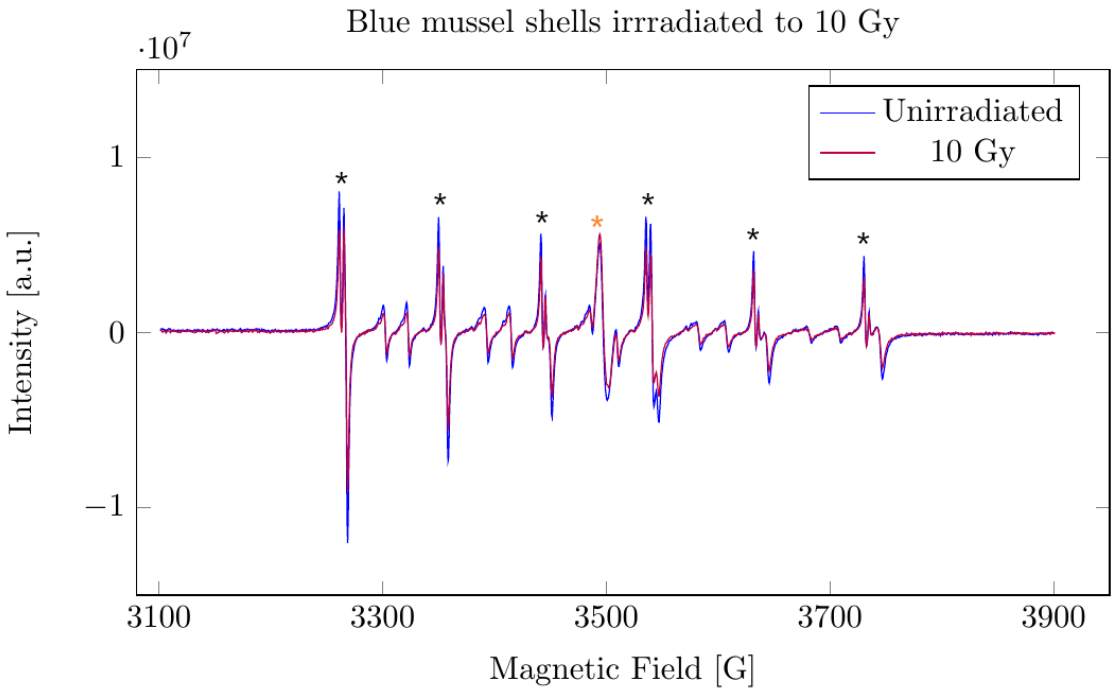

FIGURE 4.12: EPR spectra of blue mussel shells irradiated to a dose of 10 Gy. The Mn^{2+} peaks are marked with black asterisks. A central peak is also displayed and marked with an orange asterisk.

Eastern Eliptio Mussel

The spectra for unirradiated and irradiated Eastern eliptio mussel shells show a complex signal and are presented in Figure 4.13. The spectra display high intensity Mn^{2+} signals and a variety of additional impurities. With this complex signal, it is difficult to resolve any radiation-induced peaks. Therefore, the shells of Eastern eliptio mussels are not suited as environmental samples.

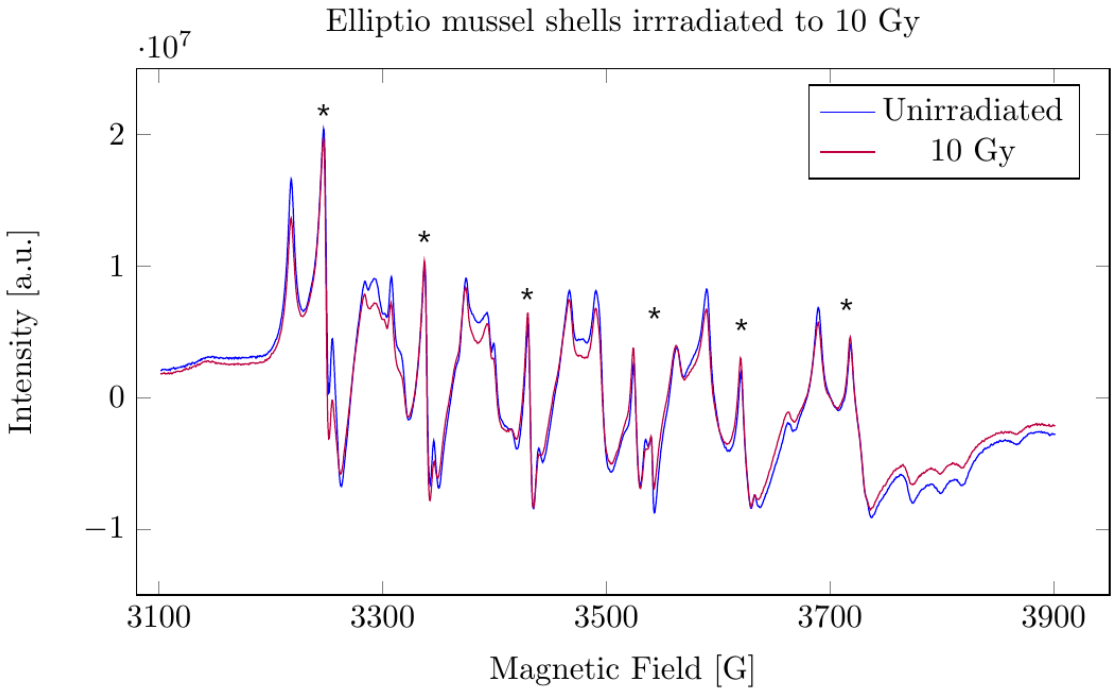

FIGURE 4.13: EPR spectra of eliptio mussel shells before and after an irradiation dose of 10 Gy. The Mn^{2+} peaks are marked with an asterisk.

The intensity of the Mn^{2+} signals is high, even though this species is a freshwater mussel. The shells of freshwater molluscs are primarily composed of aragonite as the main $CaCO_3$ polymorph [68]. However, Eastern eliptio mussel shells can contain trace amounts of calcite and rhodochrosite ($MnCO_3$) as well. The high intensity Mn^{2+} signals are likely due to the shells composed of calcite and rhodochrosite since it has been established that manganese will be more easily incorporated into the crystal structure of calcite. Furthermore, the typical habitats of Eastern eliptio

mussels are lakes, rivers, and streams where the species inhabit substrates comprised of a combination of clay, rocks, and sand. The occupancy of Eastern eliptio mussels on these substrates results in this species incorporating trace amounts of manganese into the shells.

Freshwater Pond Snail

As discussed in Section 4.1, the EPR spectra for freshwater pond snails present a complex signal, which is shown in Figure 4.14. A radiation-induced peak is not detected for this species at a dose of 10 Gy. The absence of a radiation-induced peak is due to the high Mn^{2+} signal intensities. Based on the complexity and overlapping signals from different impurities, the shells of freshwater pond snails would not be suitable for low dose studies.

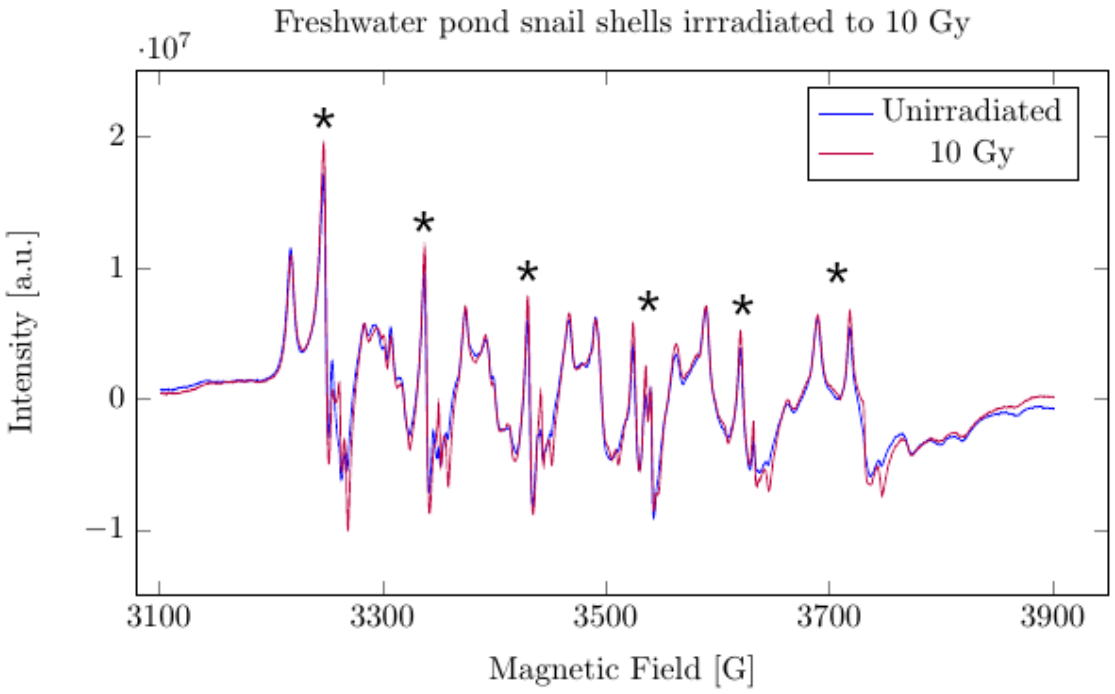

FIGURE 4.14: EPR spectra of pond snail shells before and after an irradiation dose of 10 Gy. Characteristic Mn^{2+} peaks are present and marked with an asterisk.

Based on the literature, the majority of freshwater mollusc shells are composed of the aragonite structure [68]; however, some freshwater gastropod species can have

calcite as their main crystal mineral [76]. Freshwater pond snails vary in their water column occupancy as well, as these species can swim on water surfaces or inhabit the sediment surface in their ponds. As a result, it is expected the shells will contain trace amounts of manganese based on their varying crystal structure and substrate occupancy.

Terrestrial Grove Snail

The last species tested for this experiment was the terrestrial grove snail. The EPR spectra of unirradiated and irradiated shells are presented in Figure 4.15. As discussed in Section 4.1, the terrestrial snail species display a radiation-induced peak at a dose of 10 Gy. A radiation-induced peak at $g = 2.0016$ for this species is detectable at a dose of 2 Gy as well. However, due to the relative height of the Mn^{2+} signals, detection under 2 Gy is challenging.

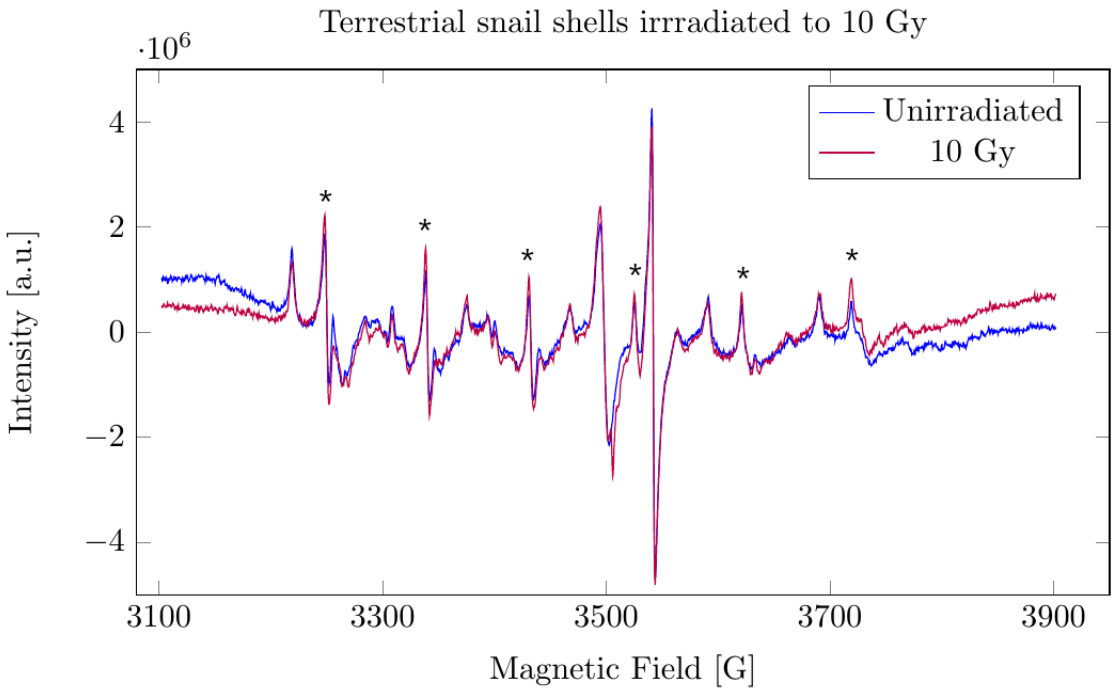

FIGURE 4.15: EPR spectra of terrestrial snail shells before and after an irradiation dose of 10 Gy. Characteristic Mn^{2+} peaks are present and marked with an asterisk.

The intensity of the Mn^{2+} signals for this species is an order of magnitude lower

than the previously studied species, and as such, it is the most promising for environmental dosimetry. This supports the assumption that manganese content can be used as an indicator for the suitability of a species for low dose studies. A study conducted on the chemical composition of a terrestrial snail species showed that the shell was comprised of 98% calcium carbonate, in the form of aragonite, and had smaller quantities of calcite, manganese, and other trace metals present [89]. Furthermore, terrestrial snails live in areas containing grass, soil, and various hedgerows, where they inhabit the top soil or grass surfaces. As discussed earlier, natural soils contain lower concentrations of manganese than sediments, and manganese accumulation in the soil is generally not on the surface of soils but rather in the subsoil layer [83]. As the terrestrial snail species live in habitats that contain lower manganese concentrations, it can be concluded that less manganese will be present in the shells.

While the intensity of Mn^{2+} signals for this species are lower than those of benthic invertebrates, studies have been conducted that correlate the shell color with metal content. The *Cepaea nemoralis* species either has a plain yellow shell or a white shell that contains dark colored bands. The results of an energy dispersive spectroscopy analysis conducted in one study showed that dark colored bands in terrestrial snail species could be due to the incorporation of iron and manganese in the shell with organic compounds [89]. As the shells collected for this experiment had dark colored bands, it can be concluded that the shells' color had an influence on the intensity of the Mn^{2+} signals present in the EPR spectra.

4.4.3 Summary

As seen in the EPR spectra for the studied shelled species, Mn^{2+} signals are prominent and limit the measurement capabilities of radiation-induced peaks. Of the seven shelled species studied, only the terrestrial snail shells displayed a radiation-induced peak observable at the dose of 10 Gy. Based on the results presented, a reasonable assumption can be made that the crystal form of $CaCO_3$ and the habitat of a species has a major influence on the manganese intensity in EPR spectra. This is further supported by the fact that most crustacea and molluscs are benthic

species with occupancy on the sediment, which contain varying amounts of manganese concentrations [83]. Therefore, trace amounts of the element will be present in shells of most species in different quantities. Table 4.3 summarizes the results for this experiment, which presented a comparative analysis of Mn^{2+} EPR signal intensities in different shelled species. The peak-to-peak heights of the Mn^{2+} signal in each species were measured (using the WinEPR software), and their intensity is presented. Additionally, the main crystal form of the shells is listed. Finally, qualitative assessments of radiation-induced peaks in the EPR spectra for each species are displayed.

TABLE 4.3: A summary of the various factors influencing EPR spectra in seven shelled species.

Species	Mn^{2+} p-p Height	$CaCO_3$ Polymorph	Radiation-Induced Peak
Giant tiger prawn	$3.05 \cdot 10^5$	Calcite	No
American lobster	$2.14 \cdot 10^7$	Calcite	No
Eastern Oyster	$3.11 \cdot 10^7$	Calcite	No
Blue mussel	$2.20 \cdot 10^7$	Calcite	No
Eliptio mussel	$2.50 \cdot 10^7$	Aragonite	No
Pond snail	$2.10 \cdot 10^7$	Aragonite	No
Terrestrial snail	$2.80 \cdot 10^6$	Aragonite	Yes

As the concentration of manganese in the shells have not been measured in this study, it is difficult to correlate the exact effect in the EPR spectra. However, based on the results summarized in Table 4.3 and the literature presented, there is evidence that the amount of manganese present in a shell due to the uptake from the environment affects both the Mn^{2+} and radiation-induced peaks in an EPR spectrum. It is further seen from Table 4.3 that the benthic species, which are composed of calcite or aragonite as their main crystal structure, display high intensity Mn^{2+} signals in the EPR spectra. The high intensity Mn^{2+} signals ultimately mask any radiation-induced peaks at low doses. The terrestrial snail shells were the only species where a radiation-induced peak was detected at the investigated dose of 10 Gy. Terrestrial snails inhabit areas that contain lower manganese

concentrations and have shells composed of an aragonite structure. These two factors combined presumably led to lower concentrations of manganese in the shells, resulting in lower intensity Mn^{2+} signals in the EPR spectrum, compared to the aquatic species.

To verify the conclusions drawn from the results of this study, it would be beneficial to sample all tested species directly from nature as opposed to purchasing them from local grocery stores. Sampling species from their natural environment would eliminate uncertainties in experimental work, as well as provide accurate data of environmental conditions for a species. Additional experiments in determining the exact crystal mineral of $CaCO_3$, such as X-ray diffraction, would be necessary to conclude structural differences of shells influencing EPR spectra.

4.5 Applicability for Retrospective Dosimetry

Depending on the application of EPR dosimetry, calcified tissues can be used to provide various information on accumulated radiation exposure. EPR dosimetry using shelled species has commonly been used for detection and identification of irradiated foodstuffs and geological dating. EPR dosimetry using shelled species for low dose studies introduces environmental factors that need to be assessed. High intensity signals present in the EPR spectra due to impurities from a species' environment have been shown to be a significant limiting factor in dose assessments. It is established that these signals obscure radiation-induced peaks at low doses. Based on the preliminary results of this work, it is evident that samples chosen for environmental EPR dosimetry will have to be selected based on multiple considerations. Factors of how a species' habitat affect shell formation need to be examined when selecting a species to use for environmental dose assessments.

As discussed in Chapter 2, and seen from experimental work, the presence of Mn^{2+} signals in the EPR spectra of crustacea and molluscs have provided a challenge in isolating and quantifying radiation-induced peaks at low doses. The results from this work have provided insight on different factors affecting the EPR spectra of various shelled species. Sampling species for environmental EPR dosimetry requires

an understanding of species' habitats and shell structures. As a result, subsequent studies in low dose EPR dosimetry using shelled species will be required.

First, knowledge of the geographic range of a species is essential, as shells of marine species have been shown to have higher Mn^{2+} intensities present in the EPR spectra. Additionally, the habitat of the species plays an equal role. The accumulation of manganese is very likely dependent on the bioavailability of this element in the substrate that species inhabit. As most crustacean and mollusc species in marine environments are benthic organisms, these species accumulate manganese into their shells during calcification, resulting in higher Mn^{2+} intensities in EPR spectra. Therefore, a species' occupancy on substrates is important to consider. Finally, knowledge of the crystal form of $CaCO_3$ is important, as calcite and aragonite minerals incorporate varying amounts of manganese in their structures. Manganese is chemically more stable in calcite [86], and as a result, shells composed of this mineral will contain more Mn^{2+} ions [32].

Although environmental factors provide a limitation in low dose detection using shelled species, it is important to note that EPR spectroscopy is species dependent. Considering only seven species were used to test their dose-response, the prospect of using shelled species for environmental EPR dosimetry is still feasible. These species represent a small selection of shelled organisms. Therefore, further research in identifying applicable shelled species to use for environmental EPR dosimetry is required. Terrestrial snail shells, for example, display promising results at characterizing a dose signal at 2 Gy. Furthermore, terrestrial snail shells are formed of an aragonite structure, they potentially have a lower concentration of manganese in their shells due to their habitat, and have light colored shells. Based on these factors, terrestrial snails could be viable for future dose assessments. Through experimental refinements, it may be possible to lower the 2 Gy limit to a range applicable for environmental dose assessments.

Though it may be challenging to resolve radiation-induced peaks at lower doses, EPR dosimetry using calcified tissues can still be useful for dose assessments. As

discussed in Chapter 2, environmental EPR dosimetry has been conducted in heavily contaminated environmental areas from unintentional releases or major accidents. The majority of EPR environmental dosimetry has been conducted in the Techa River ecosystem. For instance, in one study, doses reconstructed using EPR on calcified tissues of fish from the Techa River ecosystem were found to be in a range from 20 - 265 Gy [77]. Therefore, in the instances of accidents, EPR dosimetry using shelled species can be applicable in assessing radiation doses in heavily contaminated environments.

Chapter 5

Conclusions

5.1 Overall Summary

The objective of this work is to investigate the feasibility of using calcified tissues of aquatic and terrestrial shelled species for retrospective dosimetry using Electron Paramagnetic Resonance (EPR) spectroscopy.

This work is motivated by the continuous interest in the protection of the environment from ionizing radiation. Moreover, there has been an emphasis on estimating radiation doses to aquatic and terrestrial species after a radiological accident. Investigating the practicality of using calcified tissues of shelled species to extrapolate absorbed doses to non-human biota is relevant to both topics.

Environmental exposure to radiation from reactor accidents and unintentional radiation releases can lead to high concentrations of radioactive material in aquatic and terrestrials environments. Exposure pathways can further result in radioactive materials being dispersed throughout the environment, leading to possible radioactive contamination in multiple ecosystems. Conventional environmental sampling techniques and retrospective dosimetry techniques can be implemented in areas to provide dose assessments. Retrospective dosimetry techniques allow for dose assessments to be provided in areas even where the contamination has decayed. The dose assessments from these techniques can help inform necessary responses for long-term environmental protection and remediation. Physical retrospective dosimetry techniques are beneficial for long-term radiation detection, as they can

determine local doses to the environment by using natural or fortuitous dosimeters. EPR dosimetry, in particular, is a promising retrospective dosimetry technique. It has been successfully used in assessing radiation doses to individuals and the environment in the cases of emergencies and accidents.

EPR spectroscopy is used to study and detect materials that contain paramagnetic centers. The calcified tissues of invertebrate aquatic and terrestrial shelled species are formed as defined calcium carbonate crystal structures. The interaction of ionizing radiation with calcified tissues results in free electrons. Free electrons are captured in the lattice defects of the calcium carbonate matrix and form paramagnetic centers. EPR measurements can then be performed on the calcified tissues to quantify radiation-induced paramagnetic centers, since the number of paramagnetic centers formed in these materials is proportional to the incident radiation. This proportionality provides an opportunity for the calcified tissues of shelled species to be used as natural or fortuitous dosimeters.

The use of EPR spectroscopy was investigated as a retrospective dosimetry technique on seven shelled species from marine, freshwater, and terrestrial ecosystems. These included the American lobsters (*Homarus americanus*), giant tiger prawns (*Penaeus monodon*), Eastern oysters (*Crassostrea virginica*), blue mussels (*Mytilus edulis*), Eastern elliptio mussels (*Elliptio complanata*), freshwater pond snails (*Lymnaea stagnalis*), and terrestrial grove snails (*Cepaea nemoralis*). Sample preparation procedures for each species were developed, which included cleaning and grinding shells in a manner that did not significantly distort the EPR signals Chemical etching of shells was investigated as a sample preparation method to improve the EPR signal by removing surface defects.

Irradiation experiments were conducted on the prepared shell samples using a ^{137}Cs gamma source. Qualitative analysis of the derived EPR spectra was performed to determine if radiation-induced peaks at environmental doses could be detected. Prominent Mn^{2+} signals were present in the spectra of all species, except the giant tiger prawns. Due to the intensity of the Mn^{2+} signals, no radiation-induced peaks were detected at a dose of 10 Gy for any species except the terrestrial grove snails.

As the high intensity Mn^{2+} signals in the EPR spectra obscured any radiation-induced peaks, the shells of the aquatic species were determined to be unsuitable for low dose EPR dosimetry.

The terrestrial grove snail shells displayed a radiation-induced peak at a dose of 10 Gy and were investigated further to determine detection limits. A study on the dose-response relationship for the terrestrial snail shells was conducted, where three shell samples were irradiated to doses of 2, 10, and 20 Gy. A quantitative analysis of the radiation-induced peak using the radical species of CO_2^- at a g-value of 2.0016 was performed. The peak-to-peak height of the radiation-induced peak was measured for each sample using the WinEPR processing software. The shells of the terrestrial snail species showed a proportionality between peak-to-peak height and dose. However, the high intensity Mn^{2+} signals caused a limitation in quantifying a radiation-induced peak below 2 Gy for this species.

The high intensity Mn^{2+} signals in the EPR spectra introduced a significant limiting factor for low dose studies. As a result, various factors contributing to Mn^{2+} signals in an EPR spectrum were investigated. The shells of marine species are primarily formed of calcite and displayed high intensity Mn^{2+} signals, which masked radiation-induced peaks at low doses. Species composed of dark colored shells, such as the blue mussels, also had high Mn^{2+} signals in the EPR spectra. It was concluded that the accumulation of manganese in shells is largely dependent on the bioavailability of this metal in the substrate that a species inhabits and the crystal mineral of the shell. The Mn^{2+} signals in EPR spectra are heavily influenced by the crystal form of $CaCO_3$, the color of the shell, and the habitat of a species. Knowing the concentration of manganese present in these species' shells and habitats would be beneficial in quantifying the direct effect in the EPR spectra. Based on the study results, it was determined that environmental factors contribute a significant uncertainty for EPR dosimetry. These factors ultimately limit the number of species applicable to use as natural dosimeters for low dose retrospective dosimetry.

5.2 Improvements of Experimental Methods and Recommendations

As this work is an exploratory study investigating the feasibility of shelled species for retrospective dosimetry, the practical applications of EPR spectroscopy as a dosimetry technique are important to consider. Throughout these experiments, various improvements and recommendations on experimental methods using EPR spectroscopy and sample preparation techniques of environmental samples were identified for future work.

To use materials available in the environment for retrospective dosimetry, it is important to ensure that the material is easily obtainable. In this work, sample collection for marine species was not possible, and they were instead purchased from local grocery stores. As a result, the organism's history was unknown, which introduced uncertainties in the assumptions made for species' habitats. As the Mn^{2+} signals in EPR spectra are largely influenced by the animal's habitat, it will be important to sample species directly from the wild for more accurate knowledge of their environment. Additionally, secondary environmental sampling will be required. For instance, when measuring the concentration of manganese in the shells, it would be necessary also to sample the sediment, water, and soil of the animal's surrounding habitat. This would allow for more accurate information about the animal's surroundings and validate the conclusions of different environmental factors that contribute to EPR signals.

To use EPR dosimetry as a retrospective dosimetry technique and to implement it for a large-scale dose assessment program, an extensive number of samples need to be collected. This further requires sample preparation methods and measurement readouts to be carried out efficiently and within a reasonable time frame. During the sample preparation methods for this work, one shell for a specific species was ground individually and used as a sample. However, if the purpose of the shells is to create a generalized calibration curve used for dose assessments, then it is more practical to prepare samples using multiple shells of the same individual species. Sample preparation will ultimately be less time consuming with a larger number

of samples being prepared. Moreover, as shells of even the same species vary in structure and composition, preparing samples from a "powdered pool" allows for multiple shells to be used as one sample and provides an accurate representation of shell variances.

Grinding samples using a mortar and pestle displayed no additional mechanically-induced peaks. As a result, the method of grinding should continue to be used, since it is an effective and rapid method to obtain powdered samples. Additionally, the grain sizes used for all samples (0.1-0.5 mm) are recommended for future measurements. The samples prepared from these grain sizes are ideal for filling into EPR tubes, which have a 4 mm inner diameter. These grain sizes allow for more sample to be filled into the EPR tubes (compared to larger grain sizes), which allows for a higher packing density in the active volume of the resonator. Having more sample in the active volume of the resonator allows for more paramagnetic centers to be measured, which subsequently results in a higher EPR signal per volume of sample.

The spectrum acquisition parameters are especially important for any quantitative analysis. When changing or selecting measurement parameters, care has to be taken not to distort or alter radiation-induced peaks. As the radiation-induced peak for the 2 Gy sample of the terrestrial shells was difficult to resolve, some considerations of measurement parameters for future experiments can be implemented. For instance, selecting a larger conversion time and time constant is a potential method to decrease noise and increase signal resolution. By decreasing the noise, the radiation-induced peak for the 2 Gy sample will be higher, since the time for signal acquisition for each measurement point will be larger. However, if the time constant is too large, distorting or filtering out the radiation-induced peak is possible. Alternatively, increasing the number of runs that the signal is averaged over can also improve the signal resolution. However, the limitations of these changes is that by increasing the conversion time and the number of runs, the total acquisition time of the measurements is also increased. Extensive studies comparable to those presented in Chapter 3 on the effect of parameters on the radiation-induced peaks need to be considered if changing any measurement parameters.

Lastly, an alanine powder calibration curve was developed to provide dose estimates for the reference dosimetry performed in this work. Alanine powder is recommended to be used as reference dosimeters for future work with EPR measurements. Alanine powder has a high sensitivity to ionizing radiation, with the lowest dose detected in this work at 0.2 Gy. Furthermore, alanine powder is inexpensive and can be irradiated in the same micro-centrifuge tubes as powdered environmental samples. The formed radical is stable for many years, and it has a linear dose-response. When using the alanine powder, silica gel packs should be kept in the container to absorb excess moisture due to environmental laboratory conditions. All prepared samples should also be kept in a dark container and a desiccator to manage signal change due to moisture content.

5.3 Future Work

Environmental factors resulted in high intensity Mn^{2+} signals in EPR spectra for all studied shelled species. Possible explanations as to why prominent Mn^{2+} signals were present in the spectra of these species were discussed in Chapter 4. Though Mn^{2+} signals limited the number of species feasible to use for low dose retrospective dosimetry, continuous work for integrating EPR as an environmental dose assessment tool for large-scale accidents should still be undertaken.

The terrestrial snail shells displayed a radiation-induced peak and are a viable species to consider for retrospective dosimetry. The preliminary results of using the terrestrial snail shells displayed a promising dose-response relationship. Implementing the shells of *Cepaea nemoralis* for environmental dose assessments will require further studies using a larger number of samples to develop a more refined dose-response curve.

Implementing EPR dosimetry for low dose studies using shelled species poses some limitations. As environmental factors largely influenced quantitative results, these aspects need to be thoroughly assessed. Future work will require comprehensive studies on selecting an appropriate shelled species for low dose EPR dosimetry. For instance, extensive exploratory studies on different shelled species may need to be

developed. These studies would include a similar approach to the work presented in this thesis. Additional experiments would include secondary measurements of the animal's surrounding environment. Knowledge of the crystal form of $CaCO_3$ that shells are composed of and the concentration of manganese in the shells of the studied species would also be required. These experiments and their results can present a comparative analysis of the environmental characteristics and what is presented in the EPR spectra. Moreover, the results of these studies will allow for an opportunity to develop a framework that examines various environmental factors, such as crystal structure, chemical composition, geographical location, shell color, and habitat. By developing such a framework, a methodical approach in selecting shelled species for low dose EPR dosimetry can be facilitated by forming a set of strong indicators that a species is suitable for this purpose.

Bibliography

[1] ICRP, "Recommendations of the International Commission on Radiological Protection. ICRP Publication 26", *Ann ICRP*, p. 3, 1977.

[2] R. Pentreath, "Radiological protection criteria for the natural environment", *Radiation Protection Dosimetry*, vol. 75, no. 1-4, pp. 175–179, 1998.

[3] ICRP, "Environmental Protection - the Concept and Use of Reference Animals and Plants. ICRP Publication 108", *Ann ICRP*, vol. 38, 2008.

[4] L. Bøtter-Jensen, S. McKeever, and A. Wintle, *Optically stimulated luminescence dosimetry*. Elsevier, 2003.

[5] IAEA, "Generic Procedures for Monitoring in a Nuclear or Radiological Emergency", Tech. Rep., 1999.

[6] E. Haskell, "Retrospective accident dosimetry using environmental materials", *Radiation Protection Dosimetry*, vol. 47, no. 1-4, pp. 297–303, 1993.

[7] E. Ainsbury, E. Bakhanova, J. Barquinero, M. Brai, V. Chumak, V. Correcher, F. Darroudi, P. Fattibene, G. Gruel, I Guclu, *et al.*, "Review of retrospective dosimetry techniques for external ionising radiation exposures", *Radiation Protection Dosimetry*, vol. 147, no. 4, pp. 573–592, Nov. 2011.

[8] S. Della Monaca and P. Fattibene, "Radiation-induced damage analysed by luminescence methods in retrospective dosimetry and emergency response", *Ann Ist Super Sanita*, vol. 45, no. 3, pp. 297–306, 2009.

[9] H. Livingston and P. Povinec, "Anthropogenic marine radioactivity", *Ocean & Coastal Management*, vol. 43, no. 8-9, pp. 689–712, 2000.

[10] M. Isaksson and C. Raaf, *Environmental radioactivity and emergency preparedness*. CRC Press, 2017.

[11] P. Povinec, A. Aarkrog, and O. Buesseler, "Worldwide marine radioactivity studies (womars)", Tech. Rep., 2004.

[12] UNSCEAR, *Report of the United Nations Scientific Committee on the Effects of Atomic Radiation. UNSCEAR 1988 Report; Annex D. Exposures from the Chernobyl Accident*. 1988.

[13] IAEA, "Present and Future Environmental Impact of the Chernobyl Accident", Tech. Rep., 2001.

[14] UNSCEAR, *Sources and Effects of Ionizing Radiation UNSCEAR 2000 Report; Annex J. Exposure and Effects of Chernobyl Accident*. United Nations Publications, 2000, vol. II, pp. 453–551.

[15] K. Buesseler, M. Aoyama, and M. Fukasawa, "Impacts of the Fukushima nuclear power plants on marine radioactivity", *Environmental science & technology*, vol. 45, no. 23, pp. 9931–9935, 2011.

[16] IAEA, "The Fukushima Daiichi Accident: Technical Volume 4/5. Radiological Consequence", Tech. Rep., 2015.

[17] V. Trapeznikova, N. Kulikov, S. Nielsen, and A. Aarkrog°, "Radioactive contamination of the Techa River", *Health Physics*, vol. 65, no. 5, pp. 481–488, 1993.

[18] I. Kryshev, G. Romanov, V. Chumichev, T. Sazykina, L. Isaeva, and M. Ivanitskaya, "Radioecological consequences of radioactive discharges into the Techa River on the Southern Urals", *Journal of environmental radioactivity*, vol. 38, no. 2, pp. 195–209, 1998.

[19] A. Akleyev, L. Krestinina, M. Degteva, and E. Tolstykh, "Consequences of the radiation accident at the Mayak Production Association in 1957 (the 'Kyshtym Accident')", *Journal of radiological protection*, vol. 37, no. 3, R19, 2017.

[20] C. Prasuna, K. Narasimhulu, N. Gopal, J. Rao, and T. Rao, "The microstructures of biomineralized surfaces: A spectroscopic study on the exoskeletons of fresh water (Apple) snail, Pila globosa", *Spectrochimica Acta Part A: Molecular and Biomolecular Spectroscopy*, vol. 60, no. 10, pp. 2305–2314, Aug. 2004.

[21] M. Desrosiers and D. Schauer, "Electron paramagnetic resonance (EPR) biodosimetry", *Nuclear Instruments and Methods in Physics Research Section B: Beam Interactions with Materials and Atoms*, vol. 184, no. 1-2, pp. 219–228, Sep. 2001.

[22] B. Berger and R. Dallinger, "Terrestrial snails as quantitative indicators of environmental metal pollution", *Environmental Monitoring and Assessment*, vol. 25, no. 1, pp. 65–84, 1993.

[23] P. Fattibene and C. Callens, "EPR dosimetry with tooth enamel: A review", *Applied Radiation and Isotopes*, vol. 68, pp. 2033–2116, May 2010.

[24] M. Ikeya, *New Applications of Electron Spin Resonance. Dating, Dosimetry and Microscopy.* World Scientific Publishing Co., 1993.

[25] J. Sadło, J. Michalik, W. Stachowicz, G. Strzelczak, A. Dziedzic-Gocławska, and K. Ostrowski, "EPR study on biominerals as materials for retrospective dosimetry", *Nukleonika*, vol. 51. SUPPL.1, pp. 2–4, 2006.

[26] D. Regulla, "ESR spectrometry: A future-oriented tool for dosimetry and dating", *Applied Radiation and Isotopes*, vol. 62, no. 2, pp. 117–127, Feb. 2005.

[27] N. Nakamura, C. Miyazawa, S. Sawada, M. Akiyama, and A. Awa, "A close correlation between electron spin resonance (ESR) dosimetry from tooth enamel and cytogenetic dosimetry from lymphocytes of Hiroshima atomic-bomb survivors", *International Journal of Radiation Biology*, vol. 73, no. 6, pp. 619–627, Jan. 1998.

[28] V. Skvortsov, A. Ivannikov, V. Stepanenko, A. Tsyb, L. Khamidova, A. Kondrashov, and D. Tikunov, "Application of EPR retrospective dosimetry for large-scale accidental situation", *Applied Radiation and Isotopes*, vol. 52, no. 5, pp. 1275–1282, May 2000.

[29] H. Swartz, A. Flood, B. Williams, R. Dong, S. Swarts, X. He, O. Grinberg, J. Sidabras, E. Demidenko, J. Gui, *et al.*, "Electron Paramagnetic Resonance Dosimetry for a Large-Scale Radiation Incident:" *Health Physics*, vol. 103, no. 3, pp. 255–267, Sep. 2012.

[30] D. Viscomi and P. Fattibene, "Radiation-induced signals analysed by EPR spectrometry applied to fortuitous dosimetry", *Ann Ist Super Sanita*, vol. 45, no. 3, pp. 287–296, 2009.

[31] A. Wieser, R. Debuyst, P. Fattibene, A. Meghzifene, S. Onori, S. Bayankin, B. Blackwell, A. Brik, A. Bugay, V. Chumak, *et al.*, "The 3rd International

Intercomparison on EPR Tooth Dosimetry: Part 1, General Analysis", *Applied radiation and isotopes*, vol. 62, no. 2, pp. 163–171, 2005.

[32] W. Stachowicz, J. Michalik, G. Burlinska, J. Sadło, A. Dziedzic-Gocławska, and K. Ostrowski, "Detection limits of absorbed dose of ionizing radiation in molluscan shells as determined by E.P.R. spectroscopy", *Applied Radiation and Isotopes*, vol. 46, no. 10, pp. 1047–1052, Oct. 1995.

[33] A. Romanyukha and D. Regulla, "Aspects of retrospective ESR dosimetry (invited paper)", *Applied Radiation and Isotopes*, vol. 47, no. 11-12, pp. 1293–1297, Nov. 1996.

[34] M. Wencka, S. Hoffmann, and H. Hercman, "EPR dating of hydroxyapatite from fossil bones. Transient effects after gamma and UV irradiation", *Acta Physica Polonica Series A*, vol. 108, no. 2, p. 331, 2005.

[35] A. Romanyukha, D. Schauer, J. Thomas, and D. Regulla, "Parameters affecting EPR dose reconstruction in teeth", *Applied Radiation and Isotopes*, vol. 62, no. 2, pp. 147–154, Feb. 2005.

[36] E. Yukihara, J. Mittani, S. McKeever, and S. Simon, "Optically stimulated luminescence (OSL) of dental enamel for retrospective assessment of radiation exposure", *Radiation Measurements*, vol. 42, no. 6-7, pp. 1256–1260, Jul. 2007.

[37] D. Stoneham, I. Bailiff, S. Petrov, L. Botter-Jensen, Y. Goeksu, H. Jungner, and S. Petrov, "Retrospective dosimetry: The development of an experimental methodology using luminescence techniques", in *1st International Conference of the European Commission and the Belarus, Russian and Ukrainian Ministries on Chernobyl Affairs, Emergency Situations and Health*, European Commission, 1996, pp. 1037–1040.

[38] I. Bailiff, "Retrospective dosimetry with ceramics", *Radiation Measurements*, vol. 27, no. 5-6, pp. 923–941, 1997.

[39] I. Fiedler and C. Woda, "Thermoluminescence of chip inductors from mobile phones for retrospective and accident dosimetry", *Radiation measurements*, vol. 46, no. 12, pp. 1862–1865, 2011.

[40] D. Mesterházy, M. Osvay, A. Kovács, and A. Kelemen, "Accidental and retrospective dosimetry using TL method", *Radiation Physics and Chemistry*, vol. 81, no. 9, pp. 1525–1527, 2012.

[41] R. Wilkins, H. Romm, T. Kao, A. Awa, M. Yoshida, G. Livingston, M. Jenkins, U. Oestreicher, T. Pellmar, and P. Prasanna, "Interlaboratory comparison of the dicentric chromosome assay for radiation biodosimetry in mass casualty events", *Radiation research*, vol. 169, no. 5, pp. 551–560, 2008.

[42] R. Kleinerman, A. Romanyukha, D. Schauer, and J. Tucker, "Retrospective assessment of radiation exposure using biological dosimetry: Chromosome painting, electron paramagnetic resonance and the glycophorin a mutation assay", *Radiation research*, vol. 166, no. 1, pp. 287–302, 2006.

[43] M. Jonas, "Concepts and methods of ESR dating", *Radiation Measurements*, vol. 27, no. 5-6, pp. 943–973, Dec. 1997.

[44] F. Trompier, A. Romanyukha, R. Reyes, H. Vezin, F. Queinnec, and D. Gourier, "State of the art in nail dosimetry: Free radicals identification and reaction mechanisms", *Radiation and environmental biophysics*, vol. 53, no. 2, pp. 291–303, 2014.

[45] R. Hayes, "Electron Paramagnetic Resonance Dosimetry: Methodology and Material Characterization", PhD Thesis. University of Utah, 1999.

[46] W. McLaughlin, "ESR Dosimetry", *Radiation Protection Dosimetry*, vol. 47, no. 1, pp. 255–262, 1993.

[47] D Regulla, "Alanine Dosimetry - A Versatile Dosimetric Tool", in *World Congress on Medical Physics and Biomedical Engineering, September 7-12, 2009, Munich, Germany*, Springer, 2009, pp. 478–481.

[48] J. Raffi and P. Stocker, "Electron paramagnetic resonance detection of irradiated foodstuffs", *Applied Magnetic Resonance*, vol. 10, no. 1-3, pp. 357–373, Jan. 1996.

[49] M. Desrosiers, "Current status of the EPR method to detect irradiated food", *Applied Radiation and Isotopes*, vol. 47, no. 11-12, pp. 1621–1628, Nov. 1996.

[50] L. Douifi, J. Raffi, P. Stocker, and F. Dole, "A point about electron paramagnetic resonance detection of irradiated foodstuffs", *Spectrochimica Acta Part A: Molecular and Biomolecular Spectroscopy*, vol. 54, no. 14, pp. 2403–2412, Dec. 1998.

[51] J. Raffi, C. Hasbany, G. Lesgards, and D. Ochin, "ESR detection of irradiated seashells", *Applied radiation and isotopes*, vol. 47, no. 11-12, pp. 1633–1636, 1996.

[52] K. Köseoğlu and F. Köksal, "Detection of free radicals in gamma-irradiated seasnail hard tissues by electron paramagnetic resonance", *Applied Radiation and Isotopes*, vol. 59, no. 1, pp. 73–77, Jul. 2003.

[53] M. Desrosiers, "Gamma irradiated seafoods: Identification and dosimetry by electron paramagnetic resonance spectroscopy", *Journal of agricultural and food chemistry*, vol. 37, no. 1, pp. 96–100, 1989.

[54] B. Engin, O. Güven, and F. Köksal, "Electron spin resonance age determination of a travertine sample from the southwestern part of Turkey", *Applied Radiation and Isotopes*, vol. 51, no. 6, pp. 689–699, Dec. 1999.

[55] B. Engin, S. Kapan-Yeşilyurt, G. Taner, H. Demirtaş, and M. Eken, "ESR dating of Soma (Manisa, West Anatolia – Turkey) fossil gastropoda shells", *Nuclear Instruments and Methods in Physics Research Section B: Beam Interactions with Materials and Atoms*, vol. 243, no. 2, pp. 397–406, Feb. 2006.

[56] H. Nagasawa, "The crustacean cuticle: Structure, composition and mineralization", *Front Biosci*, vol. 4, pp. 711–20, 2012.

[57] D. Raabe, C. Sachs, and P. Romano, "The crustacean exoskeleton as an example of a structurally and mechanically graded biological nanocomposite material", *Acta Materialia*, vol. 53, no. 15, pp. 4281–4292, 2005.

[58] B. Goodman, D. McPhail, and D. Duthie, "Electron spin resonance spectroscopy of some irradiated foodstuffs", *Journal of the Science of Food and Agriculture*, vol. 47, no. 1, pp. 101–111, 1989.

[59] E. Stewart and M. Hilar, "Identification of Irradiated Norway Lobster (Nephrops norvegicus) Using Electron Spin Resonance (ESR) Spectroscopy and Estimation of Applied Dose Using Re-irradiation: Results of an In-House Blind Trial", *International Journal of Food Science & Agriculture*, vol. 74, Feb. 1997.

[60] E. Stewart, M. Stevenson, and R. Gray, "The Effect of Irradiation Dose and Storage Time on the ESR Signal in the Cuticle of Different Components of

the Exoskeleton of Norway Lobster (Nephrops nowegicus)", *Applied Radiation and Isotopes*, vol. 44, pp. 433–437, Feb. 1993.

[61] E. Stewart, "The application of ESR spectroscopy for the identification of irradiated Crustacea", *Applied Magnetic Resonance*, vol. 10, no. 1-3, pp. 375–393, Jan. 1996.

[62] E. Stewart, M. Stevenson, and R. Gray, "Detection of irradiation in scampi tails - effects of sample preparation, irradiation dose and storage on ESR response in the cuticle", *International Journal of Food Science & Technology*, vol. 27, no. 2, pp. 125–132, Jul. 1992.

[63] E. Stewart and D. Kilpatrick, "An International Collaborative Blind Trial on Electron Spin Resonance (ESR) Identification of Irradiated Crustacea", *International Journal of Food Science & Agriculture*, vol. 74, pp. 473–484, Feb. 1997.

[64] C. Aydaş, S. Tepe Çam, B. Engin, T. Aydin, and M. Polat, "The use of ESR spectroscopy for the identification and dose assessment of irradiated pink shrimp (parapenaeus longirostris) from Turkey", *Radiation Effects and Defects in Solids*, vol. 168, no. 3, pp. 212–223, 2013.

[65] K. Morehouse and M. Desrosiers, "Electron spin resonance investigations of gamma-irradiated shrimp shell", *Applied Radiation and Isotopes*, vol. 44, no. 1-2, pp. 429–432, 1993.

[66] A. Maghraby, "Identification of irradiated crab using EPR", *Radiation Measurements*, vol. 42, no. 2, pp. 220–224, Feb. 2007.

[67] E. Seletchi and O. Duliu, "Comparative study on ESR spectra of carbonates", *Romanian Journal of Physics*, vol. 52, no. 5-7, pp. 657–666, 2006.

[68] T. Vichaidid, U. Youngchuay, and P. Limsuwan, "Dating of aragonite fossil shell by ESR for paramagnetic species assignment of Mae Moh basin", *Nuclear Instruments and Methods in Physics Research Section B: Beam Interactions with Materials and Atoms*, vol. 262, no. 2, pp. 323–328, Sep. 2007.

[69] R. Köseoğlu, F. Köksal, and M. Birey, "Electron paramagnetic resonance study of defects in gamma-irradiated marine mussel and scallop", *Zeitschrift für Naturforschung*, vol. 59, pp. 773–779, May 2004.

[70] K. Ostrowski, A. Dziedzic-Gocławska, W. Stachowicz, and J. Michalik, "Accuracy, sensitivity, and specificity of electron spin resonance analysis of mineral constituents of irradiated tissues", *Annals of the New York Academy of Sciences*, vol. 238, no. 1, pp. 186–201, 1974.

[71] A. Alberti, E. Chiaravalle, P. Fuochi, D. Macciantelli, M. Mangiacotti, G. Marchesani, and E. Plescia, "Irradiated bivalve mollusks: Use of EPR spectroscopy for identification and dosimetry", *Radiation Physics and Chemistry*, vol. 80, no. 12, pp. 1363–1370, Dec. 2011.

[72] S. Della Monaca, P. Fattibene, C. Boniglia, R. Gargiulo, and E. Bortolin, "Identification of irradiated oysters by EPR measurements on shells", *Radiation measurements*, vol. 46, no. 9, pp. 816–821, 2011.

[73] R. Köseoğlu, F. Köksal, and E. Çiftçi, "EPR study of radicals produced by gamma-irradiation in marine mollusc (*Venus* sp.) fossils", *Radiation Effects and Defects in Solids*, vol. 159, no. 8-9, pp. 497–502, Aug. 2004.

[74] D. Schramm, M. Cattani, N. Mastro, A. Rossi, *et al.*, "Electron spin resonance (ESR) of gamma-irradiated oyster shells", 2015.

[75] W. Stachowicz, J. Michalik, G. Burliriska, J. Sadto, A. Dziedzic-Goclawska, and K. Ostrowski, "EPR detection of the dose of ionizing radiation with shells of molluscs", *Nuclear Chemistry and Technology*, p. 19, 1995.

[76] A. Molodkov, "ESR-dating of non-marine mollusc shells", *Applied Radiation and Isotopes*, vol. 44, no. 1-2, pp. 145–148, 1993.

[77] D. Ivanov, E. Shishkina, D. Osipov, V. Starichenko, S. Bayankin, M. Zhukovsky, and E. Pryakhin, "Otoliths as object of EPR dosimetric research", *Radiation and environmental biophysics*, vol. 57, no. 4, pp. 357–363, 2018.

[78] D. Barr, S. Eaton, and G. Eaton, "Workshop on Quantitative EPR", 2008.

[79] L. Felner, "Electron paramagnetic resonance (EPR) as an appropriate method in retrospective accident dosimetry", Bachelor's thesis. FH Technikum Wien, 2017.

[80] M. Al-Karmi and M. Morsy, "EPR of gamma-irradiated polycrystalline alanine-in-glass dosimeter", *Radiation measurements*, vol. 43, no. 7, pp. 1315–1318, 2008.

[81] F. Callens, G. Vanhaelewyn, P. Matthys, and E. Boesman, "EPR of carbonate derived radicals: Applications in dosimetry, dating and detection of irradiated food", *Applied Magnetic Resonance*, vol. 14, no. 2-3, pp. 235–254, Apr. 1998.

[82] M. Tzivaki, "Electron Paramagnetic Resonance for Dosimetry in Freshwater Aquatic Environments.", PhD Thesis. Ontario Tech University, 2020.

[83] P. Howe, H. Malcolm, and S. Dobson, *Manganese and its compounds: environmental aspects*. World Health Organization, 2004.

[84] D. Bordean, D. Nica, M. Harmanescu, I. Banatean-Dunea, and I. Gergen, "Soil manganese enrichment from industrial inputs: A gastropod perspective", *PloS one*, vol. 9, no. 1, 2014.

[85] R. Roer and R. Dillaman, "The structure and calcification of the crustacean cuticle", *American Zoologist*, vol. 24, no. 4, pp. 893–909, 1984.

[86] A. Soldati, D. Jacob, P. Glatzel, J. Swarbrick, and J. Geck, "Element substitution by living organisms: The case of manganese in mollusc shell aragonite", *Scientific reports*, vol. 6, no. 1, pp. 1–9, 2016.

[87] N. Udomkan, S. Meejoo, P. Limsuwan, P. Winotai, and Y. Chaimanee, "Electron Spin Resonance Studies of Mn^{2+} in Freshwater Snail Shells: Pomacea Canaliculata Lamarck and Fossilized Snail Shell", *Chinese Physics Letters*, vol. 22, no. 7, pp. 1780–1783, Jul. 2005.

[88] FAO, "Fisheries and aquaculture cultured aquatic species information programme - penaeus monodon", [Online]. Available: http://www.fao.org/fishery/culturedspecies/Penaeus_monodon/en#tcNA008C.

[89] D. Mierzwa, "Chemical composition and structure of the shell of Cepaea vindobonensis (Férussac, 1821) (Gastropoda: Pulmonata: Helicidae)", *Folia Malacologica*, vol. 16, no. 1, pp. 17–20, Mar. 2009.